Crevasse formation and maturation in the fluvial-tidal realm

Jelle Izaäk Maarten Moree, BSc

jelle.moree@gmail.com

In partial fulfilment of the degree of Master of Science
in the Earth Sciences

Department of Physical Geography,
Utrecht University

Supervisors:
Prof. dr. M.G. Kleinhans
Dr. H.J. Pierik

the 23rd of August, 2019

Utrecht University

Het drijven van
ondergrond

Het bezonken gelaagde

De klaarte van het wachten
op een kier

Uit de bundel “Bladgrond”
van Roland Jooris.

Statement of originality of the MSc thesis

I declare that:

1. this is an original report, which is entirely my own work,
2. where I have made use of the ideas of other writers, I have acknowledged the source in all instances,
3. where I have used any diagram or visuals I have acknowledged the source in all instances,
4. this report has not and will not be submitted elsewhere for academic assessment in any other academic course.

Student data:

Name: Jelle Izaäk Maarten Moree

Registration number: 4087747

Date: the 23rd of August, 2019

Signature: 

Abstract

A crevasse is a geomorphological unit that consists of channel, bar, and splay deposits that form at a breach in the natural levee of a river, extending into the flood basin. They are common features in river delta and tidal landscapes where they form relatively highly elevated elements in otherwise low-lying flood basins. Hence, crevasses have an effect on sediment distribution within deltas and tidal landscapes.

So far, research on crevasses is generally limited to single crevasse case-studies in fluvial settings. Due to the focus on the effects of fluvial boundary conditions, there is a knowledge gap in the understanding of the effects of tidal boundary conditions. Therefore, the objective of this thesis is to assess the effect of tidal and fluvial boundary conditions, their interplay, and the initial flood basin conditions on the formation, evolution, and morphology of crevasses in the fluvial-tidal realm.

To address the objective, the Old Rhine system was used as a case study. The Old Rhine is a former main branch of the Rhine in the Western part of the Rhine-Meuse delta in the Netherlands. Multiple abandoned crevasses are well-preserved and its palaeogeographic development and changes in boundary conditions have been generally well reconstructed. The sedimentary build-up of four long crevasses was reconstructed based on borehole data of hand-augered corings. Lithogenetic cross-sections of each crevasse were constructed. Archaeological data were used in conjunction with the crevasse stratigraphy to get an indication of crevasse ages. Hence, three crevasse phases of the Old Rhine were identified. Their timing was compared to changes in boundary conditions and flood basin configuration of the Old Rhine to infer the effect of these changes on crevasse formation and evolution.

It was found that with regular tidal flushing of the crevasse throats (*i.e.* the initial natural levee breach) due to water level fluctuations induced by the tidal backwater effect, more crevasses can be formed by preventing crevasse healing. As such, regular tidal flushing facilitates crevasse evolution and progradation. When the tidal backwater effect decreased in the Old Rhine due to gradual closure of the estuary, the number of active crevasses decreased. This occurred because of the abandonment of existing crevasses on one hand and a decrease in the formation and establishment of new crevasses on the other as infilling of the crevasse throats was no longer or to an increasingly lesser extent prevented.

Flood events cause the initial natural levee breach which starts the crevasse formation. Subsequent flood events cause crevasse maturation and progradation, given that filling-in of the crevasse throat is prevented by regular flushing by the tidal backwater effect. Periods with a high frequency of flood events coincide with phases of increased crevasse formation and extensive progradation. Periods with a decreased frequency of flood events compared to a preceding high frequency period show a decrease in number of crevasses formed and a cease of crevasse progradation. Storm surge events probably have the same effect on crevasses as flood events, but the lack of a storm surge record for the Old Rhine estuary prevents any definitive statements about their effect.

Pre-existing channels, in the case of the Old Rhine peat drainage channels draining the raised bogs in the flood basins, can be intercepted by progradating crevasses. Hence, hybrid crevasse-peat drainage channels are formed. Such channels can still function as drainage channels of the raised bogs after a decrease or cease of morphodynamic crevasse activity due to a decrease in the tidal backwater effect, in the flood frequency or both. In the case of the Old Rhine, the three most upstream located crevasses in this study were formed as hybrid crevasse-peat drainage channels.

The outcomes presented in this thesis increase the understanding of the formation and maturation of crevasses in the fluvial-tidal realm of lowland river systems. They show that changes in both upstream as well as downstream boundary conditions affect the potential of crevasse formation and maturation. The presence of raised bogs in the flood basins and associated peat drainage channels can lead to the formation of hybrid crevasse-peat drainage channels.

These outcomes have implications for the archaeology of the Old Rhine area and future natural land-building projects in deltas. The three identified crevasse phases aid archaeologists to estimate the archaeological expectation of crevasse deposits in the Old Rhine area. Crevasses could be used in natural land-building projects to provide sediment to vulnerable flood basins to match (relative) sea level rise rates. Whether crevasse sedimentation rates would be high enough cannot be concluded based on the outcomes of this thesis. Implementation of crevasses for natural land-building projects would require that enough fluvial or marine sediment is available, sufficient vegetation cover is present to trap sediment efficiently, and flood events and storm surges are allowed to flood the flood basins.

Acknowledgements

I will write the acknowledgements in this section predominantly in Dutch as the people to whom they are addressed are almost all Dutch-speaking.

Allereerst wil ik heel graag mijn beide begeleiders, prof. dr. Maarten Kleinhans & dr. Harm Jan Pierik bedanken. Harm Jan, ik ben je heel dankbaar dat je me zo'n ontzettend interessant onderzoek suggereerde toen ik bij jouw oude kamer in de Zonneveldvleugel in mei 2018 langskwam met de vraag of jij nog interessante scriptieonderwerpen voorhanden had waarbij mijn beide interesses, de geomorfologie en de archeologie, aan bod zouden komen. Ook wil ik je bedanken voor je aanhoudende geduld met mijn soms wat stroeve voortgang wat betreft het schrijven van deze scriptie. Door jouw enthousiasme over het onderzoek en goede feedback op mijn schrijven inzichten vond ik dikwijls hernieuwde energie om weer met frisse zin verder aan de slag te gaan en om mijn theorieën op een dieper niveau uit te werken. Maarten, dankjewel voor jouw altijd zeer nuttige vragen tijdens onze gezamenlijke besprekingen over mijn voortgang. Je liet me daardoor met een kritische blik naar mijn eigen theorieën en hypothesen kijken, waardoor ik deze ten goede kon herzien en beter verwoorden. Ik wil jullie allebei bedanken voor de kans die jullie mij hebben geboden om ervaring op te doen met het presenteren van mijn werk voor een breed publiek tijdens de nationale NCR-dagen. Ik dank dr. Wim Hoek en de technisch assistenten van het departement Fysische Geografie voor de begeleiding tijdens het laboratoriumwerk en voor het toegang verlenen tot het fysisch geografisch laboratorium. Dr. Kim Cohen & dr. Tjalling de Haas bedank ik voor het delen van respectievelijk oudere boringen uit het Rijn-Maas delta moederbestand en de ARCHIS archeologische data van het Oude Rijngebied uit 2015.

Verder wil ik cultuurhistorisch onderzoeksbureau BAAC bv en mijn stagebegeleider aldaar drs. Chris Kalisvaart bedanken voor het mij toestaan nog verder te werken aan deze scriptie tijdens mijn stageperiode bij BAAC.

Voorts wil ik alle landeigenaren op wier percelen wij veldwerk uit mochten richten hartelijk bedanken voor het toegang verlenen tot en uitvoeren van veldwerk op hun land. Zonder hun toestemming, medewerking en gastvrije ontvangst was het onderzoek in deze scriptie niet mogelijk geweest. Kaspar Sonnemans, Pascal Born, Paul Veldhuijzen, Joep Storms, Tim Winkels, William McMahon, Bas Knaake, Jasper Candel, Steven Weisscher en Marcio Boechat Albernaz dank voor het helpen tijdens het boorveldwerk voor mijn en Lonneke Roelofs' scripties. Lonneke, heel erg bedankt voor de goede samenwerking tijdens het veld- en labwerk, voor onze nuttige discussies over de ontwikkeling van de Oude Rijn en voor je steun en vriendschap wanneer het wat stroever ging met mijn scriptie.

Daarnaast wil ik alle medestudenten in het Vening Meineszgebouw bedanken voor de soms zeer welkome afleiding tijdens lunch- en koffiepauzes, jullie hebben me daarmee erg geholpen. All Ei saa peittää members, thank you for our already three years long friendship, which only deepened since our mutual time at UCC. You really helped me a lot at specific moments during my thesis. Hetzelfde geldt uiteraard voor al mijn (studie)vrienden uit Utrecht. Dank voor de leuke momenten die we deelden tijdens mijn scriptieonderzoek!

Paul, ik wil jou iets uitgebreider bedanken. Vanuit het diepst van mijn hart dankjewel voor je steun tijdens het schrijven van mijn scriptie. Ik denk dat ik het er zonder jou een stuk slechter vanaf had gebracht. Niet alleen als ik even vastzat met het schrijven bood je altijd een luisterend oor, begrip en advies, maar juist en

vooral ook wat betreft andere voor mij moeilijke kwesties sleepte je me er doorheen door te luisteren en me vrijblijvend van advies te voorzien. Goed kunnen luisteren is een eigenschap die niet veel mensen gegeven is, koester dus alsjeblieft die eigenschap.

Mama en papa, heel erg bedankt voor jullie steun en vertrouwen. Ik zal jullie voor altijd dankbaar zijn voor de open en nieuwsgierige blik naar onze mooie wereld die jullie me hebben meegegeven.

Content

List of figures & tables

1. Introduction

Crevasses are well-known phenomena in river systems around the world. They form when a natural levee of a river is breached due to excess discharge during a flood (Van Dinter & Van Zijverden, 2010) (see figure 1). Sandy to silty clayey sediments are subsequently deposited as a complex of splays and bars in the flood basin. Crevasses have different sizes and shapes, depending on a range of boundary conditions (*e.g.* river system size, discharge, sediment supply, etc.).

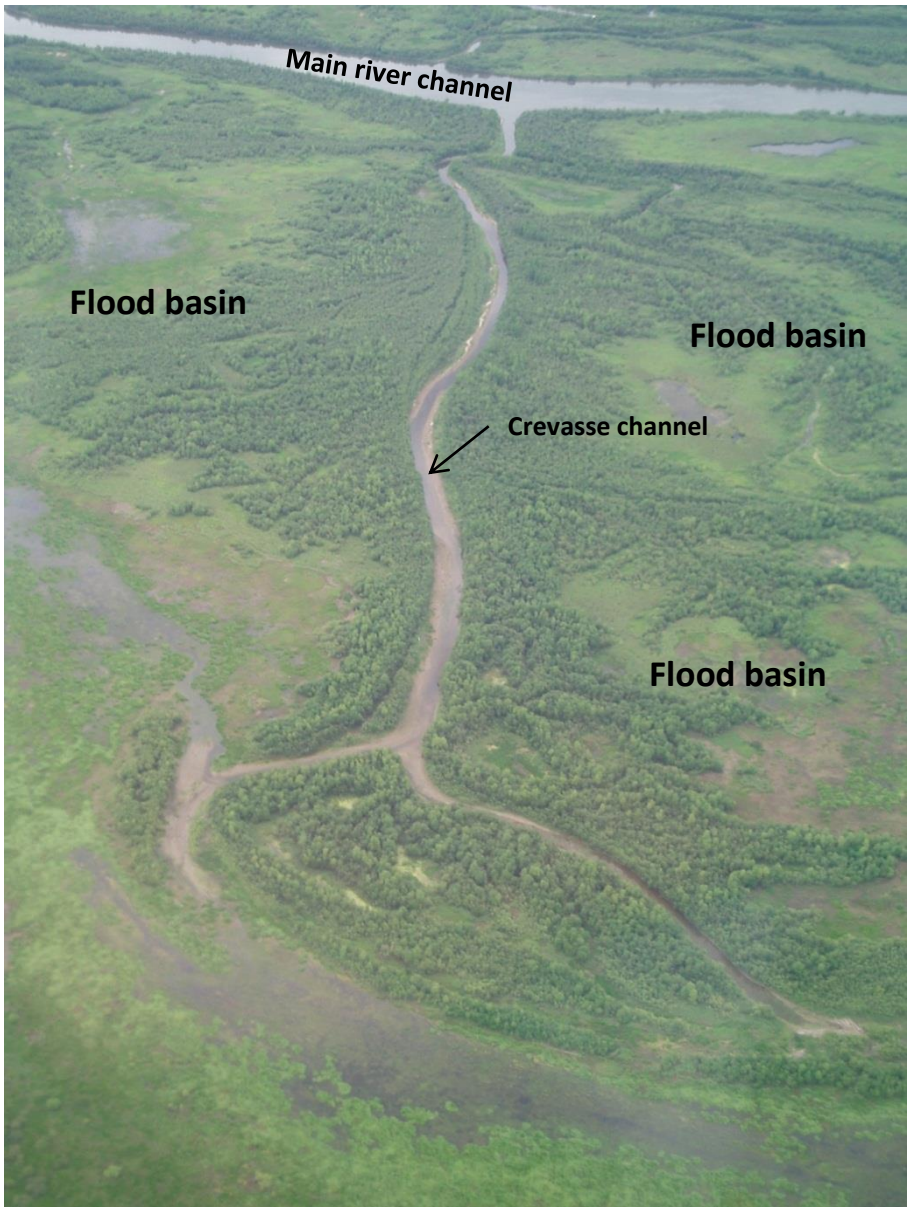

Figure 1: Active crevasse of the Saskatchewan river, Canada (photo by Maarten Kleinhans).

1.1 Problem definition

Research on crevasse formation, evolution and occurrence has predominantly focussed on single crevasse case-studies in purely fluvial settings. A general understanding of the effect of tidal processes on crevasses and their interplay with fluvial processes and autogenic feedback mechanisms, therefore, lacks.

The research aim of this thesis is therefore:

- *To understand the effects of fluvial and tidal boundary conditions, their interplay, and changes in initial flood basin conditions on crevasse evolution.*

To gain more knowledge about the formation and development of crevasses in the tidal-fluvial realm of a river system, this thesis focusses on the case study of the Old Rhine (‘*Oude Rijn’* in Dutch) with generally well-known changes in boundary conditions throughout its lifespan. By doing so, the effect of changes in both upstream (*e.g.* river discharge and flood frequency) and downstream (*e.g.* tidal range and backwater effect) boundary conditions on the spatio-temporal development of crevasses can be assessed.

The Old Rhine formed the main branch of the Rhine from its formation ca. 6500 cal. years BP and has since formed many crevasses in the surrounding peatlands. After ca. 3000 cal. years BP, it became gradually abandoned in favour of the new *Nederrijn* and *Waal* distributaries (Berendsen & Stouthamer, 2000; De Haas *et al*., 2018a). The Old Rhine’s upstream and downstream boundary conditions as well as its palaeogeographic development have been reconstructed in the literature in the past two decades. Besides, its architectural elements (*e.g.* natural levees, final channel course, crevasses, etc.) are generally well-preserved in the present-day landscape and subsurface, since the Old Rhine’s channel belt was not incised and eroded by younger river systems because of its isolated location in (former) peatlands. This makes the Old Rhine a suitable case study to achieve the above-mentioned research aim of this thesis.

1.2 Relevance

Crevasses have a large potential to counter the negative effects of land loss due to sea level rise induced by global climate change in subsiding, and thus vulnerable, densely populated deltas around the world.

Shen et al. (2015) found that episodically deposited sediment bodies dominate the overbank deposits of all Holocene channel belts of the Mississippi River system. Breaching of the natural levee of these channel belts and consequent formation and development of a crevasse is much more common than gradual (continuous) sedimentation due to overtopping of the natural levees in the Mississippi delta.

Subsequently, a recent study by Esposito et al. (2017) explored the potential of crevasse splay formation in the delta plains of the Mississippi to counter the negative effects of the combination of high rates of wetland loss and eustatic sea level rise. They concluded that sediment diversions (*e.g.* in the form of crevasse splays) in currently still vegetated settings have the largest potential to mitigate land loss due to sea level rise.

The two above-described studies in the Mississippi delta highlight the importance of episodic overbank deposition. Therefore, a better understanding of crevasse formation and development dynamics in the fluvial-tidal realm, will aid in answering questions related to sedimentation processes in subsiding deltas. Consequently, it will improve the possibilities for sustainable management (*e.g.* by natural land-building projects) of such large-scale delta systems.

Furthermore, from the first half of the 1st up until the 3rd century CE the Old Rhine formed the northern border of the Roman Empire. The various fortifications along its southern banks are known as the *limes* and stretched from the North Sea coast near Katwijk well into present-day Germany. Van Dinter (2013) hypothesized that the locations of the Roman fortifications along the Old Rhine were chosen based on the location where crevasse channels connected to the main Old Rhine branch, to guard these potentially dangerous transport routes from the lands north of the border. The reconstruction of the spatio-temporal crevasse evolution in this thesis will aid in further testing this hypothesis.

1.3 Approach

The aim of this study is to understand effects of boundary conditions, their interplay and the changes in initial flood basin conditions on the evolution of crevasses. Therefore, different types of data and recent insights into the Old Rhine system have to be combined in a coherent analysis.

To achieve the research aim:

1. The chronology of the crevasses will be reconstructed.

2. First, the chronology will be linked to changes in boundary conditions of the Old Rhine.

3. Second, the chronology will be linked to changes in the flood basin configuration of the Old Rhine.

For ***1*** Borehole data, archaeological data, recent palaeogeographic reconstructions and literature will be used to assess the chronology and phasing of the crevasses.

For 2, changes in downstream and upstream boundary conditions will be inferred from literature. Knowledge about mechanisms affecting crevasse evolution from the literature will be summarized and later in the discussion compared to the results found in this thesis.

For 3, palaeogeographic reconstructions of the Old Rhine will be used in conjunction with insights from the literature into the effects of the initial flood basin configuration on crevasses to assess the effect of changes in flood basin configuration on the crevasses in the fluvial-tidal realm of the Old Rhine.

2. Literature review

This literature review consists of two parts. In the first part crevasses will be discussed in relation to other fluvial geomorphologic features in lowland delta settings. Based on the knowledge gap inferred from the overview of crevasse literature, hypotheses about the formation and evolution of crevasses along the Old Rhine will be formulated. In the second part the Holocene evolution of the Old Rhine and the changes in its boundary conditions that are known from the literature are described.

2.1 Geomorphological elements in lowland river systems

River systems are natural alluvial complexes of single or interconnected waterways and associated landforms. In the lowland, downstream reaches of river systems, with generally small gradients, large-scale deltas can be formed due to sediment deposition when the river flows out into a lake or sea (*e.g.* Nichols, 2009; Stouthamer *et al*., 2015). Both in delta and valley settings they consist of diverse geomorphological features. The river system can be severely affected by tides and other marine processes up to a certain distance from its mouth. Within this tidal-fluvial realm the landforms associated with lowland river systems are thus affected by fluvial processes, marine processes and their interplay.

Figure 2 shows a facies model for meandering rivers in the Rhine-Meuse delta, adopted from Gouw & Erkens (2007). A broad-brush distinction can be made between the alluvial ridge and the flood basin of a meandering river.

The alluvial ridge consists of channel belt deposits and the discharge conveying channel. Channel belt deposits comprise channel lag and natural levee sediments. The former consist of coarse sand and gravel in the deepest parts of the channel and fining upwards point bar deposits in the inner meander bends. In the case of an abandoned channel, the residual channel fill consists of peats and organic rich fine-grained deposits. The point bar deposits can be overlain by scroll, chute, and tail bars.

The natural levee alongside the river channel on its banks comprises a sloping landform consisting of clay, silt and fine sand which are deposited when sediment is transported out of the channel and subsequently deposited in the vicinity of this river channel (Roelofs, 2019). Depending on the river system size, the dimensions of the natural levees vary accordingly (to a maximum of ca. 2 m in height and ca. 1 kilometre in extent). The transition from natural levee to flood basin is generally gradual.

The flood basin can consist of organic-clastic deposits and peats. Clastic deposits become progressively more fine-grained at increasing distance from the channel belt. Peatlands may develop in areas where the groundwater level is consistently high.

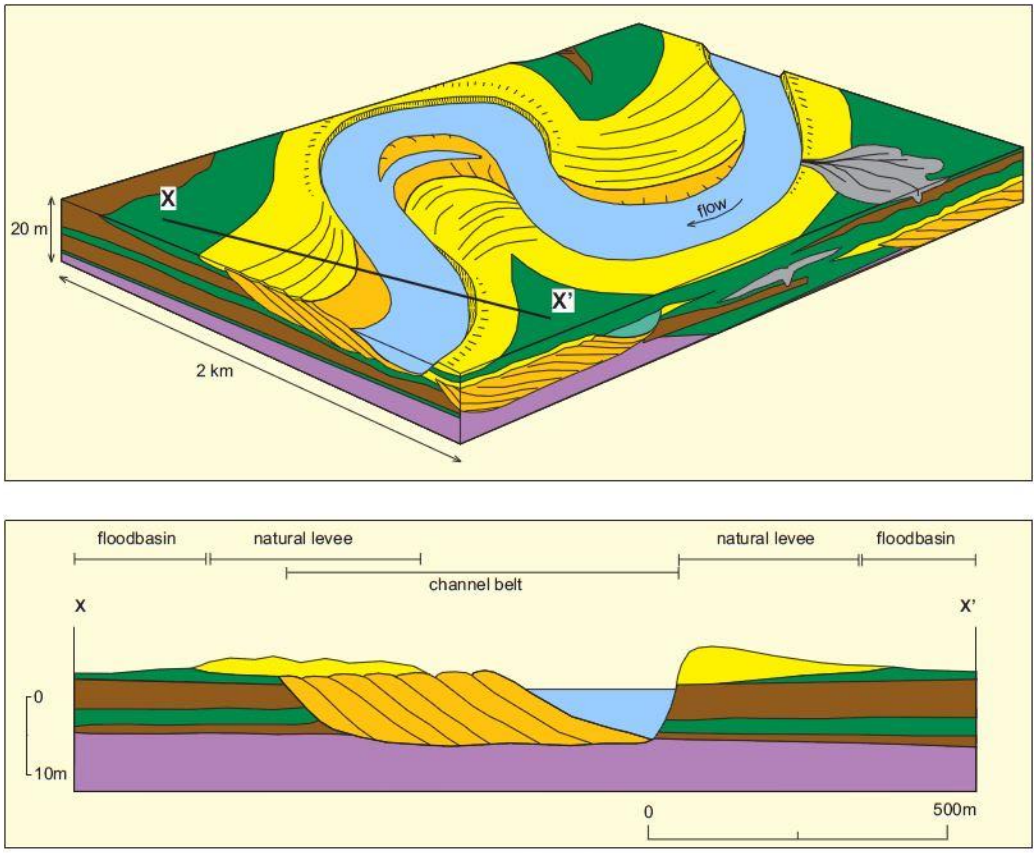

Figure 2: Schematic block diagram and cross-section of lowland meandering river facies. The legend shows to which lithostratigraphic units the Holocene fluvial deposits of the Old Rhine system belong; this scheme is used to classify the different facies encountered in the Results chapter (Chapter 4) too. Adapted from Gouw & Erkens (2007, figure 3).

Crevasses are peculiar features in the channel-flood basin continuum of river systems, as they are part of the natural levee deposits and of the flood basins. An unequivocal definition of crevasses used in the literature does not exist. In this study crevasses are defined as:

a channel or a network of channels and associated levee and bar deposits in the flood basin which is connected to a river system through a breach in the natural levee of the river system, which discharges water discontinuously.

They consist of overbank channel complexes branching off the main river channel into the flood basin (see figure 3), which form when the natural levee of the main river is breached under (more than) fullbank discharge conditions (Allen, 1965; Smith *et al*., 1989; Slingerland & Smith, 1998). After initial levee breach, a portion of the flow and sediment load is redirected into the flood basin adjacent to the natural levee, and sediment is deposited in the form of a splay with a dendritic pattern of interconnected channels (Smith *et al*., 1989; Farrell, 2001; Stouthamer, 2001b). Consequently, a crevasse may either *i)* 'heal', *i.e.* become inactive already within a relatively short time after initialization (which is typically a few years) and fill in; *ii)* develop into a single main feeder channel from the interconnected smaller channels close to the levee breach, which progradates into the flood basin and forms crevasse natural levees during overbank deposition (this is sometimes called a partial-avulsion in the literature, and these crevasses might be active for decades or even centuries); *iii)* take over the entire discharge of the main river channel when its course is more favourable than the original river course, after which the channel belt downstream of the crevasse breach location becomes increasingly inactive and eventually abandoned. This process is known as avulsion (Slingerland & Smith, 2004). Extensive crevasses have a large potential to transform large areas of the distal parts of flood basins by channel progradation and deposition of relatively coarse suspended sediment.

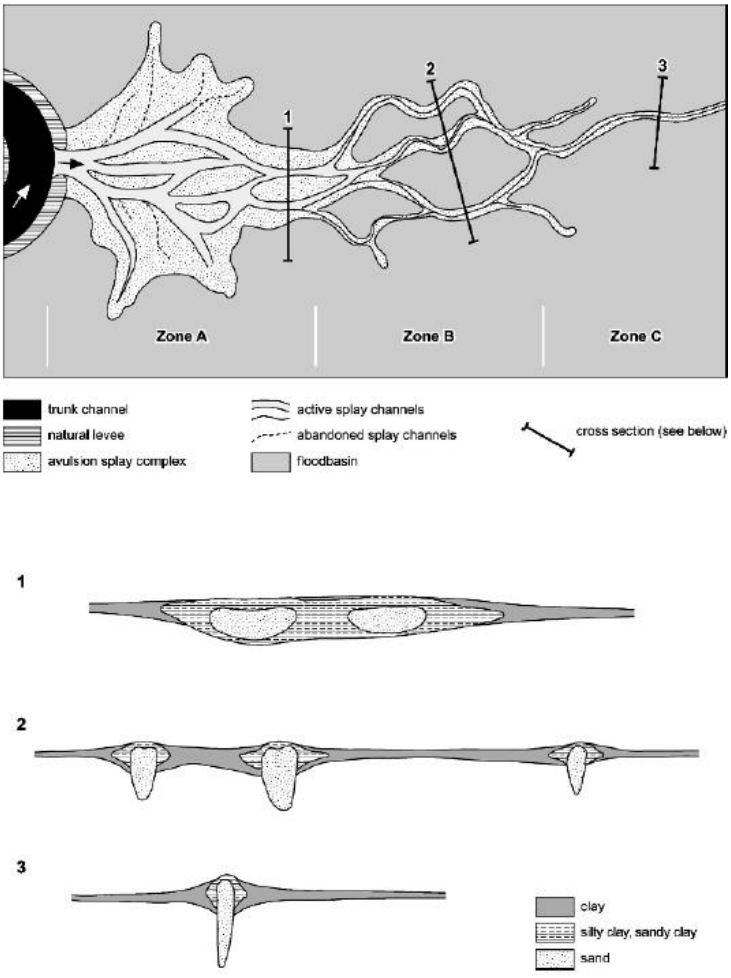

Figure 3: Schematic planform view and cross-sections after abandonment of the Schoonrewoerd crevasse. Note the exaggeration of the vertical axes of the cross-sections. Adapted from Makaske *et al*. (2007, figure 9)

2.2 Formation and evolution of crevasse splay complexes

Crevasses - active, well preserved or partly preserved in the geological record - have been studied by researchers from diverse backgrounds.

Processes and sedimentological and geomorphological characteristics of crevasses have been studied in geomorphology by means of numerical modelling studies to infer processes affecting initial formation and development (*e.g.* Slingerland & Smith, 1998; Hajek & Wolinsky, 2012; Millard *et al*., 2017; Nienhuis *et al*., 2018), and in geology by studying crevasse facies in outcropping geological formations, doing borehole surveys and by assessment of (time-series of) aerial imagery to reconstruct their development (*e.g.* Stouthamer, 2001b; Makaske *et al*., 2007; Van Dinter & Van Zijverden, 2010; Toonen *et al*., 2016; Burns *et al*., 2017; Gulliford *et al*., 2017). Still, relatively little is known about the geomorphological and sedimentary development of crevasses on decadal and centennial scales. This is especially important to understand the potential of a crevasse to i) develop into full avulsion, having a significant impact on the evolution of the landscape and hydrodynamics on a delta-scale; and ii) provide sediments and thus build out new land in low-lying flood basins.

There are three phases during crevasse development: the long-term set-up leading to favourable conditions for crevasse formation; the short-term trigger that leads to crevasse formation, and consequently the maturation of the crevasse. Initial conditions that can affect these phases are for example the flood basin configuration, the composition of the substrate, and boundary conditions.

First, the three above-mentioned phases will be described shortly. Thereafter follows an overview of the effect of initial conditions during these phases. It is important to distinguish between the three phases because changes in boundary condition have a different effect on each of them on different time-scales. Finally, a knowledge gap is identified.

2.2.1 Phases of crevasse development

Long-term setup

Slingerland and Smith (2004), after Jones and Schumm (1999), determined that the conditions required for river avulsion (here taken to equate crevasse formation) can be divided in two categories: a long-term setup during which the conditions for successful formation of a crevasse progressively increase (or decrease), and a short-term trigger of crevasse formation, the initial natural levee breach. Many researchers consider the ratio of the natural levee slope perpendicular to the channel to the downstream main river channel slope to be most important for determining whether a crevasse channel might successfully progradate (eventually leading to an avulsion) (Slingerland and Smith, 1998; 2004; Ethridge *et al*., 1999; Makaske, 2001; Törnqvist & Bridge, 2002; Millard *et al*., 2017). A high slope from the channel belt to the flood basin thus promotes crevasse formation and consequently crevasse enlargement. Hence, high channel bed and natural levee aggradation rates increase the chance of successful crevasse formation. Subsidence and tectonics can raise or lower flood basins and river channels and thus also affect energy and transport gradients (Kleinhans *et al*., 2013).

Short-term crevasse trigger

The short-term crevasse trigger is an event that initiates crevasse formation via a natural levee breach. Such events are mostly (extreme) flood events but can also include debris dams, beaver dams, ice or log jams, vegetative blockages and bank failures (Slingerland & Smith, 2004). The local river bank, the natural levee, and the flood basin substrate in the direct vicinity of the natural levee are eroded strongly by high-velocity flows through the natural levee breach. The time-scale of crevasse formation typically comprises several hours to a few weeks at most (Toonen *et al*., 2016). Slingerland & Smith (2004) further note that initial crevasse formation commonly occurs at the outer banks of meander bends. Here the confining natural levees are generally narrow (see figure 2), flow velocities are relatively high and floods strike the natural levee at high angles. Furthermore, weak spots in the channel banks, such as buried sand bodies of former channel belts, are more prone to initial levee breach and thus more potential locations for crevasse formation (Smith *et al*., 1998; Slingerland & Smith, 2004).

Maturation

The natural levee height and the flood regime of the main river system are important for the maturation of a crevasse. Increased alluviation of the main river channel leads to increased overbank flooding and hence increased natural levee sedimentation (Slingerland & Smith, 2004). Higher natural levees increase the water-surface slope and thus the energy and transport gradients, which increase the crevasse channel progradation potential. Likewise, frequently recurring flood events promote crevasse development from an initial lobate splay system to an extensive single-channel crevasse (Knigthon & Nanson, 1993; Slingerland & Smith, 2004). It has not been determined yet, however, what the threshold frequency of flood events of a certain magnitude is for maintaining a crevasse in dynamic equilibrium or progradation.

The final extent and shape of a crevasse depends on the shape and dimension of the crevasse throat (*i.e.* the beginning of the crevasse channel at the natural levee breach) and the suspended sediment. The crevasse throat controls the distribution of water and sediment to the crevasse (Toonen *et al*., 2016). The crevasse lip height, which is the height of the crevasse throat bottom relative to the main channel water depth, determines how much suspended sediment load a crevasse channel receives during a flood, especially so for the finer grained suspended sediments (Slingerland & Smith, 1998, 2004; Kleinhans *et al*., 2013). Hence, it affects the likelihood that a crevasse channel enlarges and progradates. Millard *et al*. (2017) found that a large supply of relatively coarse suspended sediment (*i.e.* coarse silt to fine sand in sand-bed rivers) is a prerequisite for extensive crevasse progradation. They based this on insights from the combination of observations and measurements of real-world river systems (*i.e.* the Columbia and Saskatchewan in Canada and the Sandover River in Australia) with modelling studies.

Based on the above, it is expected that an increase in the flood frequency of a river system enhances crevasse maturation and thus leads to longer and more numerous crevasses, since floods not only promote progradation but also alter the shape and dimensions of the crevasse throat (*e.g.* by widening or deepening). Besides, the presence of tidal flows and a tide-induced backwater effect could affect the crevasse throat by regular flushing, which would prevent it from rapid filling in. Consequently, tides and floods have comparable effects on the crevasse throat, but the effects of the tides have a smaller magnitude, and act on a smaller (albeit more regular) time-scale (*i.e.* daily or twice daily). Hence, the presence of tides in a river system could increase the number of crevasse being active simultaneously.

Smith et al. (1989) introduced a conceptual model of three intergradational stages of crevasse development, based on research in the Saskatchewan River system. This river has no tidal influence and hence differs from the Old Rhine. Therefore, the crevasses of the Saskatchewan are expected to differ in appearance and formation from the crevasses of the Old Rhine. The conceptual model comprises three stages of crevasse development in space (both in planform shape as well channel configuration) and time after initial formation, roughly corresponding to the three possible development pathways in figure 3 and figure 4. Stage 1 comprises the deposition of lobate splays by multiple small-scale channels directly next to the natural levee of the main river. Consequently, the multiple smaller channels develop into fewer relatively stable channels, which bifurcate and re-join in the more distal parts of the flood basin and deposit more elongated sand bodies (*i.e.* Stage 2). Ultimately, from these channels a single dominant channel might develop which becomes the single active crevasse channel, with small-scale natural levees along its course (*i.e.* Stage 3). Especially in the proximal parts of the flood basin, directly adjacent to the channel belt, the sedimentary facies of older stages (*e.g.* lobate splay deposits) can be partly preserved when the crevasse develops into a stage 2 or 3 crevasse. The latter stage is sometimes hard to distinguish from a full avulsion without sufficient knowledge about the surrounding channel belt configuration and stratigraphy. The model was later adapted and slightly modified by Farrell (2001) and geomorphologists in the Dutch Rhine-Meuse delta (*e.g.* Stouthamer, 2001b; Stouthamer *et al*., 2015; Makaske *et al*., 2007), and in other lowland deltaic settings (*e.g.* Toonen *et al*., 2016 who proposed a new conceptual model describing the general characteristics, sedimentary products and controls and feedback mechanisms for the different stages).

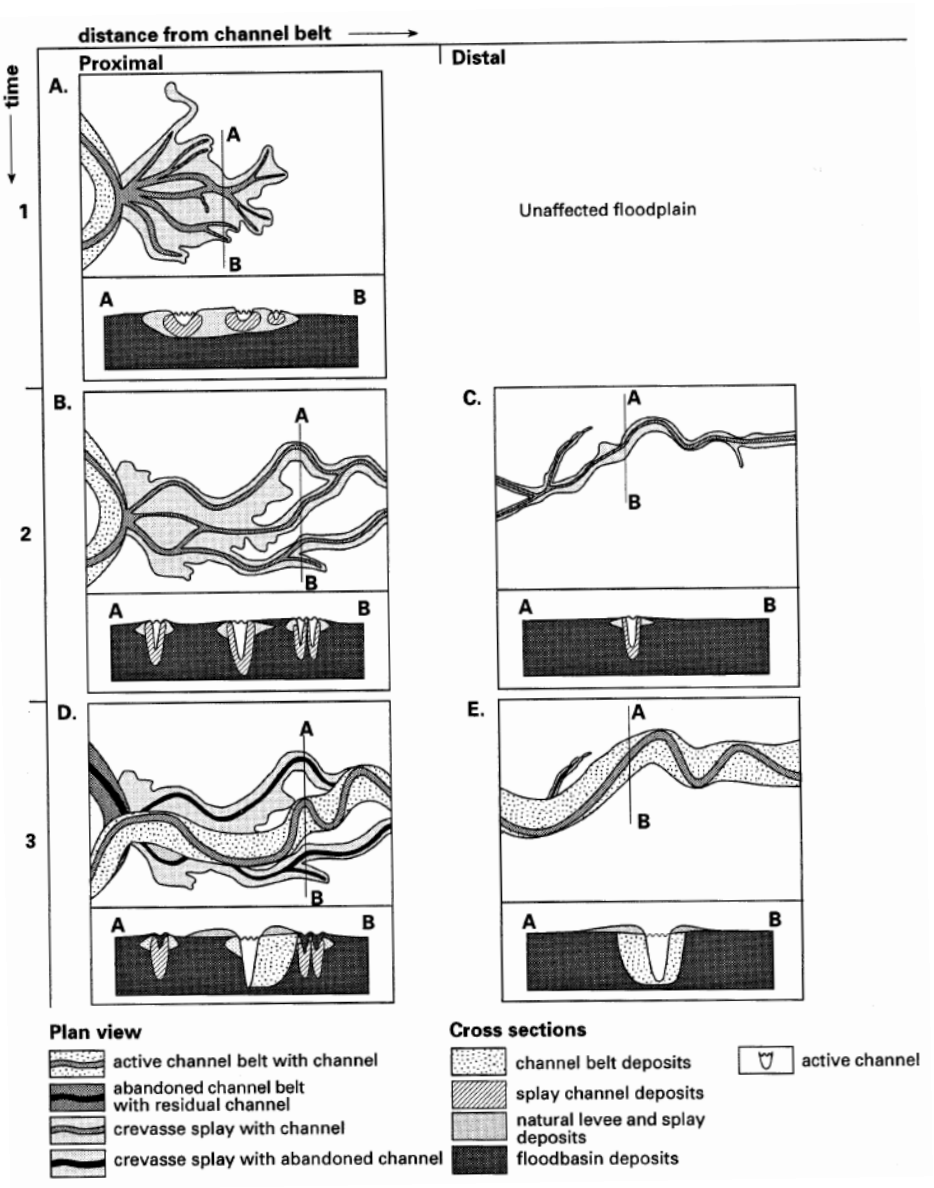

Figure 4: Three stages of crevasse development, adapted from Stouthamer (2001b, figure 13) after Smith *et al*. (1989, 1998) and Farrell (2001).

2.2.2 The effect of initial conditions

The initial conditions under which crevasses are formed affect the phases of crevasse development. They mostly concern the environmental setting in which a (lowland) river system is situated, and how this setting evolves. Especially the flood basin configuration of a river system is important for the development of crevasses.

Flood basin relief

Slingerland & Smith (2004) note that a wide unobstructed flood basin, which is able to drain down-valley, is needed to maintain crevasse flow, since it permits water surface slopes from the main river channel to the flood basin to remain high during a flood event. Besides, an open flood basin promotes crevasse maturation (Berendsen, 1982; Toonen *et al*., 2016). If a flood basin is closed, sediment is not transported effectively downstream to the distal reaches of the basin, since ponding, infilling of the crevasse channel, and deposition in the proximal parts of the basin is stimulated.

Pre-existing flood basin channels such as abandoned channel belts of older river systems can be intercepted by progradating crevasses and, once annexed, can enlarge considerably (Slingerland and Smith, 2004). This phenomenon is termed 'avulsion by annexation' by Slingerland & Smith (2004). Occupation of abandoned channels in the flood basin, potentially leading to river avulsion was identified for a minimum of 24 cases in the Rhine-Meuse delta by Stouthamer (2001a).

Alternatively, it is possible that pre-existing (abandoned) channel belts with their natural levees form an obstruction for a progradating crevasse. If the orientation of the channel belt is perpendicular to the direction of crevasse progradation, this can severely affect the subsequent direction of progradation or even prevent progradation at all (Stouthamer, 2001b; Slingerland & Smith, 2004; Toonen *et al*., 2016). Thus, the presence and orientation of pre-existing channel or depressions in the flood basin can have a promoting or limiting effect on crevasse progradation and maturation. Hence, when peat drainage channels with a favourable course direction are present in the flood basin it is expected that more extensive crevasses form.

Subsurface composition

The composition of the flood basin subsurface layers influences the development of crevasses as well. The erosion resistivity of the substrate, particularly in the more distal parts of the flood basin, affects crevasse progradation, dimensions, and lateral movement (Makaske *et al*., 2007; Toonen *et al*., 2016; Pierik *et al*., 2018). Compressed peat layers are more erosion-resistant than for example aeolian cover sands and thus impede quick crevasse progradation, and hamper lateral channel migration (*e.g.* Makaske *et al*., 2007; Pierik *et al*., 2018). Crevasse channels in a thick peat substrate have therefore generally lower width-depth ratios than crevasse channels in other more easily erodible substrates (Makaske *et al*., 2007).

Vegetation

The last factor that affects crevasse maturation is vegetation. Vegetation growth on the banks of a crevasse channel strengthens its banks and levees by making them more erosion-resistant and thus stabilizes the channel (Toonen *et al*., 2016). Channel stabilization causes flow concentration, which in turn increases the crevasse channel's stream power, resulting in incision. It thereby also promotes natural levee formation (Toonen *et al*., 2016). The vegetation cover of the flood basin itself can have both negative as well as positive

effects on crevasse expansion (Nienhuis *et al*., 2018). As mentioned before, vegetation can reduce erosion in the flood basin as it consolidates sediments whilst also enhancing sediment trapping (Esposito *et al*., 2017; Nienhuis *et al*., 2018). Therefore, it can have seemingly contradictory effects on crevasse expansion: it can hamper crevasse channel progradation whilst simultaneously stabilizing its course (which enhances crevasse development). Nienhuis *et al*. (2018) inferred from their morphodynamic model simulation of crevasse development that intermediate vegetation strengths lead to the highest rates of net sedimentation of crevasses in flood basin.

Based on the above-described flood basin configuration factors, it can be stated that the initial relief, subsurface composition and vegetation have a large influence on the maturation of crevasses and their potential extent. The presence of pre-existing channels with a favourable course relative to the crevasse's can accelerate crevasse progradation. Likewise, with easily erodible subsurface layers throughout large areas of the flood basin which promote progradation, it is expected that longer crevasses are present and that the number of mature crevasses is higher. Vast areas of vegetation can initially hamper crevasse progradation, but in a later stage stabilize the crevasse's course and hence promote progradation.

2.2.3 Knowledge gap

The description of the processes and factors affecting crevasse formation and development in the previous two sections shows that already a lot of has research has been done into crevasse dynamics. However, crevasse dynamics have been mostly studied in fluvial environments and on a small scale only (*i.e.* focusing on the evolution of a single crevasse). The importance of tidal backwater effects on the effective energy gradient and their positive effect on the avulsion potential of new channels (*e.g.* crevasse channel) over old channels was already mentioned by Kleinhans *et al*. (2013). Model runs with large tides and strong tidal flows showed an increase in the number of crevasses that are formed, which remained open for a longer time, in a combined field and modelling study into the effects of changes in fluvial and tidal boundary conditions on natural levee morphology and evolution by Roelofs (2019). However, this observation has not been validated with evidence in the geological record of crevasses yet. Hence, the long-term effect of tidal processes and their interplay with fluvial processes on the dynamics of multiple crevasses in the tidal-fluvial realm of a river system should be studied. Besides, the impact of autogenic flood basin processes on more than a single crevasse have not been studied either. Therefore, the two main knowledge gaps are:

- The effects and combined effects of (changes in) tidal and fluvial boundary conditions on crevasse dynamics and morphology.
- The effect of autogenic or internal processes on crevasse development and morphology in the tidal-fluvial realm of a river system.

2.3 Hypotheses

From the overview in the previous section of the processes and factors affecting crevasse formation and development as well as the identified knowledge gap, the following hypotheses are proposed concerning the crevasses along the Old Rhine:

- Regular tidal flushing and tides-induced backwater-effects promote the formation and prolonged activity of crevasses and prevent (quick) crevasse-healing. An increase in the magnitude of the tidal wave and an increase in the (reach of) the tidal backwater effect lead to an increase in the absolute number of active crevasses.
- Periods with a relatively high frequency of extreme flood events enable proximal crevasse splays to develop into kilometres-long single-channel crevasses. Moreover, do they increase the amount of natural levee breaches within a major river system as a result of which the number of crevasses increases too.
- The flood basin configuration (*e.g.* relief, vegetation, subsurface compositions, and presence of (abandoned) channel belts) affects the (potential) course, extent and morphology of crevasses. Peat drainage channels in the flood basin could be intercepted by crevasses, accelerating progradation and significantly increasing the crevasse extent.

2.4 Setting and Old Rhine system history

In this section the development of the Old Rhine system will be summarized. First, the geographic setting of the Old Rhine within the geographic setting of the Rhine Meuse delta will be described. Thereafter follows a summary of the Early-Holocene inherited relief and conditions, complemented by a description of the Middle-to Late-Holocene Old Rhine system evolution and abandonment. Last, the changes in down- (offshore) and upstream (fluvial) boundary conditions of the Old Rhine system are discussed.

2.4.1 Geographical & geological setting

The well-preserved Old Rhine channel belt is located in the Western part of the present-day Dutch Rhine-Meuse delta, which extends for approximately 140 km from the Dutch-German border in the east (where the delta apex is located) to the beach-barrier North Sea coast in the west (Pierik *et al*., 2017) (see figure 5). The two main branches of the Rhine are now the Nederrijn and the Waal, which commence at a bifurcation close to the delta apex. Consequently, both branches bifurcate further in downstream direction, creating an interconnected network of distributaries, which eventually, together with the more southern located Meuse, flow into the North Sea via the Rhine-Meuse outlet just west of Rotterdam. The Old Rhine, like other now minor Rhine branches such as the Hollandse IJssel, is a former main branch which was abandoned due to upstream avulsions.

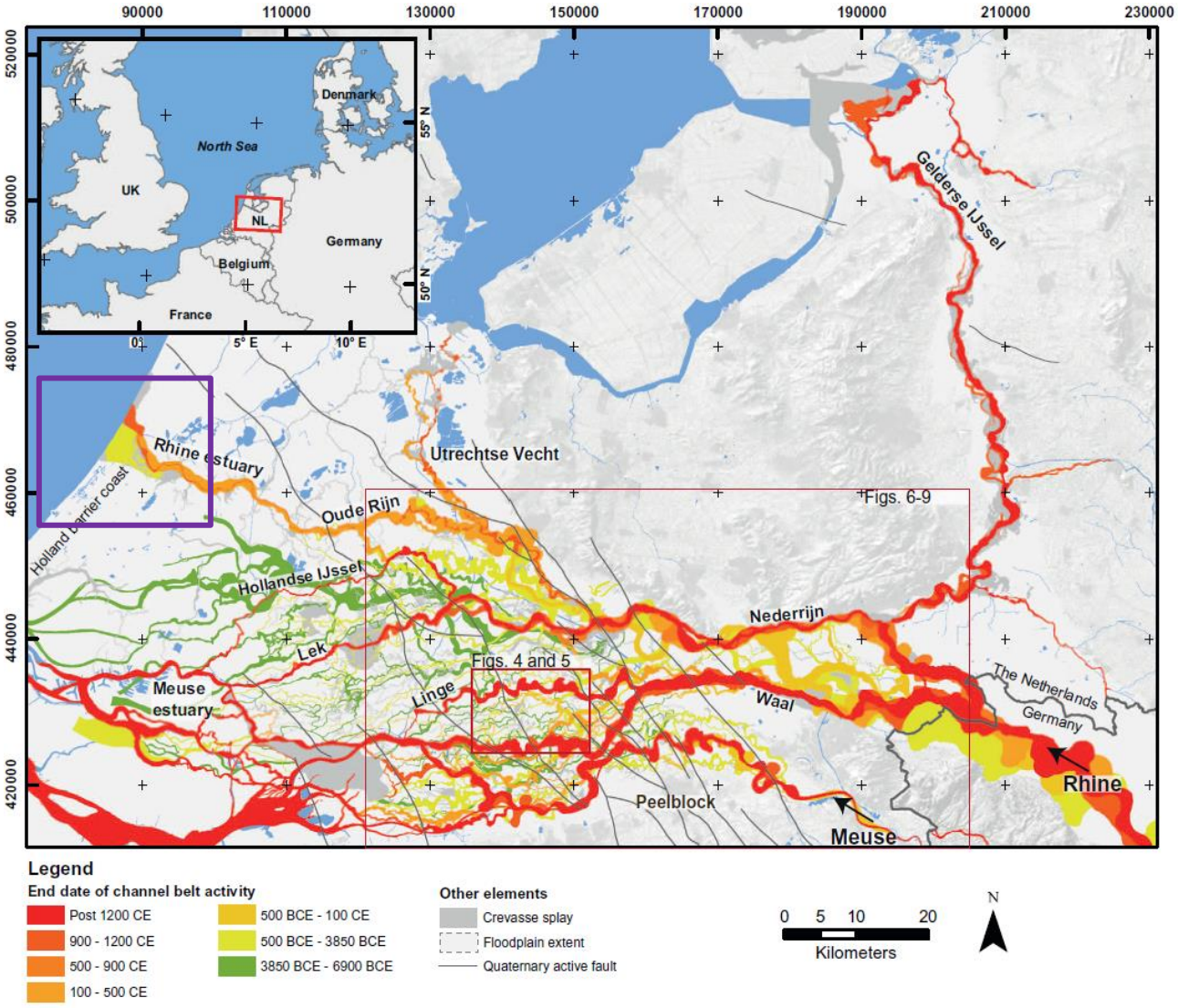

Figure 5: Location of the preserved Old Rhine channel belt (*i.e.* 'Oude Rijn' and 'Rhine estuary' in the map) within the Rhine-Meuse delta in the Netherlands. The purple quadrangle denotes the area of the palaeogeographic reconstructions in figures 6 and 7. Adopted from Pierik et al. (2017, figure 1).

The Old Rhine system is located between the city of Utrecht in the east and Katwijk aan Zee at the North Sea in the west. It traverses the Holocene coastal plain of the Western Netherlands which consists of barrier, peat, flood basin, and several channel belt deposits (see section 2.1) on top of a gently sloping Pleistocene substrate (Vos, 2015). The thickness of the Holocene deposits varies from ca. a few metres in the upstream parts to a maximum of ca. 20 metres near the coast (Pierik *et al*., 2017).

2.4.2 Early Holocene inherited relief & Old Rhine establishment

The Old Rhine was established between 7300 and 6100 cal. years BP after two successive avulsions of the Rhine river in northward direction (De Haas *et al*., 2018a) (figure 6). In the preceding period from 8500 till 7500 cal. years BP a substantial estuary was present in former Rhine-Meuse palaeovalley, which was inundated due to ongoing Holocene relative sea level rise, and which received most of the discharged water

of both the Meuse and Rhine (De Haas *et al*., 2018b; Hijma & Cohen, 2011; Vos, 2015). An infilling tidal back-barrier basin was present north of this Rhine-Meuse estuary, consisting of tidal flats and an established tidal channel network on top of early Holocene basal peats (Vos, 2015; De Haas *et al*., 2018a). Consequently, around 7300 cal. years BP a first avulsion caused a Rhine distributary to flow into this tidal back-barrier basin (Berendsen & Stouthamer, 2000; Hijma & Cohen, 2011; De Haas *et al*., 2018a). A second avulsion ca. 6500 cal. years BP initiated the formation of the Old Rhine river, which probably captured a former tidal channel belonging to the aforementioned tidal channel network (Vos, 2015; De Haas *et al*., 2018a). The formation phase of the Old Rhine estuary thereafter took place until ca. 5700 cal. years BP, whilst already around 6100 cal. years BP the Old Rhine had become the main Rhine branch in the Rhine-Meuse delta, discharging most of the Rhine river water (De Haas *et al*., 2018a).

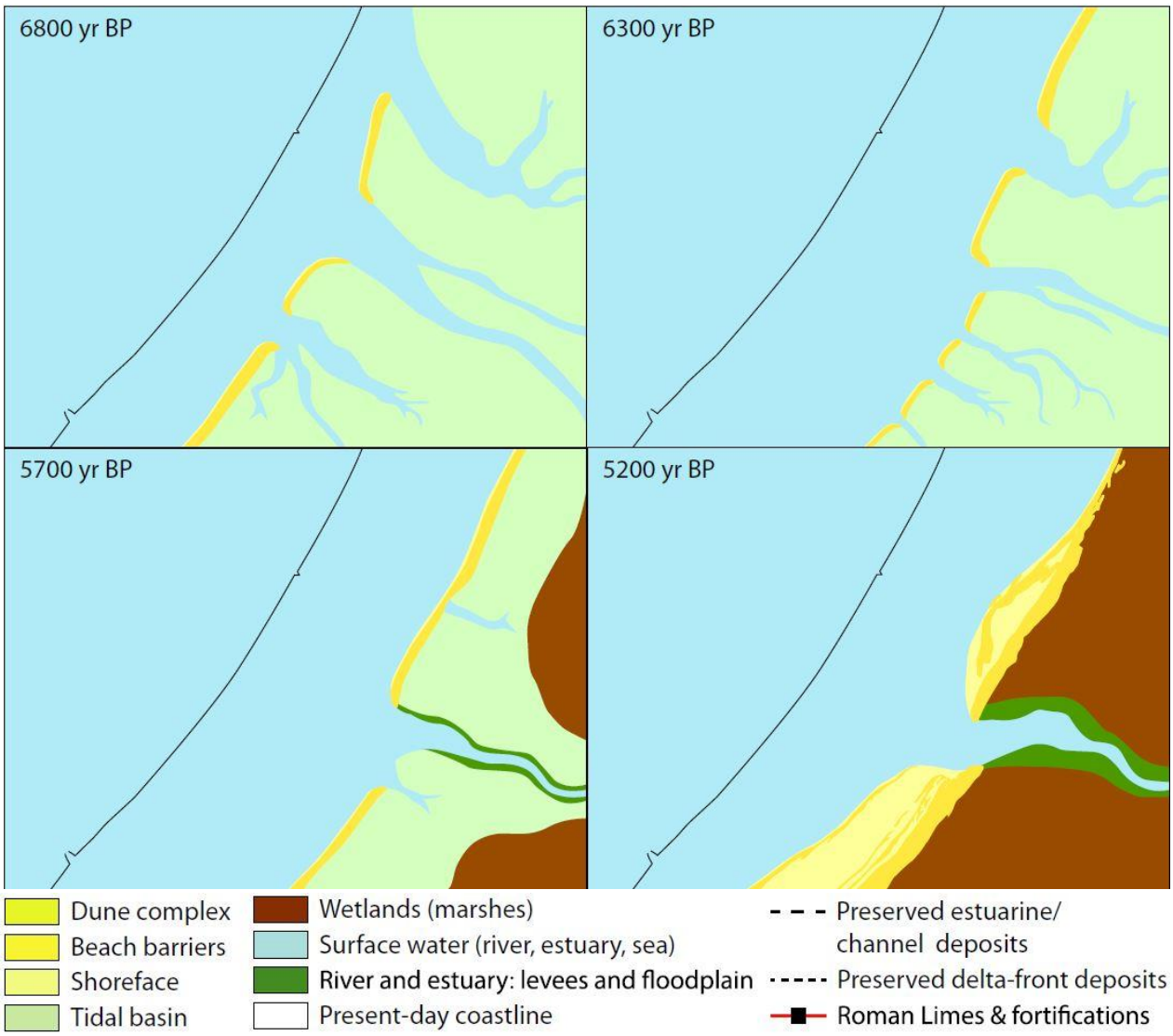

Figure 6: Palaeogeographic reconstructions of the Old Rhine estuary by De Haas et al. (2018a). North is up and all ages are in cal. years BP. The purple quadrangle in figure 5 denotes the area of the palaeogeographic reconstructions. Adopted from De Haas et al. (2018a, figure 10).

2.4.3 Middle to Late Holocene Old Rhine evolution and abandonment

Around 5700 cal. year BP an established river channel had formed, along which tidal-fluvial natural levees were developing (De Haas *et al*., 2018a) (figure 6). Simultaneously, the rate of relative sea level rise decreased and as a result fluvial and marine sedimentation was able to keep up with and at some point surpass the rate of creation of accommodation space. This caused silting up of most of the back-barrier basin and eventually to closure of most of its tidal inlets by merging beach barriers (Vos, 2015; De Haas *et al*., 2018b; Van Heteren *et al*., 2011). The combination of the lateral confinement of river flow (due to the development of tidal-fluvial natural levees) with the change in the distribution pattern from cross-shore to alongshore due to the closing off of the back-barrier basin, led to progressive peat development from the margins of the back-barrier basin in seaward direction due to increasingly freshwater conditions (Pons, 1992; Vos, 2015; De Haas *et al*., 2018a-b). Coastal progradation started as well, as new beach barriers were formed in seaward direction caused by the change in direction of marine sediment distribution (Vos, 2015; De Haas *et al*., 2018a).

From ca. 3800 cal. years BP onwards the course of the Old Rhine estuary started to shift in northwards direction (figure 7). An increasing amount of sediment was deposited at the beach barriers south and north of the estuary mouth, most prominently at the north flank. In the same period, a substantial spit had formed at the southern part of the estuary mouth, which closed off a part of this inlet. Therefore, the Old Rhine estuary was forced to move in northward direction (De Haas *et al*., 2018a). The dimensions and configuration of the estuary mouth, a broad and relatively deep single channel, didn't change significantly until ca. 3000 cal. years BP though (Wilbers, *pers. comm.*, 2019).

Also around 3800 cal. years BP, extensive peatlands had been formed in the former back-barrier basin, comprising a varied landscape of peaty marshes, eutrophic fens and oligotrophic raised bogs (Pons, 1992; Vos, 2015; Erkens *et al*., 2016; Pierik *et al*., 2017; De Haas *et al*., 2018). The raised bogs had developed via a succession of eutrophic groundwater-fed woodland fens to mesotrophic sedge and reed mires to oligotrophic rain water-fed sphagnum bogs, which gradually increased in height (Van Dinter, 2013; De Haas, 2018a). Eventually they reached a height of ca. 2 – 4 m above storm surge sea levels and high tide, and are estimated to have been several kilometres in diameter (Van Dinter, 2013; Pierik *et al*., 2018). Drainage of stored rain water in the raised bog domes most likely occurred via (a complex of) shallow peat drainage channels (also called brooks or peat rivers) which discharged excessive water to nearby fluvial systems (*e.g.* the Old Rhine and the Vecht) (Van Dinter *et al*., 2013). The raised bog domes themselves served as watersheds between the (longer) peat drainage channels and are believed to have stabilized their courses (Pierik *et al*., 2017).

Besides, De Haas *et al*. (2018a) state that between 4000 to 3500 cal. years BP what they call 'perimarine' crevasse channels were formed up to 30 kilometres inland from the estuary mouth, due a tidal backwater effect-induced rise of river water, which they base on earlier work by Berendsen (1982) and Van Dinter (2013). The perimarine crevasse channels are thought to have been well-established around 3000 cal. years BP (Berendsen, 1982; De Haas *et al*., 2018a). The extensive kilometres-long crevasses are studied in this thesis.

Consecutive avulsions in the upstream parts of the Rhine-Meuse delta from ca. 2850 cal. years BP led to a decrease in discharge conveyed through the Old Rhine system (De Haas *et al*., 2018a) (figure 7). Gradually the Old Rhine lost its role as main Rhine distributary in favour of other branches. The estuary mouth

developed into an increasingly sinuous ('swan-neck') shape as the alongshore sediment transport (by the northward-directed littoral drift) became progressively more dominant relative to the river discharge. As a result, tidal influence in the estuary decreased (section 2.5.1). River floods and storm surges, however, continued to transport sediments into the Old Rhine system (Van Dinter *et al*., 2017; De Haas *et al*., 2018a; section 2.5.1). Eventually the Old Rhine was dammed in 1122 CE (*i.e.* 828 cal. years BP) at the town of Wijk bij Duurstede, which ended the natural fluvial activity in this river system that was already almost completely abandoned (Van Dinter *et al*., 2017; De Haas *et al*., 2018a) (see section 2.5.1). The marine connection of the Old Rhine estuary (*i.e.* now tidal inlet) ended ca. 1300 CE (*i.e.* 700 cal. years BP) as the sea entrance was filled-up completely by the alongshore sediment transport in the absence of river flow which formerly enhanced ebb flows, flushing the entrance and keeping it open (De Haas *et al*., 2018a-b).

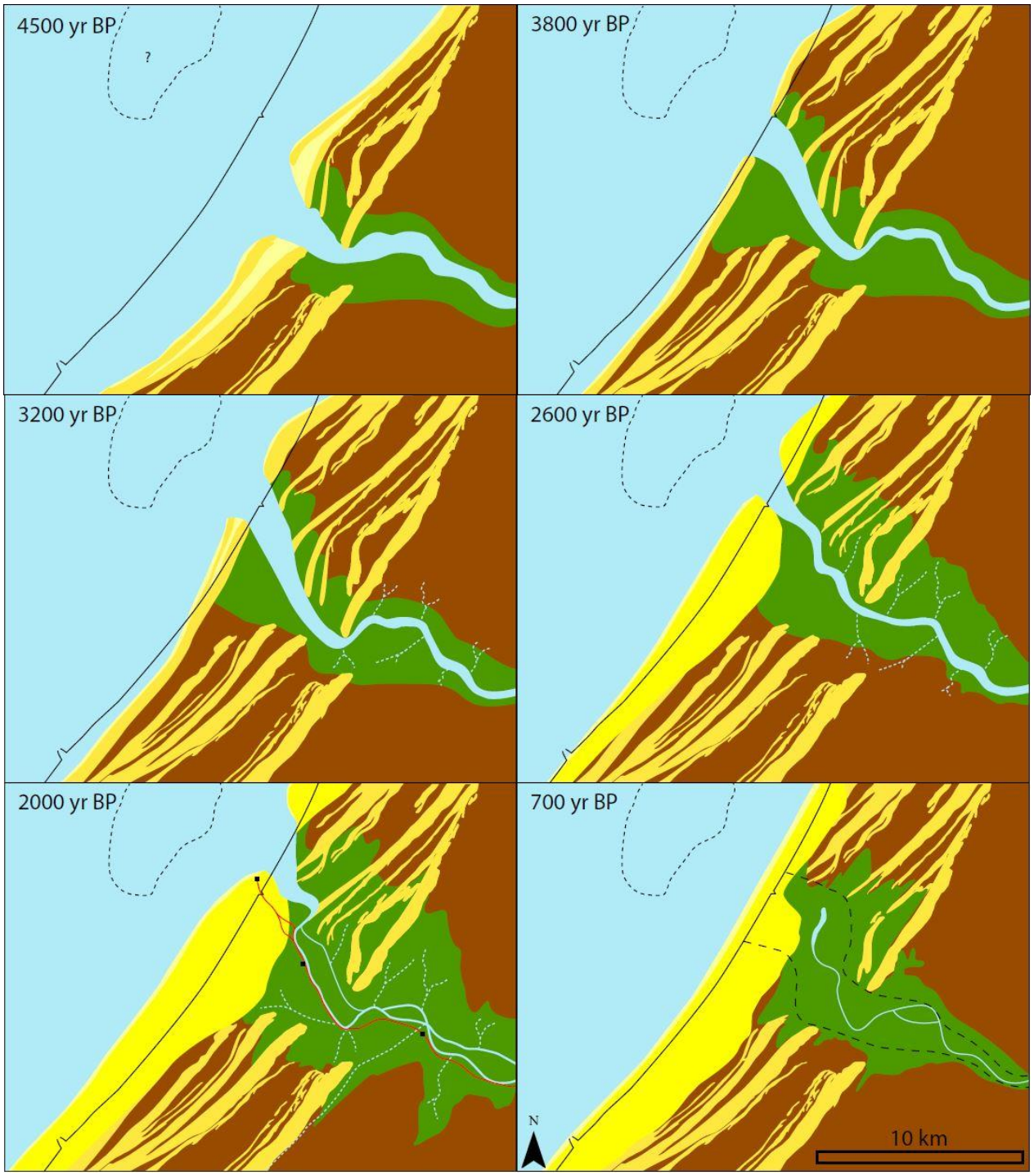

Figure 7: Palaeogeographic reconstructions of the Old Rhine estuary by De Haas et al. (2018a). Legend is the same as in figure 6 and all ages are in cal. years BP. The purple quadrangle in figure 5 denotes the area of the palaeogeographic reconstructions. Adopted from De Haas et al. (2018a, figure 10).

2.5 Boundary conditions of the Old Rhine system

In this section the most important reconstructed boundary conditions and changes therein throughout the Old Rhine system's lifespan are described. Changes in upstream (*i.e.* fluvial) and downstream (*i.e.* offshore) boundary conditions and the palaeogeographic reconstruction of the Old Rhine system, in figure 8. First, the changes in relative mean sea level (at the approximate location of the Old Rhine estuary mouth), mean significant wave height, tidal range, and storm surge frequency are described. Thereafter the changes in discharge, flood frequency, and sediment supply are discussed.

2.5.1 Offshore boundary conditions

Relative sea level rise

Relative sea level at the Western –Netherlands coast rose ca. 120 m since the Last Glacial Maximum (ca. 20,000 cal. years BP), due to the combined effects of eustatic sea level rise on one hand and glacio-isostatic subsidence of the Netherlands both caused by deglaciation of the Northern Hemisphere glaciers (see figure 8). The rate of relative sea level rise started to decrease severely from 8500 cal. years BP onwards (Hijma *et al*., 2010). Around 6000 cal. years BP relative sea level rise had decelerated so much that fluvial and marine sedimentation exceeded the creation of accommodation space, which led to coastal progradation and beach barrier formation (Beets & Van der Spek, 2000). The rate of relative sea level rise slowed down from ca. 5.5 mm/year around 7000 cal. years BP until ca. 0.5 mm/year around 2000 cal. years BP (Hijma & Cohen, 2010). The rate remained more or less constant for the last 2000 years.

Mean significant wave height & longshore drift

The mean significant wave height at Old Rhine estuary mouth increased from ca. 0.8 to ca. 0.9 m during the lifespan of the Old Rhine (De Haas *et al*., 2018a). The current mean significant wave height might be ca. 0.1 to 0.5 m higher than the mean significant wave height during the Middle-Holocene due to a larger depth of the North Sea as a result of relative sea level rise (Van der Molen & De Swart, 2001a; De Haas *et al*., 2018a) and shoreface-steepening due to wave-induced erosion of the sea bed (Van Heteren *et al*., 2011). A wave-induced longshore current and associated littoral sediment transport has been mainly south-west to north-east-directed along the Western-Netherlands coast since approximately 7500 to 6500 cal. years BP due to prevailing westerly winds (Hijma *et al*., 2010; De Haas *et al*., 2018a; Van der Molen & De Swart 2001a).

Tidal range

The tidal range at the location of the Old Rhine estuary mouth during the Holocene was microtidal, and remained approximately 1.5 m from 6500 cal. years BP until the Old Rhine system was abandoned ca. 1000 cal. years BP (Van der Molen & De Swart, 2001b; Hijma & Cohen, 2011; De Haas *et al*., 2018a). The upstream reach of the influence of tidal processes in the Old Rhine system changed throughout its lifespan due to two processes. Progradation of the Western-Netherlands coastline until ca. 3000-2000 cal. years BP, due to decelerating relative sea level rise (see above), caused the Old Rhine estuary mouth to move westwards too. The second process was the northward shift of the Old Rhine estuary mouth during ca. 3000 – 2000 cal. years BP, due to the fact that the northward littoral drift became relatively more important compared to the decreasing Old Rhine discharge (see section 2.5.2). The northward shift of the Old Rhine

estuary mouth led to an increasingly sinuous shape of the estuary (De Haas *et al*., 2018) which hampered upstream progradation of the tidal wave (Bodewes, 2014) and thus also decreased the reach of the tidal backwater-effect.

Storm surges

A record of (prehistoric) marine storm surges which occurred in the Old Rhine estuary has not yet been published. However, Sorrel et al. (2012) identified five Holocene storm periods of increased storminess in northern coastal Europe, based on sedimentary data from coastal coring locations in north-western Europe and marine coring sites in the North-Atlantic. These five stormy intervals were from 5800 to 5500, 4500 to 3950, 3300 to 2400, 1900 to 1050, and 600 to 250 cal. years BP (see figure 8).

2.5.2 Upstream boundary conditions

Old Rhine discharge & Rhine delta avulsion history

Since the Old Rhine river was established ca. 6500 cal. years BP it became the main Rhine branch in the Rhine Meuse delta (De Haas *et al*., 2018a). The mean annual discharge of the Old Rhine is assumed to have remained more or less constant - ca. 2000 m^3/s - from ca. 6100 until 2850 cal. years BP (Van Dinter *et al*., 2017; De Haas *et al*., 2018), see right-hand side of figure 8. The variation in total mean annual discharge of the Rhine river is approximated to have been less than 10 % (De Haas *et al*., 2018a), since the Rhine is assumed to have been mostly insensitive to intra-Holocene climate changes due to the size of its catchment (Erkens, 2009; Stouthamer *et al*., 2011).

After 2850 cal. years BP, upstream avulsions led to a gradual decrease in Rhine discharge conveyed to the Old Rhine in favour of newly established Rhine branches in the Rhine-Meuse delta (Stouthamer & Berendsen, 2007; Van Dinter *et al*., 2017; De Haas *et al*., 2018). Already around 2200 cal. years BP the Old Rhine didn't discharge the vast majority of Rhine water anymore (Berendsen & Stouthamer, 2002; De Haas *et al*., 2018). The rate of the loss of discharge in the Old Rhine increased considerably after ca. 2200 cal. years BP due to the formation of the Hollandse IJssel and Lek branches (just upstream of the inland margin of the Old Rhine branch) around 1850 and 1700 cal. years BP respectively (Pierik *et* al., 2018; Van Dinter *et al*., 2017; De Haas *et al*., 2018a). This was further amplified by a decrease in total Rhine discharge to the northern Rhine-Meuse delta due to changes in channel configuration induced by chute cut-offs and meandering behaviour at the delta apex (Kleinhans *et al*., 2011; De Haas *et al*., 2018a). Later avulsions leading to the formation of the for example the Waal and the Gelderse IJssel, farther inland from the upstream margin of the Old Rhine, decreased the discharge conveyed to the Old Rhine system even more (Van Dinter *et al*., 2017). The nearly completely filled-in Old Rhine was definitively closed off from Rhine discharge by the construction of a river dam near Wijk bij Duurstede in 1122 CE (*i.e.* 828 cal. years BP).

Flood frequency

The flood event record for the Lower Rhine from ca. 8200 cal. years BP until present was reconstructed based on a palaeoflood dataset obtained form 7 oxbow-fill sedimentary records from the Rhine-Meuse delta apex region (Toonen, 2013). Specific periods of increased flood frequency we later identified by Cohen et al. (2016). They also related the record to the avulsion history of the Rhine-Meuse delta and to its potential applications for archaeology in riverine settings in the Netherlands. Naturally, since flood event discharges are not necessarily evenly distributed among different Rhine distributaries in the Rhine-Meuse delta,

especially considering the process of (on-going) gradual avulsion, it cannot be presumed that the Lower Rhine flood event record can be extrapolated directly to the Old Rhine flood event record. Nonetheless, considering the Lower Rhine flood event record is the only one of its kind available for the Holocene Rhine in the Rhine Meuse delta and that the Old Rhine system was the main Rhine branch during most of its lifespan, it is assumed to be largely representative for the (frequency of) flood events that occurred in the Old Rhine system. The flood frequency per century of various flood magnitudes, exceeding recurrence time of 25, 50, 100, and 250 years is plotted next to the reconstructed mean annual Old Rhine discharge in figure 8.

Flood frequency in the Rhine was (and is) affected by climate variability within the Holocene. Phases with relatively higher (large magnitude) flood frequencies, are linked to the phase and seasonality of the Atlantic Multi-decadal Oscillation and of the North Atlantic Oscillation (Toonen *et al*., 2016; Toonen *et al*., 2017), which can cause favourable general climate conditions for the generation of flood events of large magnitudes (Toonen *et al*., 2016). Several periods of increased flood frequency are identified by Cohen *et al*. (2016) and can be recognized in the flood record plotted in figure 8 too. The period from 7700 until ca. 3300 cal. years BP, is characterized as a period with an average frequency of large flood events, with many relatively large flood events for a century around 3300 cal. years BP. During the next ca. 1500 years until ca. 1750 cal. years BP the flood frequency is remarkably low, especially the frequency of extreme flood events. Afterwards, the flood frequency increased again. This increase could have been affected by deforestation in the upstream catchment area of the Rhine in present-day Germany since the Bronze Ages (ca. 4000 cal. years BP) which increased general magnitudes and flow velocities of run-off into the river leading to an increase in flood magnitude and frequency in downstream areas (Cohen *et al*., 2016; Toonen, 2013; Dikau *et al*., 2005). From ca. 1750 cal. years BP until present the flood frequency remained more or less constant (Cohen *et al*., 2016).

Sediment supply

The suspended sediment delivery to the Old Rhine was reconstructed by Erkens (2009) in his PhD thesis for 500-year time-steps. It is plotted on the right-hand side of figure 8. Until ca. 2500 cal. years BP the suspended sediment delivery doesn't vary much for the Old Rhine system. The above-mentioned deforestation since the Bronze Ages led to a substantial increase in suspended sediment delivery from ca. 2500 cal. years BP onwards (Erkens, 2009; Hoffmann *et al*., 2009; Cohen *et al*., 2016). This increase is roughly concurrent with the increase in flood frequency, considering the relation between deforestation and flood frequency described above. Moreover, is it thought to have increased the avulsion frequency from ca. 2500 cal. years BP too (Cohen *et al*., 2016; De Haas *et al*., 2018a). De Haas *et al* (2018a) mention that the suspended sediment delivery during the period from ca. 3000 cal. years BP until the end of the Old Rhine system around 1000 cal. years BP increased by 60% compared to the period from the Old Rhine formation around 6500 cal. years BP until ca. 3000 cal. years BP, which they base on the reconstructions of Hoffmann *et al*. (2007) and Erkens (2009).

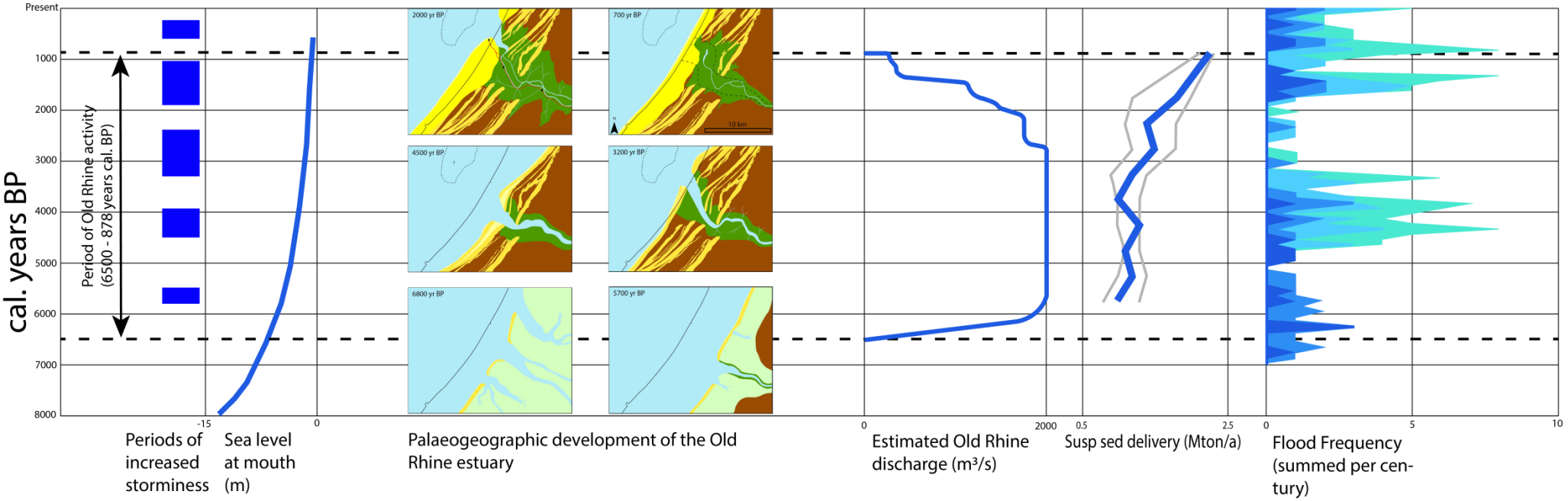

Figure 8:Boundary Conditions of the Old Rhine system. Downstream boundary conditions are plotted at the left-hand side of six palaeogeographic reconstructions of the Old Rhine estuary (see figures 6 & 7,adopted from De Haas *et al.*, 2018a), whereas the upstream boundary conditions are plotted on the right-hand side. Downstream boundary conditions plotted: **Periods of increased storminess** - (after Sorrel *et al.*, 2012, figure 3); **Relative mean sea level near the Old Rhine estuary mouth** – (after De Haas *et al.*, 2018a, figure 3, see references therein). Upstream boundary conditions: **Estimated Old Rhine discharge** – (after De Haas *et al.*, 2018a, figure 7, after Van Dinter *et al.*, 2017); **Suspended sediment delivery** – (after De Haas *et al.*, 2018a, figure 3, after Erkens, 2009); **Flood frequency (summed per century) for the Holocene Rhine** – (after Toonen, 2013, chapter 7, figure 3) - illustrated by the frequency of various flood magnitudes, exceeding recurrence times of 250, 100, 50, and 25 years and respectively corresponding with increasingly lighter shades of blue. The period of Old Rhine activity (indicated by the dashed black lines) is based on De Haas et al. (2018a) after Cohen et al. (2012) and Van Dinter et al. (2017).

3. Materials & Methods

To gain a solid understanding of the formation and evolution of the crevasses of the Old Rhine, geological reconstructions and the palaeogeographic development of the Old Rhine were combined with changes in upstream and offshore boundary conditions of the system. The latter were inferred independently from literature. Geological data from the literature and institutional databases (*i.e.* the Utrecht University lowland genesis borehole database and the open-source online data portal TNO-DINO from the Dutch Geological Survey) was used to gain insight in the large-scale sedimentary build-up along the Old Rhine channel belt and flood basins. Archaeological reports and sparse geological data from the literature were used to assess the build-up and phasing of crevasses along the Old Rhine.

Additionally, lithogenetic cross-sections of four extensive single-channel crevasses were constructed based on borehole data acquired during a two-week field campaign in September 2018. The aim of this field campaign was two-fold: i) to infer the sedimentological build-up of crevasse facies and ii) to reconstruct the age of formation and abandonment of the crevasses. Transects were located at roughly similar distance from the Old Rhine channel belt to equally compare crevasses. The insights from field (using borehole data from the same field campaign) and modelling studies into natural levee dimensions and dynamics by Roelofs (2019) were used to better understand crevasse dynamics in relation to natural levee dynamics and tidal boundary conditions.

3.1 Field data acquisition & analysis

3.1.1 Borehole location strategy

To assess spatial differences in the stratigraphic build-up and planform shape of crevasses along the course of the Old Rhine, four crevasses along the entire stretch of the river system were chosen as fieldwork locations. These were the Grecht, Meije, Alphen Zuid, and the Zwiet (see figure 9). By doing this is was possible to assess the spatial and temporal differences in the effects of changes in boundary conditions of the Old Rhine on crevasse formation and evolution. Borehole locations were planned by combining the interpretation of the extent of the crevasses around 100 CE (*i.e.* ca. 1900 cal. years BP) in the palaeogeographic map published by Van Dinter (2013, Appendix A) with detailed LiDAR data of the Dutch surface (AHN3, ahn.nl) and aerial imagery. Criteria based on which a specific agricultural parcel was deemed a potential location for gathering borehole data were: accessibility (*i.e.* easy to travel to and permission of landowner(s) to conduct fieldwork on their premises), distinguishability of crevasse features, and proximity of other archaeological or geological research locations.

Per fieldwork location, boreholes were positioned along a transect over the crevasse channel belt which was aligned roughly perpendicular to the crevasse channel direction. This enables accurate interpretation of crevasse facies. Specific borehole locations were planned based on field observations of the different preserved geomorphological crevasse features (*e.g.* levees and filled-in residual channels) per case. Therefore, individual boreholes were typically at 5 – 50 m distance from each other.

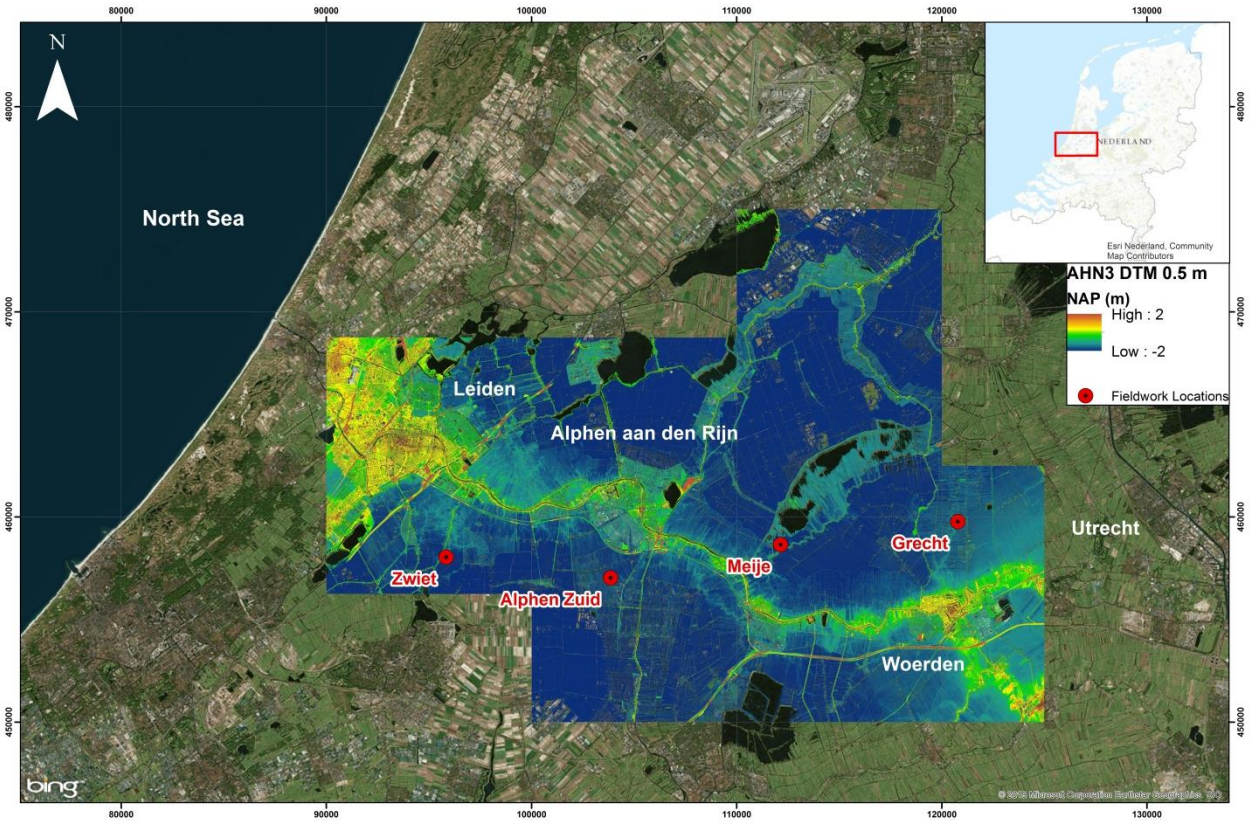

Figure 9: Fieldwork locations of crevasses along the Old Rhine plotted on BING aerial imagery and AHN3 elevation data.

3.1.2 Borehole logging

An Edelman hand auger (7 cm diameter) and gouge were used to obtain the borehole data. Sedimentary characteristics were logged in the field at 10 cm intervals for sediment texture (via the De Bakker and Schelling's (1989) classification scheme, Appendix B), calcium carbonate content (tested with 5% hydrochloric acid), colour, plant remains and oxidation/reduction (following methods for sediment classification in the field as described by *e.g.* Berendsen & Stouthamer (2001). The field-logged data (Appendix D) was digitalized using LLG2012 software. Sediment texture and organic contents classifications via the De Bakker & Schelling scheme were subsequently converted to their USDA counterparts using a standard UU-LLG conversion scheme (Appendix C). This was done to improve international accessibility to the data. Surface elevations (in m NAP, the Dutch ordnance datum) of individual borehole locations were inferred by plotting their field-logged *Rijksdriehoekstelsel* (national coordinate system) coordinates on AHN3 LiDAR data. The coordinates were acquired with a field GPS device, generally with a ca. 4 m accuracy in the horizontal plane. Transitions from peat to clastic crevasse deposits (based on sedimentary characteristics logged in the field) and vice versa were sampled in 1 m intervals and stored in sealed PVC tubes at 7 ^{o}C to minimize oxidation of organics after sampling. By means of the application of the Loss on Ignition (LOI) method the organic content of the sediments was determined at a 1 cm interval in the laboratory at Utrecht University. Laboratory procedures followed methods regarding LOI analysis as described by Schuring (2016) based on Heiri *et al*. (2001).

3.1.3 Lithogenetic and lithostratigraphic cross-section assemblage

Lithogenetic cross-sections were constructed based on the logged sedimentary characteristics of each borehole. LLG2012 was used to visualize each borehole with correct distance and elevation relative to each other per cross-section. Consequently, the recurring lithogenetic units identified in multiple boreholes in the cross-section were connected to each other based on knowledge about the common configuration of elements encountered in crevasse and other alluvial systems as previously described (see Chapter 2). TNO's DINOloket national subsurface data portal, of which the corings are generally spaced at greater distances from each other with more generic borehole data descriptions, provided an indication of the maximum depth of the top and bottom as well as the spread of lithogenetic units in the area of the crevasse. This aided in the accurate construction of the cross-sections. Assemblage of these different lithogenetic units into lithogenetic cross-sections followed methods as described and applied by Gouw and Erkens (2007), Toonen et al. (2012) and Kleinhans et al. (2011) (for the Dutch Rhine-Meuse in general) and Toonen *et al*. (2016) (for crevasses more specifically). This was done using Adobe Illustrator software.

Lithostratigraphic formations were assigned to the deposits in the lithogenetic cross-sections based on facies and stratigraphic criteria (TNO, 2013).

3.2 Laboratory Analysis

LOI analysis determines the organic content of sediments and thus enables the identification of the exact depth of the point of transition from a layer with high and constant organic content (*i.e.* peat) to a layer with increasingly higher clastic content, and vice versa (Appendix E). Samples from the peat layers under- or overlying these transition point were considered to be suitable for ^{14}C-dating as they mark the earliest (*terminus post quem*) or oldest (*terminus ante quem*) phase of activity of the crevasse respectively. Subsequently, after the samples had been taken, they were prepared for AMS ^{14}C-dating by removing calcareous and clastic matter (see Schuring (2016) for a detailed description of the applied procedure). From the remaining material macro remnants were selected suitable for ^{14}C-dating by dr. Nelleke van Asch. In a final step, they were treated one more time, removing any of the remaining calcareous and clastic matter before sending them to the Centre of Isotope Research for Radiocarbon Dating in Groningen at Groningen University early January 2019 (see Appendix F for an overview of the samples sent). The dating results are expected earliest at the beginning of May 2019, too late to use in the analysis in this thesis.

3.3 Age estimation

Pending the results of the AMS ^{14}C-dating, reports of archaeological investigations (*e.g.* borehole surveys and excavations) at locations of crevasses along the Old Rhine were assessed to get an indication of the minimum age of crevasse deposits. These reports were used to trace the extent, stratigraphic position (*i.e.* relative age) of the crevasses. In some cases, artefacts on top of the crevasses provided a more accurate minimum age estimate. Furthermore, an extract from the ARCHIS database (National Database of Archaeological reports, stray finds and observations) from 2015 limited to the Old Rhine Area was supplied by dr. Tjalling de Haas. The database consists of the location and the type and minimum and maximum age of archaeological artefacts. Consequently, the data were subdivided in five archaeological periods and plotted on separate maps (based on the Dutch subdivision of archaeological periods in the Netherlands, see table 1). Additionally, De Haas provided a database of ^{14}C-dated samples from the Old Rhine area and

vicinity, which was used in the study of Cohen *et al*. (2012) too. Both databases were plotted on a georeferenced version of the palaeogeographic reconstruction of the Old Rhine from ca. 100 CE (1900 cal. years BP) by Van Dinter (2013, Appendix A). This made it possible to get an indication of the minimum and maximum age of beginning and end of crevasse activity along the Old Rhine. Archaeological remains and traces being preserved in deposits lying under or on top of crevasse deposits (or even in crevasse deposits themselves) provide *terminus ante quem* and *terminus post quem* ages of crevasse activity respectively.

Archaeological period	**Age in BCE/CE**	**Age in cal. years BP**
Middle ages	450 to 1500 CE	1500 to 450
Roman age	12 BCE to 450 CE	1962 to 1500
Iron age	800 to 12 BCE	2750 to 1962
Bronze age	2000 to 800 BCE	3950 to 2750
Neolithic	5300 to 2000 BCE	7250 to 3950

Table 1: Subdivision of archaeological periods in the Netherlands.

3.4 Integration of results for synthesis

The results of the fieldwork discussed in this study will thus comprise detailed cross-sections of each of the four concerned crevasses of which the relative ages of the different crevasse facies will be inferred from stratigraphic correlation and archaeological remains. Coupling this information to the sedimentary characteristics of different facies enables the reconstruction of spatio-temporal crevasse formation and development. Subsequently, the reconstructed development of each crevasse along the Old Rhine can then be correlated to changes in upstream and downstream boundary conditions of the river system (see section 2.5) and integrated into the system-scale development of the Old Rhine area. By doing so, dominant processes and mechanisms affecting crevasse formation and development.

4. Results

This chapter comprises three sections. The first section describes the sedimentary build-up as reconstructed per crevasse cross-section. The second section summarizes the archaeological remains in the Old Rhine area from Neolithic until Early-Medieval times, focussing on archaeology on or near crevasse deposits. The last section compares the studied crevasses in terms of facies and relative chronology.

4.1 Sedimentary build-up: lithogenesis and lithostratigraphy of crevasses

4.1.1 Grecht

Figure 10 shows the location of the transect aligned roughly perpendicular to the Grecht crevasse channel belt in Kanis (municipality of Woerden) along which 5 boreholes were cored (see figure 9 for the location of the Grecht crevasse fieldwork location). The cross-section, figure 11 is roughly in line with the cross section of the Holocene sequence beneath Kanis in figure 4 of Van Asselen *et al*. (2018) (see Appendix G and figure 10 for the location of the cross-section). The latter cross-section is located directly east of the Grecht crevasse and has some with the cross-section in figure 11.

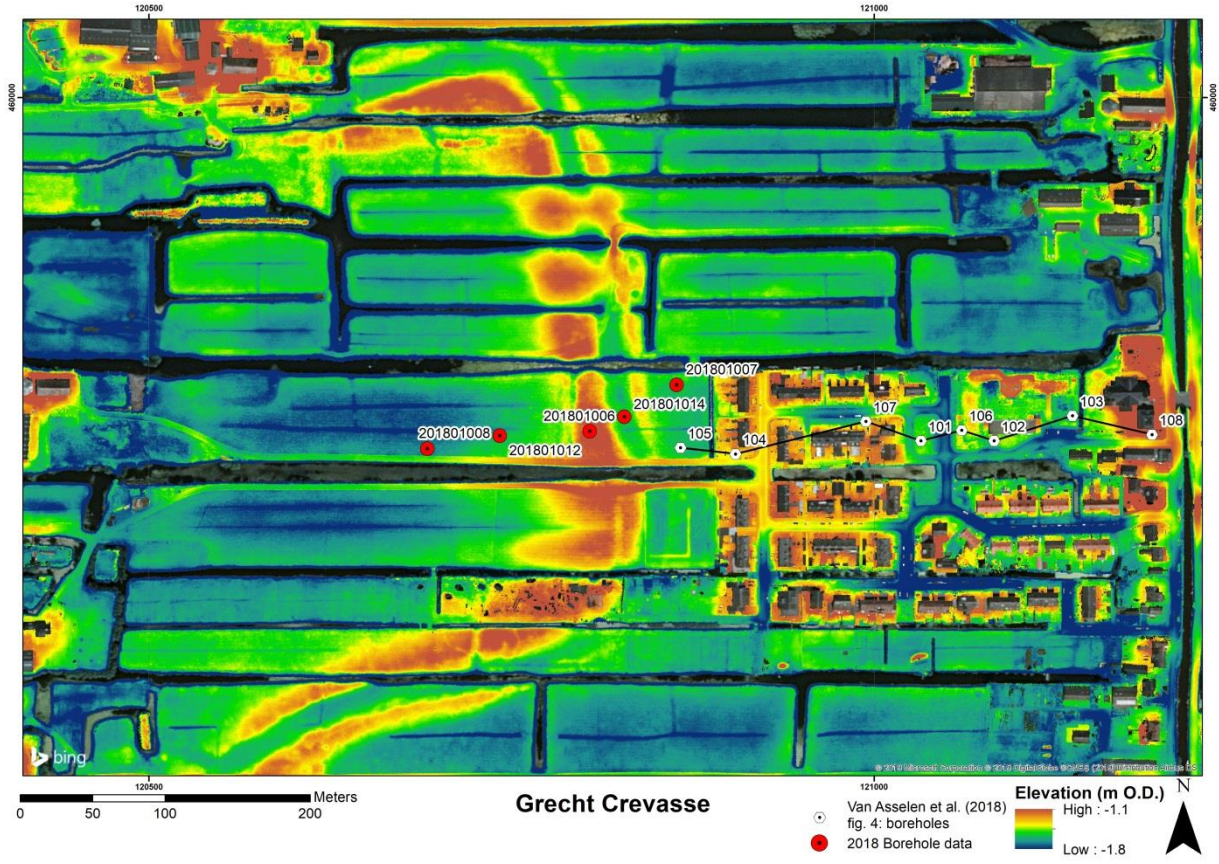

Figure 10: Borehole locations of the Grecht crevasse lithogenetic cross-section.

At a depth of ca. -8.8 m NAP in coring 008 well-sorted fine sands with low calcium carbonate content are encountered. These are interpreted to be Late-Pleistocene to Early-Holocene aeolian cover sand deposits of the Boxtel formation, in line with sand layers at the same position in DINOloket.

Overlying these fine sands are alternating peats and peaty mucks. These differ in thickness from ca. 4.5 m in the West of the profile (coring 008) to ca. 3 m towards the east of the profile (corings 006 and 007). They belong to the Nieuwkoop formation, basal peat member. In coring 012 the peat deposits are intersected by ca. 1.3 m of (silty) clays containing reed remains (occasionally *in viva*), of which the bottom 0.6 m are laminated with very fine sand and detritus laminations. They are interpreted to be deposited by a minor crevasse channel or (tidal) creek (Naaldwijk formation, Wormer member). Van Asselen *et al*. (2018) identified a similar potential crevasse channel or (tidal) creek at a comparable depth in their cross-section at Kockengen, ca. 4 kilometres upstream of the Grecht along the Old Rhine (figure E.4 in the supplementary data of Van Asselen *et al.*, 2018).

In both coring 007 and 008 around -6.5 m NAP, ca. 0.3 m of peaty clay deposits occur, of which the deposits at coring 007 are abundant in reed. Since these peaty clay layers are very similar in composition and stratigraphic position they are interpreted as one layer. Here they are interpreted to be the easternmost wedge of the tidal deposits of the Naaldwijk formation, Wormer member, from the Middle Holocene (see chapter 2), based on comparison with other cross-sections and DINOloket data.

On top of the peat deposits the deposits from the Grecht crevasse were encountered. These consist of channel, natural levee and flood basin facies.

Crevasse deposits

Coring 014 is located in the approximate middle of the crevasse channel. The base of the channel was not reached, but the depth of the former channel of the Grecht is at least ca. 3 m and is estimated to be at maximum ca. 6.5 m based on comparable crevasses in the Rhine-Meuse delta (*e.g.* Stouthamer, 2001; Makaske *et al*., 2007; section 4.1.3). The residual channel consists of a typical fining upwards sequence of laminated sandy loams to humic silty clay loams which grade into peats towards the top. They mark the stage of gradual decrease of activity and eventually abandonment of the Grecht. The top of the peat is oxidized with reed and wood parts and largely intact leafs identifiable in the bottom 60 cm of the peat.

The natural levee deposits consist of laminated loamy sand to silty clays, rich in calcium carbonate with shell gritt and *in viva* reed remains.

The western natural levee of the Grecht at this location is approximately 30 m wide, whereas the eastern levees is only ca. 15 m wide (figure 10). This pattern stays more or less constant along the course of the Grecht. The thickness of the western natural levee deposits is assumed to be slightly thicker than the thickness of the eastern floodplain deposits encountered in coring 007 (see figure 11 and in corings 105 and 104 in Van Asselen *et al*. (2018).

The natural levee deposits grade into flood basin clays, becoming less thick, less abundant in sand and more organic away from the channel.

On top of both the western as well as the eastern flood basin deposits a younger peat layer is encountered just beneath the surface (*i.e.* at ca. 40 – 50 cm below the surface). It becomes progressively thicker at

increased distance from the natural levees of the Grecht (*i.e.* 40 cm in coring 007, 70 cm in coring 012, and 200 cm in coring 008).

The top distinguished layer in the in the profile is an anthropogenically affected clay layer of ca. 40 – 50 cm, found at the top of each coring along the transect.

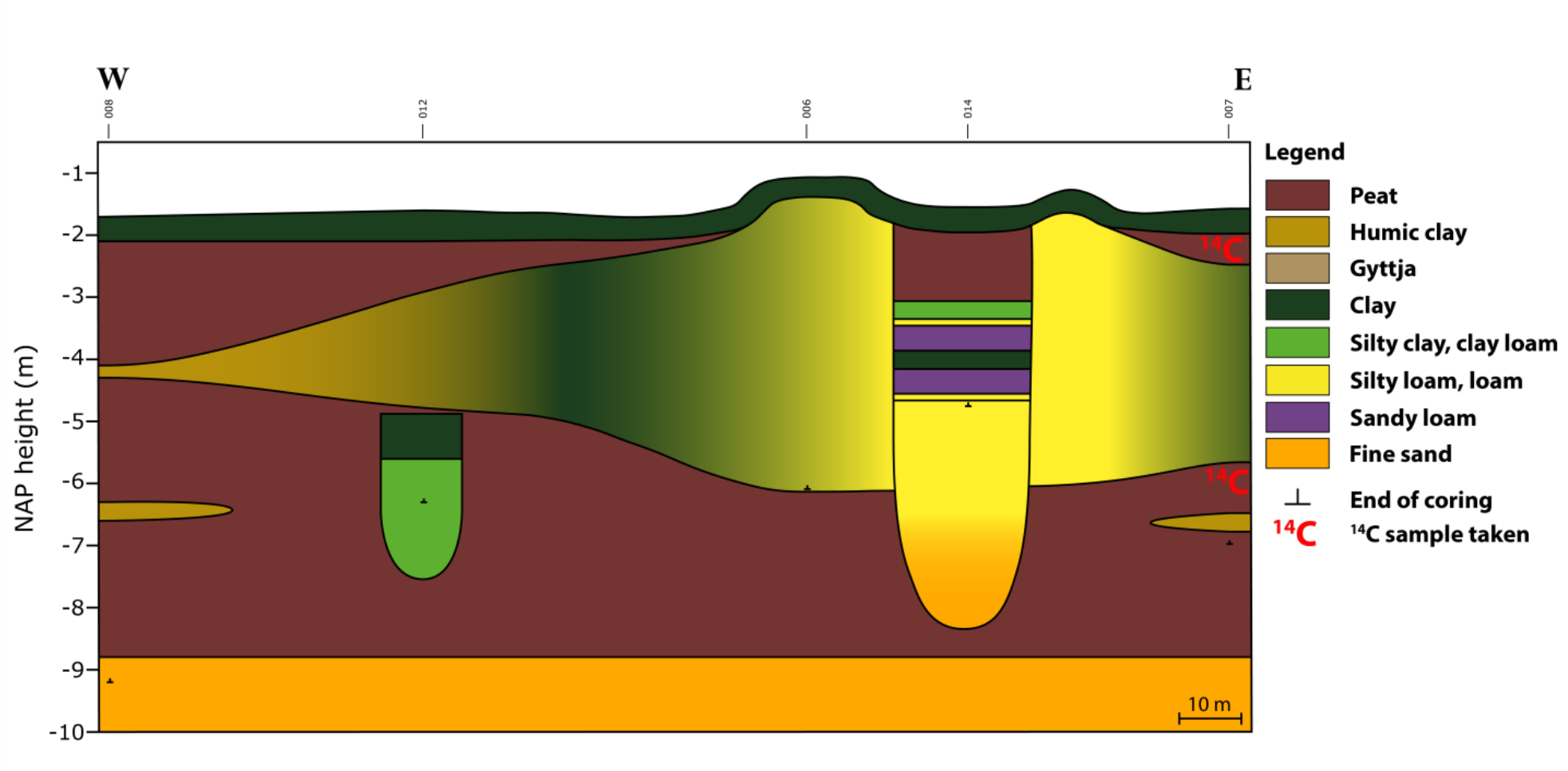

Figure 11: Lithogenetic cross-section of the Grecht crevasse.

4.1.2 Meije

Moving downstream along the Old Rhine, figure 12 shows the location of the transect of boreholes aligned roughly perpendicular to present-day course of the Meije. As the Meije is still discharging water (although there is no morphodynamic activity) the transect lacks boreholes located in the channel and the natural levee of the Meije. Therefore, the most south-easterly located borehole, 022, is observed to be at or near the distal parts of the natural levee of the Meije or the proximal parts of its floodplain deposits. As can be inferred from the LiDAR (AHN) elevation in figure 12 the agricultural parcel in which the transect is located differs from its neighbours because its surface is levelled by the owner with material from the natural levee of the Meije. Hence, the upper ca. 30 – 40 cm of the field are anthropogenically disturbed. Figure 13 shows the lithogenetic cross-section which was constructed on basis of logged borehole data.

Figure 12: Borehole locations of the Meije crevasse lithogenetic cross-section.

Aeolian deposits are not found at the bottom of the geological profile of the Meije. Instead, the bottom of the cross-section consists of peat deposits of the Nieuwkoop formation, basal peat member. The basal peat layer is intersected by a wedge of humic clayey deposits in the south-east part of the geological cross-section (see coring 022 and 024).

The top of the peat layer is characterized by a gradual transition to humic clay deposits, which eventually grade into mostly inorganic clays. The humic clays and the top of the underlying peat in coring 024 are intersected by (silty) clay loams deposited by a small creek system.

From ca. -5 m NAP the predominantly clastic deposits are believed to belong to the major crevasse phase of the Grecht (Echteld formation). In the north-western part of the profile (corings 023 and 025) they are more clayey and have a higher organic content (coring 023), whereas they are siltier and thicker in the south-eastern part of the profile, closer to the channel of the Grecht. Therefore, the former are interpreted as flood basin deposits and the latter as the distal parts of the natural levee deposits of the Grecht crevasse.

The flood basin deposits consist of clays, which become increasingly humic towards the top and contain wood remains. Farther away from the channel the flood basin deposits become less humic and the number of wood remains decreases.

The distal natural levee deposits have a lower organic but a higher silt content than the flood basin deposits and consist of silty clays to silty loams. They contain washed down plant remains and occasionally wood fragments. Sometimes parts of thick branches could be identified.

In the north-western part of the cross-section, the flood basin deposits are overlain by peats which grade into humic clays towards the south-eastern end. The humic clays are characterized by abundant wood remains. They belong to the Nieuwkoop formation, Hollandveen member. No suitable organic material from the bottom parts of these deposits could be sampled for subsequent ^{14}C-dating to get an indication of the age of the end of crevasse activity.

On top of the peaty and humic clayey deposits and distal natural levee deposits lay clay deposits which are increasingly silty towards the south-east end of the cross-section. They were probably deposited during a reactivation phase of the Old Rhine crevasses.

The anthropogenically-disturbed clays have a minor sand component and contain crushed brick remains. They were extracted from the natural levee.

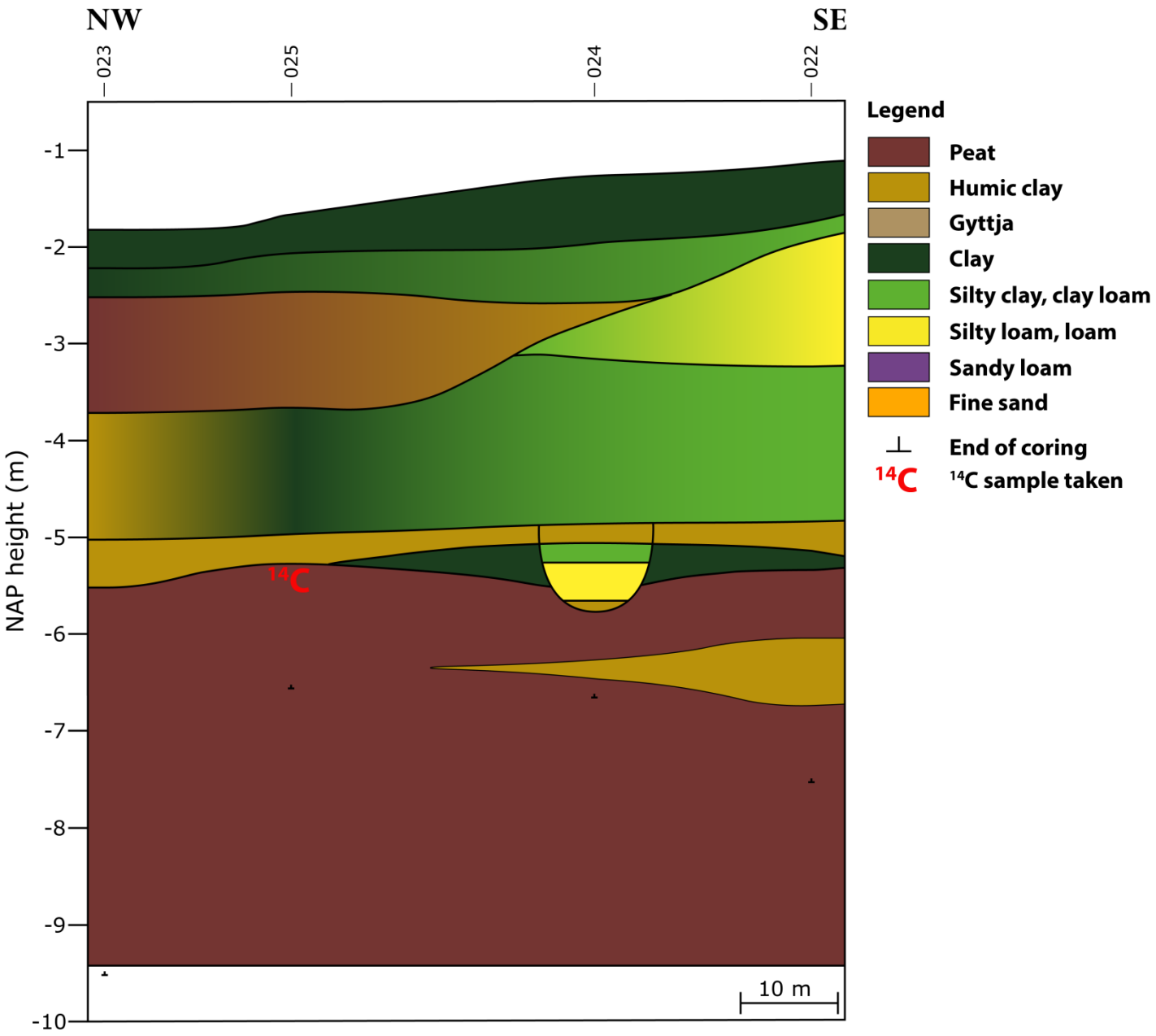

Figure 13: Lithogenetics cross-section of the Meije crevasse.

4.1.3 Alphen Zuid

Being located more downstream the Alphen Zuid crevasse is expected to be more tidally influenced than the Grecht and Meije. Figure 14 shows the location of the lithogenetic cross-section, figure 15. The crevasse creek and its natural levees were easily identifiable in the field due to differential subsidence of the clastic deposits compared to its surrounding peat.

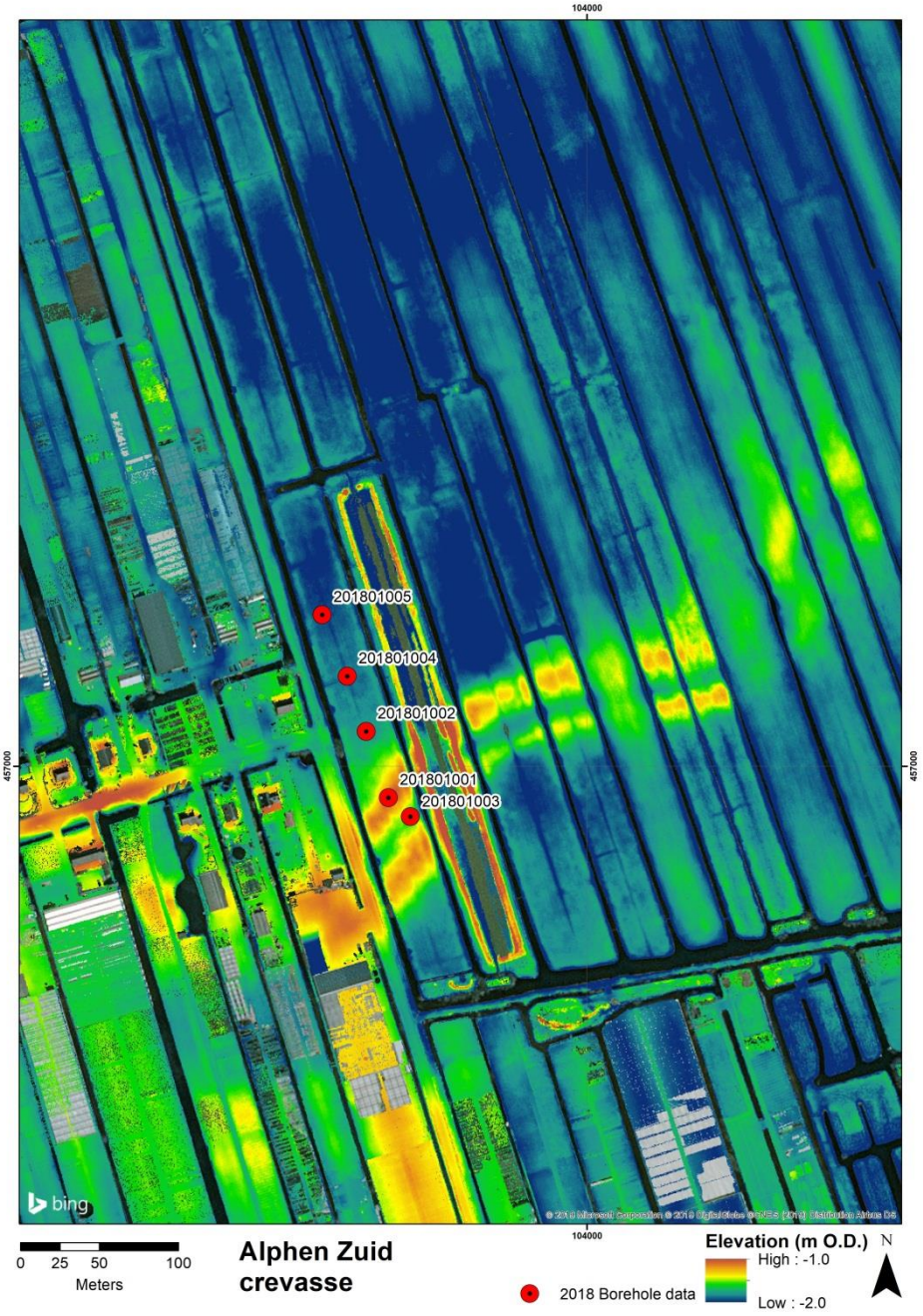

Figure 14: Borehole locations of the Alphen Zuid crevasse lithogenetic cross-section.

The bottom of the cross-section consists of tidal deposits of the Wormer member (Naaldwijk formation, around ca. - 4.5 m NAP). They consist of medium to extremely fine sands to silty clays loams and clay loams. Shell fragments, shell gritt and tidal laminations of very fine sand are present.

Peat (Hollandveen Member, Nieuwkoop Formation) lies on top of the tidal deposits. The peat is relatively thin (ca. 50 cm) throughout the entire cross section. Below the northern natural levee of the crevasse, the peats are slightly more compressed (ca. 30 cm) due to the extra weight of the overlying levee deposits. The peat mainly consists of reed below -3.5 m NAP, whereas more wood remains are present in its top.

A humic clay 'pulse' is present in the peats from 3.62 – 3.42 m below NAP, possibly indicating a minor, earliest phase of clastic input of a channel which preceded the Alphen Zuid crevasse.

The Alphen Zuid crevasse consists of a channel, levee, and flood basin facies. The transition from the tidal deposits to base of the channel is abrupt.

The bottom of the channel deposits (from ca. 7.5 to ca. 6.7 m below NAP) consists of very fine sands with abundant detritus laminations and a high calcium carbonate content. They gradually grade into loams (from ca. 6.7 to 5.8 m below NAP) with an equally high calcium carbonate content, a lack of clearly identifiable laminations, but occasionally shell gritt and fragments as well as plant, wood and reed remains (not *in viva*, though). Subsequently, the loams gradually change into clay loams (from ca. 5.80 to ca. 3.60 m below NAP). These contain both detritus laminations (towards the top), shell fragments and gritt, and leaf and wood remains. A sample of the leafs was taken for ^{14}C-dating.

At a depth of 3.60 m below NAP the clay loams become silty clay loams deposited during the abandonment phase of the Alphen Zuid crevasse. They to ca. 2.40 m below NAP and contain shell gritt and plant remains and have a high calcium carbonate content.

The natural levee deposits consist of clay loams overlying the Holland peats which grade into silty clay loams and silty clays towards the top (from 2.20 to 1.60 m below NAP). The lower part of the clay loams contains fine sand and detritus (*i.e.* possibly reworked peat) laminations of a few mm thick and abundant plant remains. The clay loams have a high calcium carbonate content and contain shell fragments and gritt below – 3.1 m NAP. Small wood remains are present in the top part of these deposits (from 2.70 to 2.20 m below NAP), as are fine sand laminations. The silty clay loams and silty clays lack plant remains and laminations.

The transition from peat to humic clays in the northern (flood basin) part of the cross-section is rather gradual. The clastic flood basin deposits consist of humic silty clays with reed remains close to the crevasse natural levee, whereas they become humic clays farther away.

On top of the crevasse flood basin clays, a very thin (from ca. -2.7 to -2.2 m below NAP), largely oxidized mucky peat layer is present (Nieuwkoop formation, Holland peat member). The transition from humic flood basin deposits to is gradual. They are oxidized due to their presence close to the surface and the generally low local ground water level.

The top layer present below the surface of the cross-section consists of anthropogenically-disturbed silty clays with a sandy admixture and occasionally an earthenware fragment.

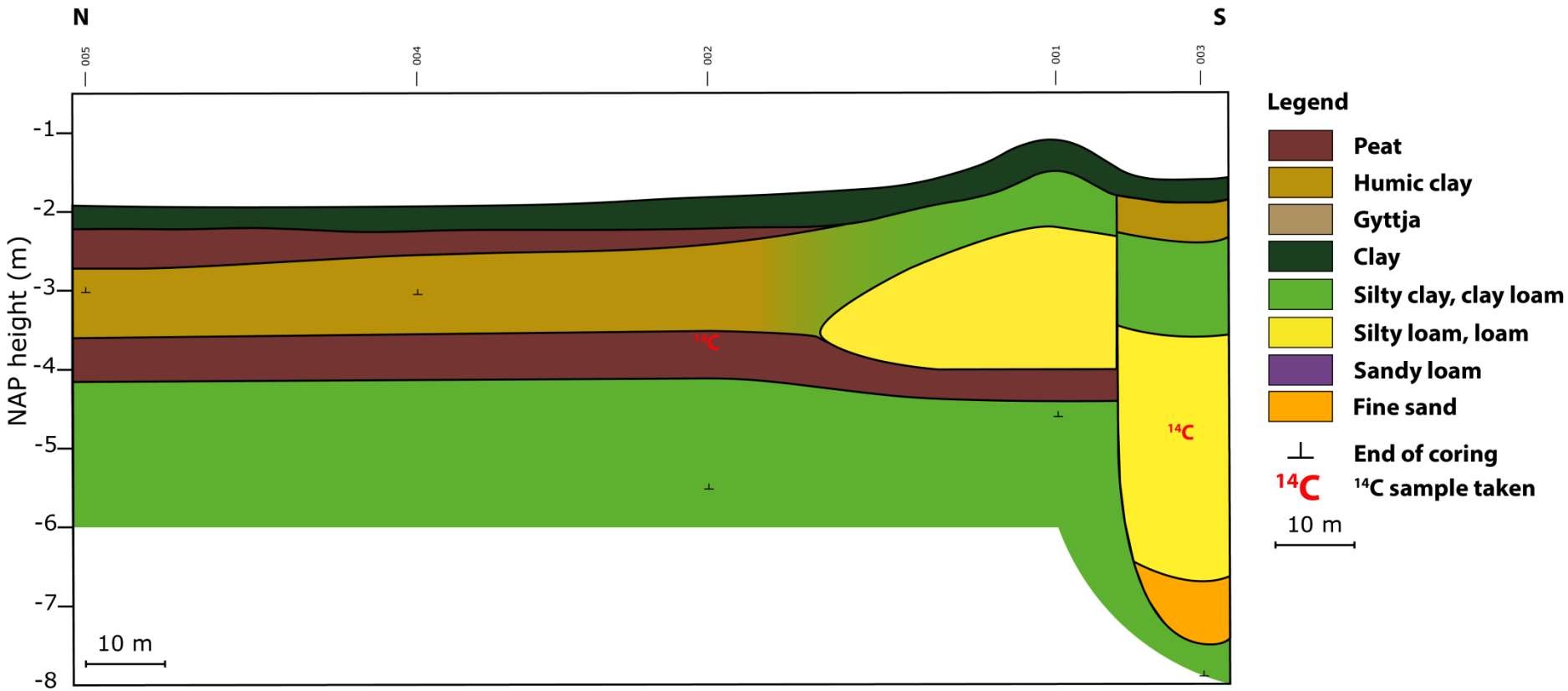

Figure 15: Lithogenetic cross-section of the Alphen Zuid crevasse.

4.1.4 Zwiet

The stratigraphic build-up of the Alphen Zuid crevasse is the most tidally-influenced of the four crevasses studied in this thesis, as it is located most downstream. Figure 16 shows the location of the transect along which 5 boreholes were cored: 033-03; figure 17 shows the lithogenetic cross-section of the Zwiet crevasse based on the logged borehole data. The Zwiet crevasse differs significantly in terms of stratigraphy and planform shape from the three more upstream located crevasses. Three intersecting peat layers are present (*i.e.* instead of two). Therefore, at least three and possibly even four phases of clastic activity can be distinguished. Besides, the Zwiet has smaller side-channels branching of the main channel, which are absent in the other three crevasses.

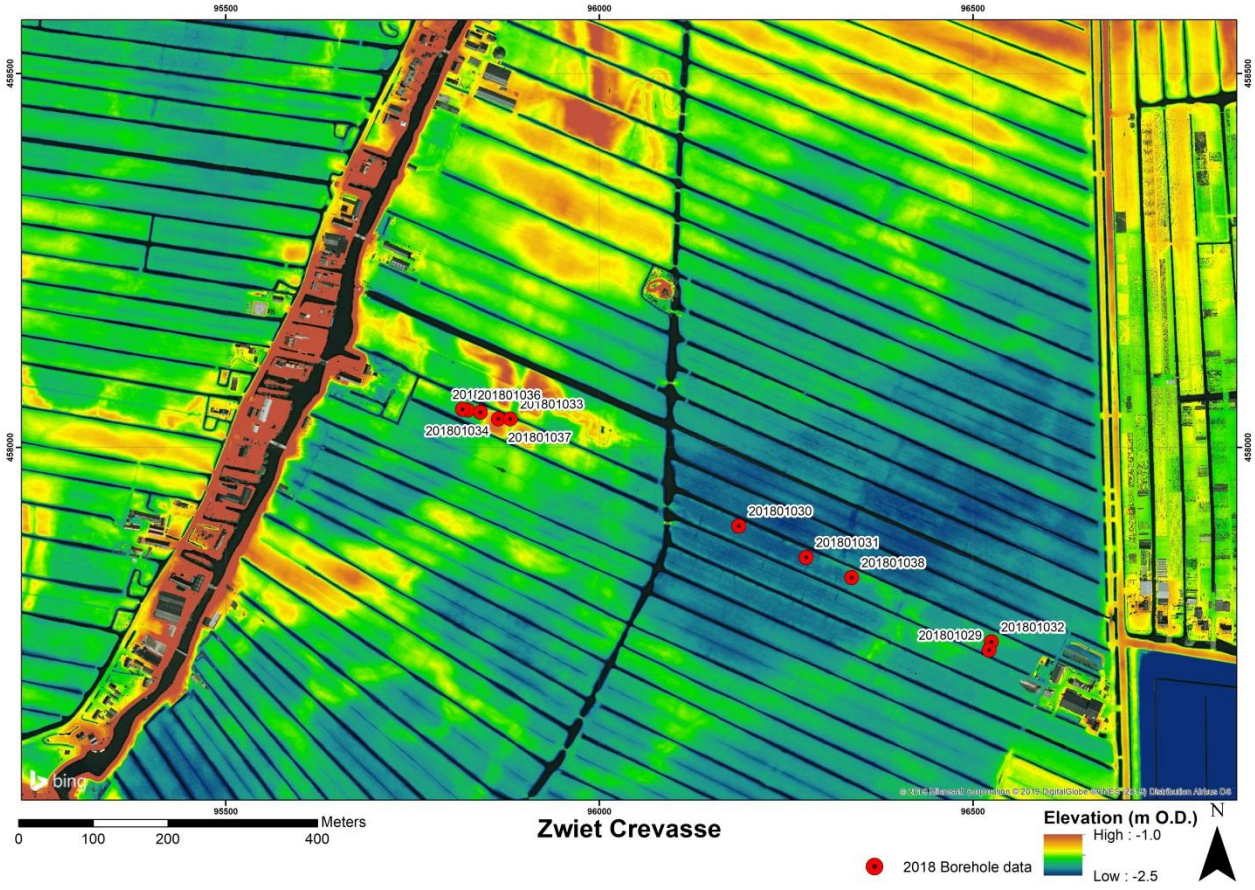

Figure 16: Borehole locations of the Zwiet crevasse cross-sections.

The bottom of the cross-section consists of tidal deposits (Naaldwijk formation, Wormer member). They consist of silty clays and silty clay loams. Detritus and fine sand laminations, shell gritt, and reed roots (*in viva*) are present. They indicate a *rietgors* environment (Van de Wallenburg, 1966).

Another indication for the presence of a *rietgors* environment is an overlying thin layer of gyttja. It is present in the cross-section from the western edge until presumably just west of the natural levee, where it is most likely eroded by an incising or migrating tidal creek. The gyttja consists of a mixture of clastic and organic sediments, deposited under low-energetic conditions. Gyttja on top of tidal deposits is a strong

indicator of a decrease in tidal influence and eventually gradual terrestrialisation. The clastic component of the gyttja consists of silts with reed remains and some very thin clay laminations.

Peat (Nieuwkoop formation, Hollandveen member) was formed on top of the gyttjas. Reed remains continue to be present throughout the peat, and occasionally thin humic clay laminations and sedge are present. The clay laminations indicate that the area received irregular clastic input from a nearby located waterway (*e.g.* a remnant of an older tidal creek) due to floods or storm surges. Sedge, which typically grows in low-energetic raised bog, might suggest that the area experienced periods of relative calm, low-energetic conditions too, during which clastic input was low or virtually absent. A sample from the top of this oldest peat layer was taken for ^{14}C-dating to determine the age of the beginning of crevasse activity.

The depth of the channel is at least 5.25 m below NAP, although the base of the channel was not reached. It is estimated to be at least ca. 7 m below NAP, which is based on the depth of the above-mentioned tidal creek bar deposits at the bottom half of coring 037, and on comparable crevasses (*e.g.* Stouthamer, 2001; Makaske *et al.*, 2007; section 4.1.3).

The tidal creek deposits consist of silty clay loams with sand and detritus, plant and shell gritt remains and lumps of leaf remains at two intervals: from 4.65 to 4.60 m (sampled for ^{14}C-dating) and from 3.85 to 3.05 m below NAP. Wood remains are present in the upper 30 cm (from ca. 3.65 to 3.35 m below NAP).

On top of the silty clay loams lay approximately 40 cm of clay loam deposits (from ca. 4.70 to 4.30 m below NAP), with a high calcium carbonate content too. The transition from the silty clay loams to these clay loams is gradual. These are most probably deposited during prime crevasse activity in the Zwiet. They contain wood remains and shell gritt as well as lumps of leaf and other plant remains. A macrofossil (*Alnus glutinosa*, *i.e.* Alder) was sampled from the plant remains for ^{14}C-dating.

The clay loam deposits change relatively rapidly into silty clays, with a high calcium carbonate content and wood remains. This strong decrease in supply of relatively coarse sediment, probably indicate a gradual abandonment of the crevasse.

The uppermost undisturbed deposits from the channel are 20 cm of severely oxidized former Holland peats (unsuitable for ^{14}C-dating), dating from the later stages of abandonment of the Zwiet when filling in of the channel infilling took place.

On top of the oldest peats lay the crevasse flood basin and natural levee deposits. The flood basin deposits are encountered in corings 034-036. The more distally located corings 035 & 036 are slightly humic silty clay loams, which contain wood remains and have a high calcium carbonate content, without laminations. In between the flood basin deposits is an intermittent peat layer, which wedges out west of coring 034. Hence, two phases of crevasse overbank deposition can be distinguished. In coring 034, where the two phases cannot be distinguished from each other directly, the lower silty clay loams contain detritus and extremely fine sand laminations at the bottom. They also differ from the 1st phase of crevasse flood basin deposits in corings 035 & 036 because they contain abundant reed remains. Coring 034, therefore, seems to be located in the transition zone from natural levee deposits to flood basin deposits.

The intermittent peat layer in between the 1st and 2nd crevasse deposits phase consists of very mucky peat with much wood. Three additional samples for ^{14}C-dating were taken to determine the age of: *i)* the end of

the 1st crevasse deposits phase, *ii)* renewed clastic input, and *iii)* the beginning of the 2nd phase of crevasse sediment deposition.

The deposits from the 2nd crevasse deposits phase in corings 035 & 036 are humic silty clays, which have a very low calcium carbonate content and contain plant and wood remains.

The youngest peat layer consists of very thin oxidized peats (unsuitable for ^{14}C-dating) and lies on top of the 2nd crevasse deposits phase facies in the western half of the cross-section.

The natural levee deposits of the Zwiet, (coring 037) are clearly more laminated than the natural levees of the other crevasses. They consist of sandy loams with shell gritt and occasionally plant remains and have a high calcium carbonate content. Alternating fine sand and clay laminations of ca. 2 mm thick are present at regular intervals. Given the position of coring 037 directly next the channel of the Zwiet, these bundled relatively coarse tidal deposits are probably point bar deposited by a migrating tidal creek pre-dating the Zwiet crevasse. The Zwiet crevasse can have taken over or evolved from the pre-existing tidal creek. Consequently, the Zwiet channel could be seen as a rather continuous development from a minor tidal creek to a mature crevasse channel belt system including all crevasse architectural elements.

The top layer in the Zwiet cross-section consists of anthropogenically-disturbed silty clays with a sand admixture and some earthenware brick fragments and debris.

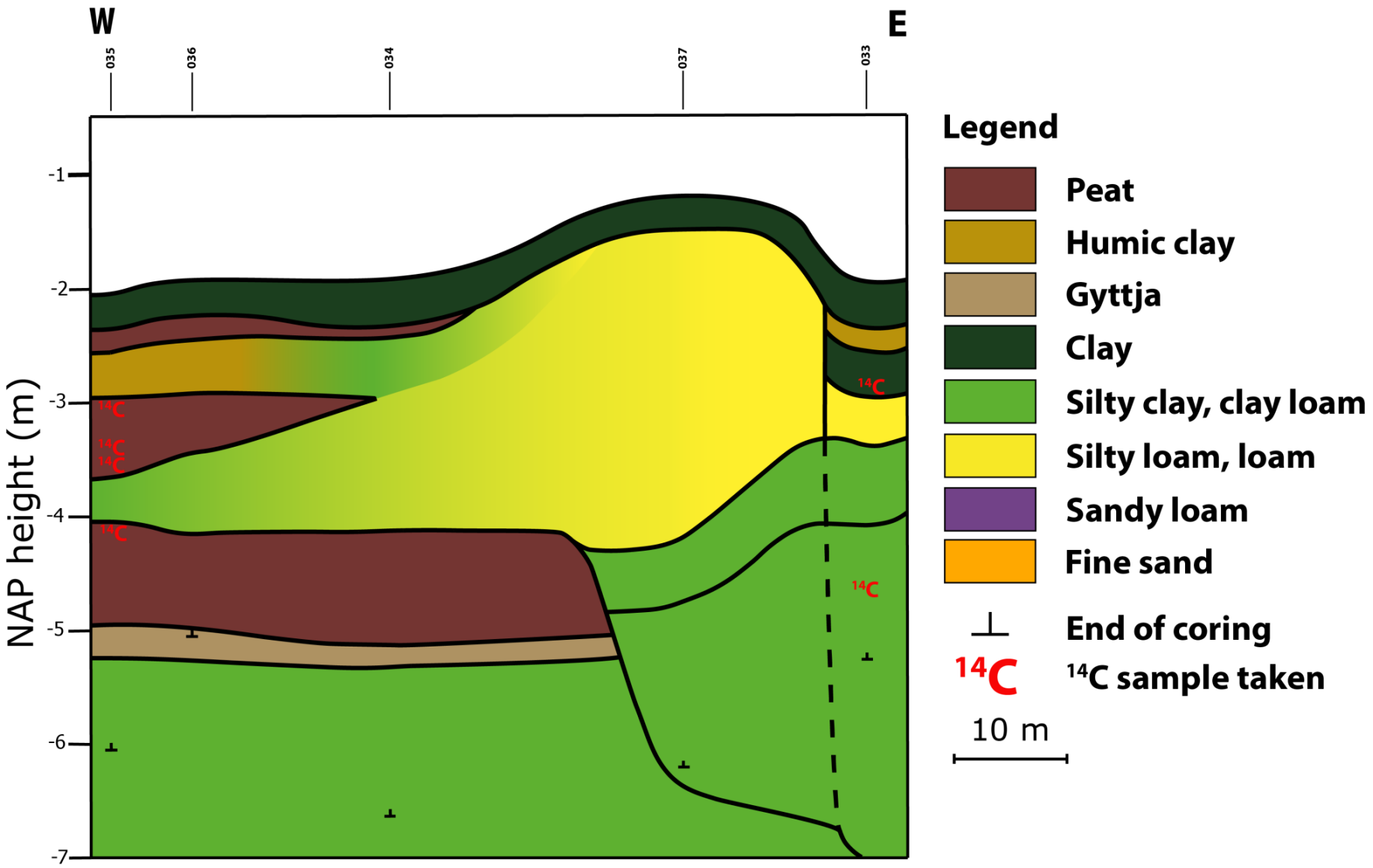

Figure 17: Lithogenetic cross-section of the Zwiet crevasse.

4.2 Archaeological reports of crevasses along the Old Rhine

This section describes the archaeological remains in the Old Rhine area found on and in the vicinity of crevasses as inferred from a selection from 2015 of the Dutch national archaeological database ARCHIS and archaeological reports from the last two decades, categorized per archaeological period. The spatio-temporal dynamics in (type of) anthropogenic activity on crevasses provides an indication of the age of such systems and an insight into their dynamic behaviour within the spatio-temporal development of the Old Rhine system.

4.2.1. Neolithic & Bronze Age remains and sites

Archaeological remains and traces from the Neolithic period (ca. 5300 to 2000 BCE or 7250 to 3950 cal. years BP) are the oldest ones that can be found in the Old Rhine channel belt or flood basin deposits, considering the Old Rhine itself was established around 6500 cal. years BP (De Haas *et al*., 2018a, see section 2.4). Figure 18 and figure 19 show the archaeological finds and traces in the Old Rhine area from the 2015 ARCHIS extract for the Neolithic period and Bronze Age period respectively. In both figures the data points are plotted on top of the 100 CE palaeogeographic reconstruction of the Old Rhine by Van Dinter (2013). This might give a somewhat distorted view of the location of the finds in relation to the configuration of the Old Rhine channel belt, as the palaeogeography during the Neolithic as well as during the Bronze Age differed considerably from the palaeogeography during the Roman Age. Nonetheless does plotting the archaeological data on said palaeogeographic reconstruction provide some indication of the provenance of the anthropogenic activity in the Old Rhine area, especially when compared to human habitation in later periods.

Archaeological remains from the Neolithic from the 2015 ARCHIS database are very sparse in the Old Rhine area and occur only in the downstream part of what was then the Old Rhine channel belt, just behind its contemporary estuary mouth and the beach barriers (*i.e.* the Western Netherlands coastline was still progradating, thus the coastline was still inland from its present-day position, see also section 2.4 and figure 7). The remains which are located in the vicinity of the Old Rhine channel belt during that period (see figure 18, four yellow hexagons downstream from the Zwiet crevasse denote the location of individual finds) comprise 2 Late-Neolithic (from ca. 2850 to 2000 BCE or 4800 to 3950 cal. years BP) flint tools (an axe and a drill), a Middle-Neolithic (from ca. 4200 to 2850 BCE or 6150 to 4800 cal. years BP) stone axe, and a Neolithic ‘weapon’ (both the age and type of weapon not further specified). It could not be inferred whether these fids were located on or in the vicinity of crevasse deposits.

Archaeological reports from the Old Rhine area, however, do indicate anthropogenic activity on (buried) crevasses. Most notably, 10,838 ceramics sherds from the Middle-Neolithic B (from ca. 3450 to 2850 BCE or 5400 to 4800 cal. years BP) and Late-Neolithic were found during a(n) (geoarchaeological) excavation on the southern banks of a buried crevasses of the Old Rhine (Diependaele & Drenth, 2010, see figure 20, yellow dot). The site is called ‘Spookverlaat’ and is located in Hazerswoude-Rijndijk in the municipality of Rijnwoude. The ceramic traditions were the Vlaardingen, Trechterbeker and Enkelgraf Culture. ^{14}C-dating of representative sherd samples specified the period during which anthopogenic activity on the crevasse took place, namely from 3360 BCE at minimum (calibrated age of the oldest Vlaardingen Culture sherd, no uncertainty given) to 2850 to 2470 BCE at maximum (calibrated age of soot remains on an Enkelgraf Culture sherd). Diependaele & Drenth hypothesize that the crevasses must have been active during this period too, which is mainly based on the presence of the ceramic sherd in crevasse deposits.

Crevasses of the same stratigraphic level were encountered in the Hondsdijkse polder (Verboom-Jansen & Wullink, 2011) at Park Prinsenschouw (Van Dasselaar & Depuydt, 2009) and in polder Nieuwkoop (Kroes & Feiken, 2011) red hexagons in figure 20). Based on their comparable depth below the surface, similar stratigraphy and close location relative to each other these crevasses are correlated to the crevasse at Spookverlaat (see above).

Concerning the Bronze Age archaeology, almost no remains from the ARCHIS 2015 database are located in the Old Rhine area, see figure 19. The only location where merely one ceramic sherd was found is close to the Middle- to Late Neolithic 10,838 ceramic sherds-complex (compare the location of the yellow dot in figure 19 to the location of the yellow square in figure 20). Its age is unspecified, and it might thus date from the whole range of the Bronze Age period (*i.e.* 2000 to 800 BCE or 3950 to 2750 cal. years BP), nor is anything known about whether it is located on or in crevasse deposits or in stratigraphically correlated layer(s). The general lack of Bronze Age archaeological remains in the Old Rhine area might therefore indicate absence of anthropogenic activity in most parts of the Old Rhine Rhine channel belt and flood basin during the Bronze Age or poor taphonomic conditions.

Neolithic archaeology 5300-2000 BCE (7250-3950 cal. years BP) along the Old Rhine

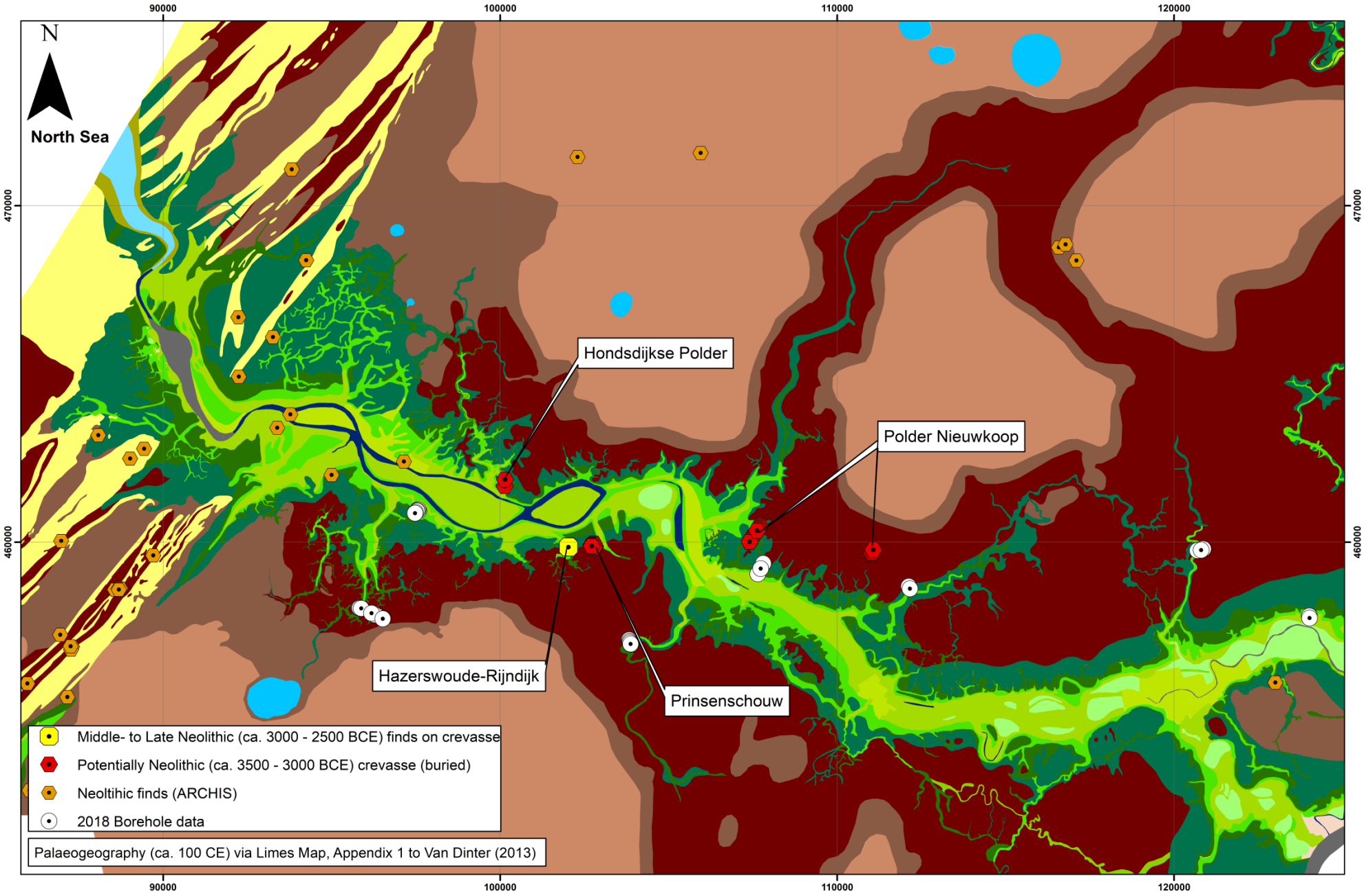

Figure 18: Neolithic Archaeology in the Old Rhine area.

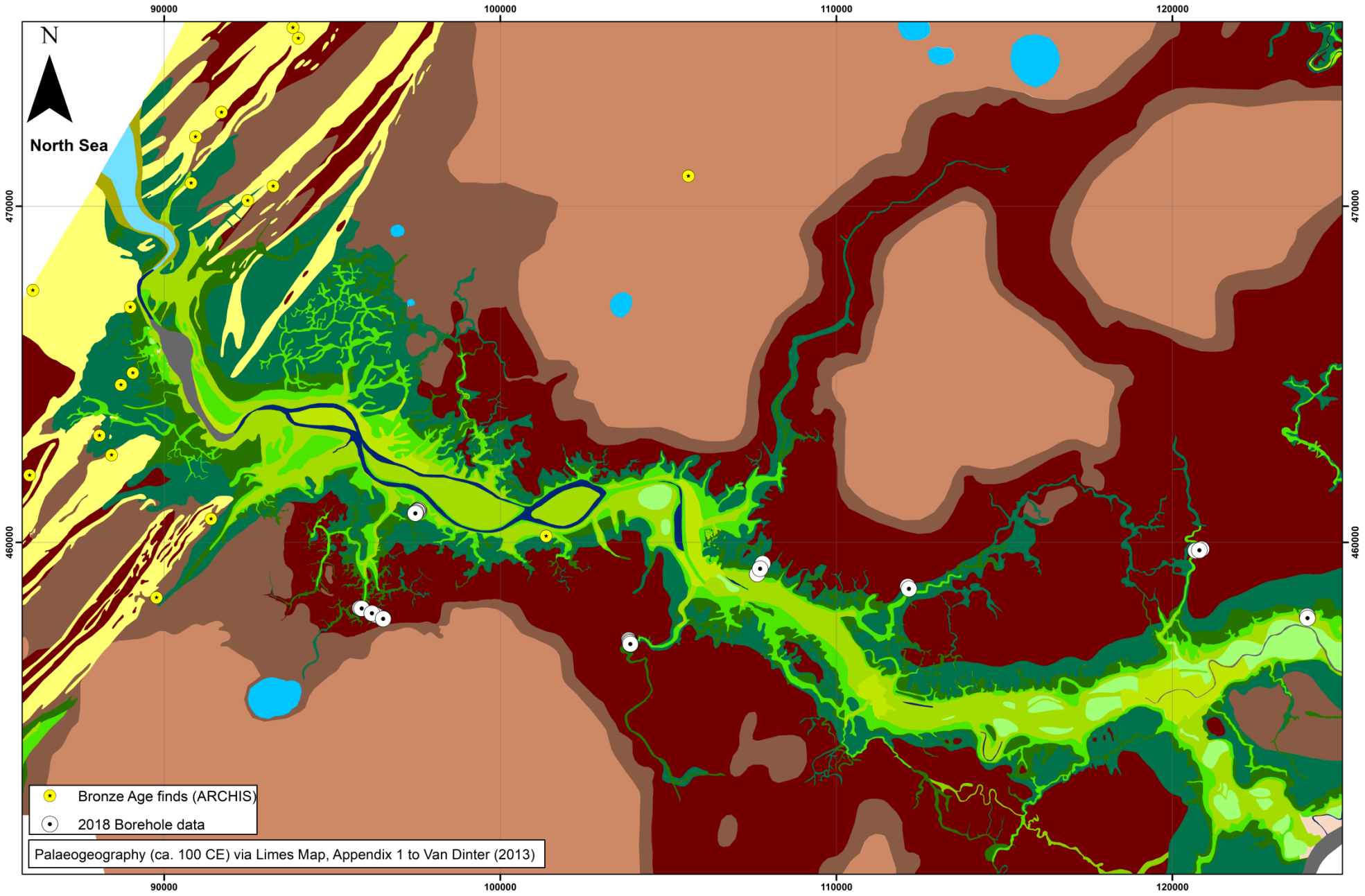

Figure 19: Bronze Archaeology in the Old Rhine area.

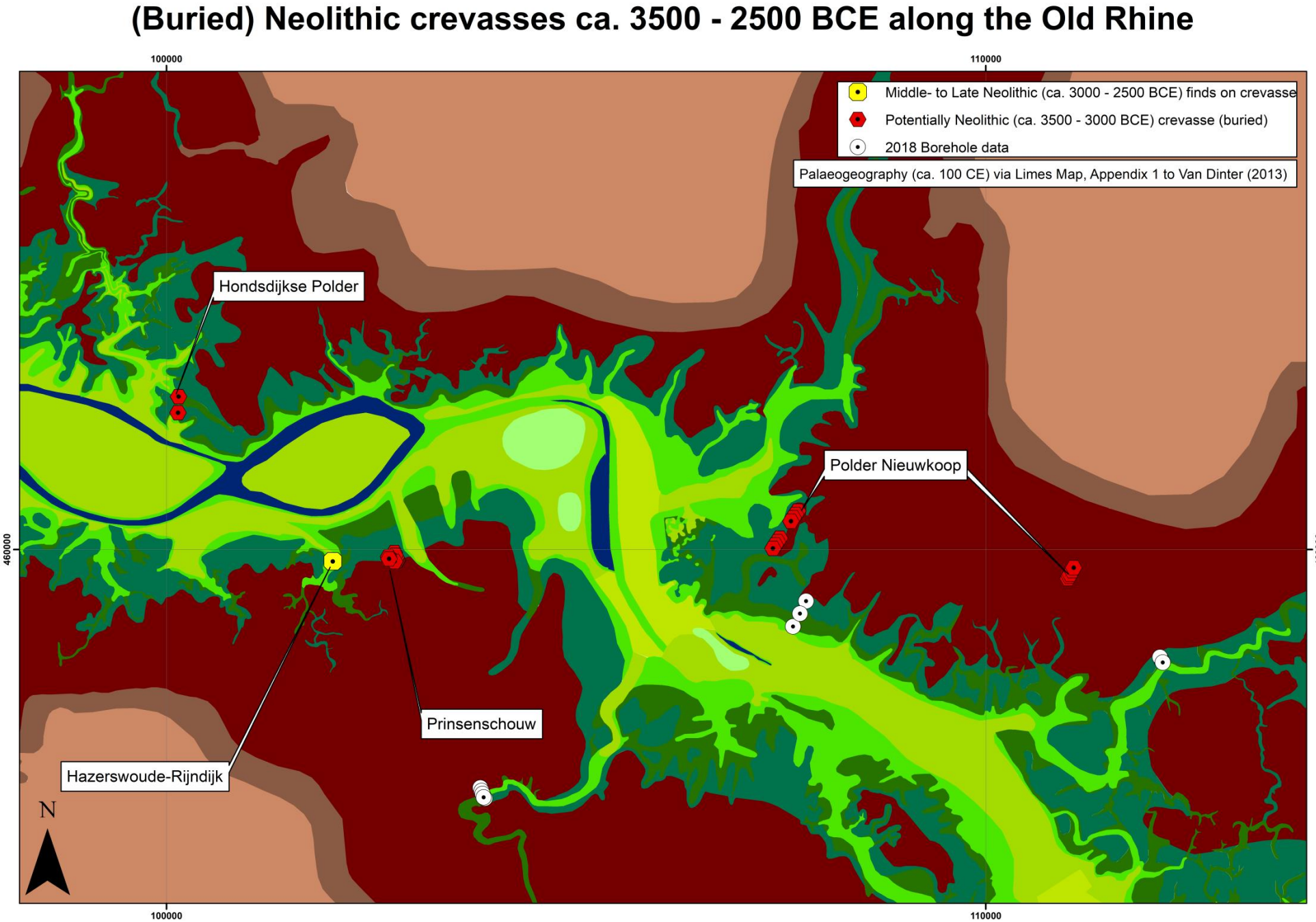

Figure 20: Neolithic archaeological sites and buried crevasses along the Old Rhine.

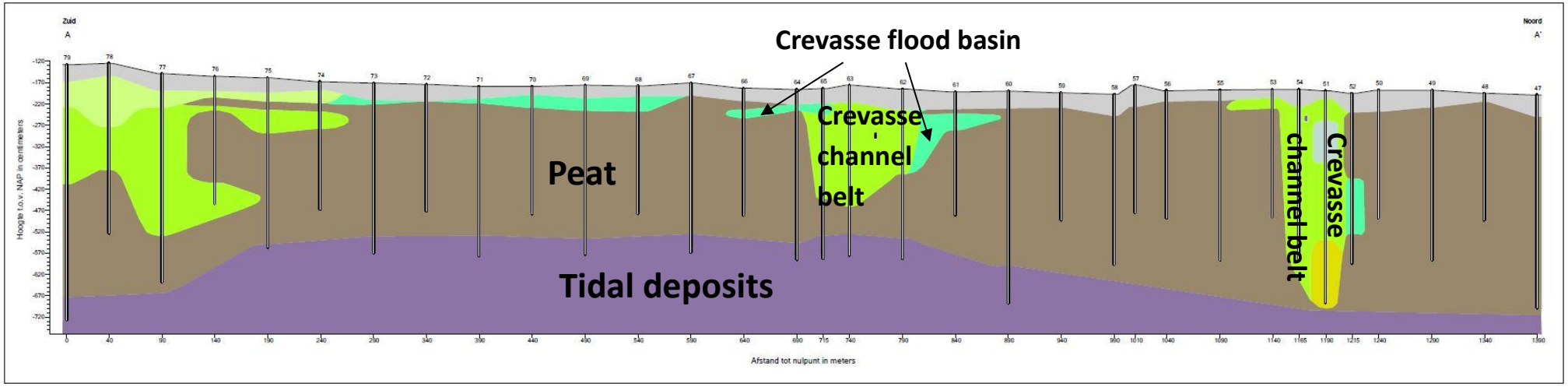

Figure 21: Lithogenetic cross section adopted from Kroes & Feiken (2011).

4.2.2. Middle-Iron Age and Roman remains and sites

The Iron Age (800 to 12 BCE or 2750 to 1962 cal. years BP, figure 22) and especially the following Roman Age (12 BCE to 450 CE or 1962 to 1500 cal. years BP, figure 23) show a marked increase in archaeological remains along the Old Rhine compared the preceding Bronze Age (figure 19) and Neolithic period (figure 18). Nonetheless, during both the Iron and the Roman Age not many archaeological finds from the 2015 ARCHIS database are located on crevasses.

From the Iron Age, archaeological remains are located on three extensive single-channel crevasses at relatively downstream locations, proximal to the Old Rhine's estuary mouth (see figure 24). The most important one regarding this thesis concerns the Zwiet. A cluster of 16 Iron Age finds (toponym Weipoortse Vliet, Municipality of Zoeterwoude), comprising mainly Middle Iron Age (ca. 500 to 250 BCE or 2450 – 2200 cal. years BP) ceramics, wooden poles and animal bone material is located along the course of the Zwiet as preserved in the present-day relief at approximately 1 kilometre distance from the Old Rhine channel belt. This find complex on crevasse deposits thus provides a good indication (*terminus ante quem*) of the age of the Zwiet, namely that its course should have been established at least before the Middle Iron Age. The two other locations, one crevasse ca. 2.5 kilometres downstream from the Zwiet (*i.e.* with the very 'dendritic' pattern), the other ca. 3 kilometres upstream from it (*i.e.* an extensive single-channel crevasse), contain Late-Iron Age (ca. 250 to 12 BCE or 2200- 1962 cal. years BP) ceramics and Iron Age ceramics and features respectively (See figure 24). The latter find complex, on crevasse deposits, is even located along the crevasse channel at roughly 3 to 3.5 kilometres from the Old Rhine channel belt (*i.e.* in the distal reach of the crevasse). This suggests that at least most of the crevasse course was established prior to the (Middle-)Iron ages. These two additional archaeological find complexes thus strengthen the indication of the minimum age of the Zwiet and similar crevasses along the Old Rhine.

Furthermore, Middle Iron Age remains have also been found at crevasse deposits from a reactivation phase of the crevasse stemming from Neolithic times at Hazerswoude-Rijndijk (yellow dot in figures 18 and 20, see also the previous section 4.2.1). The sparse ceramic finds date from the latter half of the Middle Iron Age, which is between roughly 400/390 BCE (*i.e.* 2350/2340 cal. years BP) and 270/250 BCE (*i.e.* 2220/2200 cal. years BP), and indicate only short-lived anthropogenic activity at this location (*i.e.* no permanent settlement) (Diependaele & Drenth, 2010). Kroes & Feiken (2011) reconstructed the build- up of crevasses (purple triangles 'Polder Nieuwkoop' in figures 18 and 20, see the cross-section in figure 21), which are recognizable in the field due to relief differences in the polders of Noordereinder, Zuideinder, and south of Aarlanderveen (were also the buried potentially Neolithic crevasses were found, see previous section 4.2.1). They are hypothesized to have been formed during Middle Iron Age reactivation phase of the crevasse at Hazerswoude-Rijndijk and to thus be of approximately the same minimum age as all the above described crevasses.

Most of the archaeological finds registered in the 2015 ARCHIS database in the Old Rhine area are from the Roman Age period. However, Roman Age remains on crevasses are still relatively sparse. An interesting exception is a find complex at the Zwiet (toponym Zwieten, municipality of Zoeterwoude), albeit at a more proximal location to the Old Rhine channel belt than the Middle Iron Age find complex described above (*i.e.* only ca. 150 – 200 metres away, figure 23). Four ceramic sherds, a feature and part of a revetment, dating from the Early- (12 BCE or 1962 cal. years BP) to the Middle (270 CE or 1680 cal. years BP) Roman Ages indicate human habitation directly on the banks of the Zwiet. Moreover, do the revetments at least

indicate that there was (occasionally) some activity in the Zwiet, although they could also hint at an attempt to prevent an on-going process of in-filling of the channel.

At the upstream border of the Old Rhine area, in the present-day neighbourhood of Leidsche Rijn (municipality of Utrecht) two so-called 'marsh-bridges' over in-filling (former) crevasse channels south of the Old Rhine were found during excavations (Wynia *et al*., 2018). They were part of the limes road, the road which ran along the southern banks of the Old Rhine, which was constructed to enable fast transport between the Roman fortifications along the Old Rhine (see chapter 1). The marsh bridge at Rijnvliet (in the Leidsche Rijn neighbourhood), found in 2018, was most likely built around 100 CE (*i.e.* 1850 cal. years BP) based on the similarity in setting and construction of this bridge compared to a bridge found in the 1990s in Veldhuizen (another part of Leidsche Rijn). Wynia et al. (2018) note that the crevasse channel must have been filled-in for its largest part, based on the stratigraphic sequence underneath the bridge's surface remains. They also state that it was still rather swampy at this time and that it might be fully inundated during occasional Old Rhine flood events, which explains the need to build a bridge.

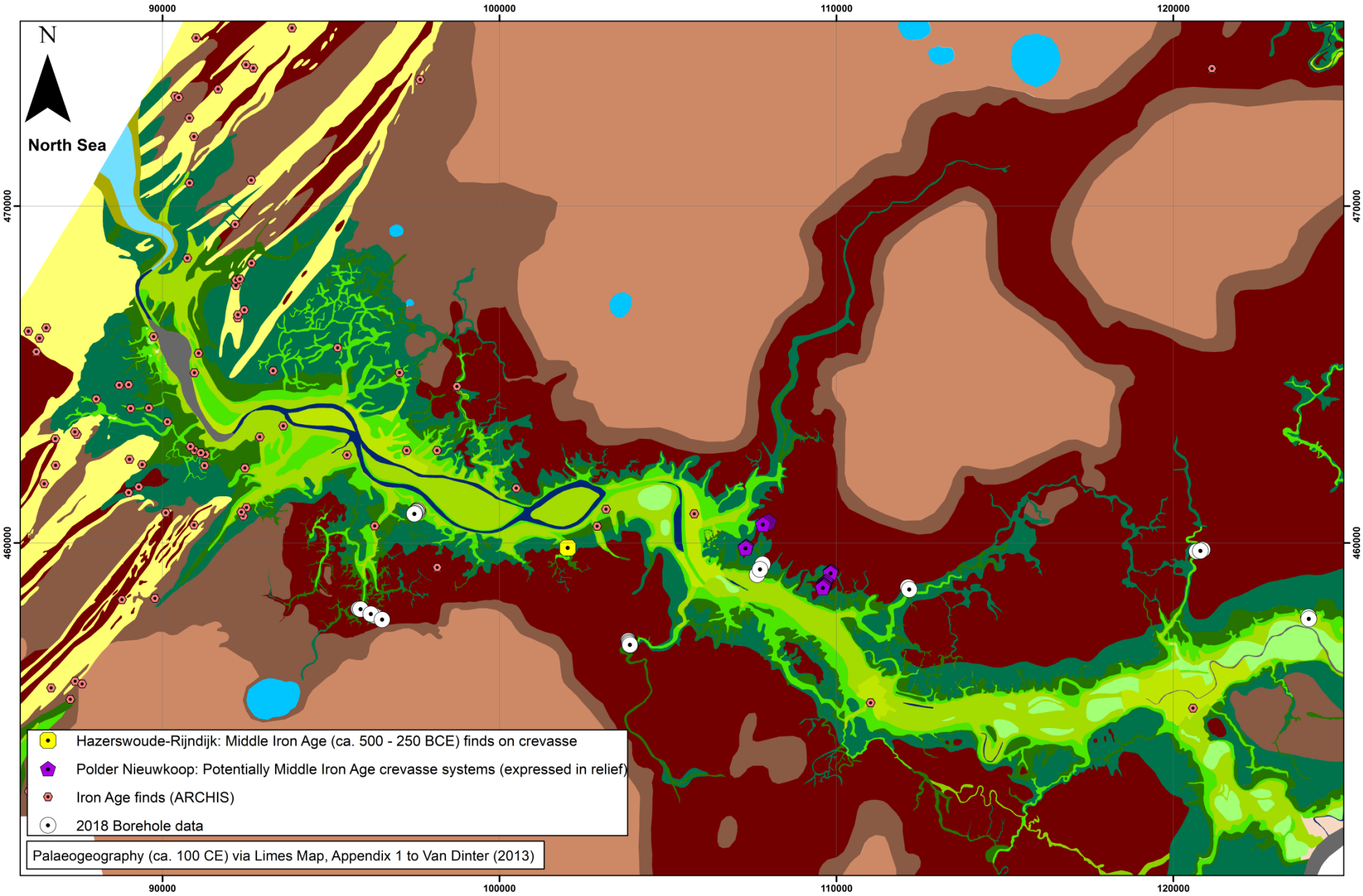

Figure 22: Iron Age archaeology in the Old Rhine area.

Roman Age archaeology 12 BCE - 450 CE (1962-1500 cal. years BP) along the Old Rhine

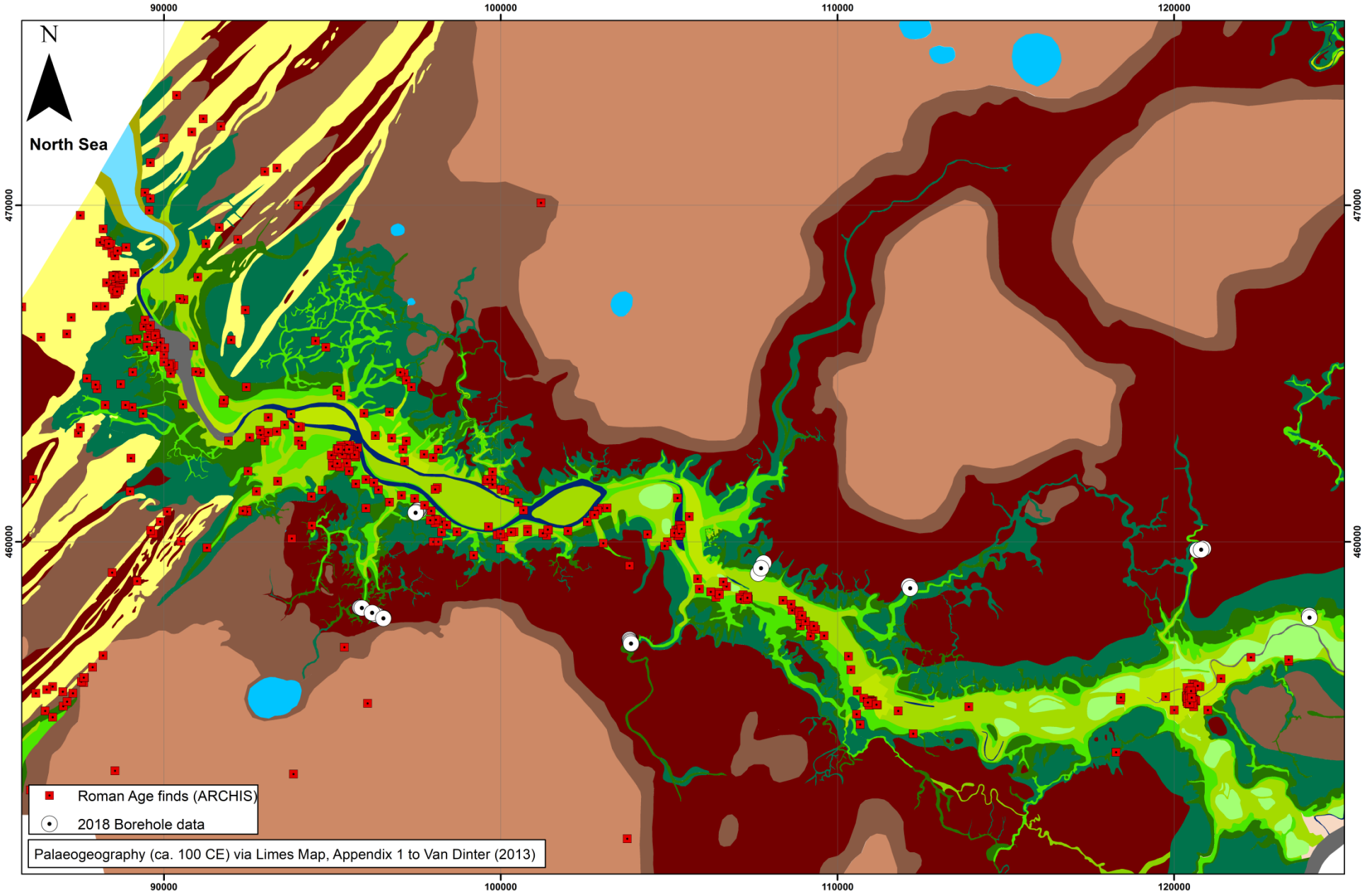

Figure 23: Roman Age archaeology in the Old Rhine area.

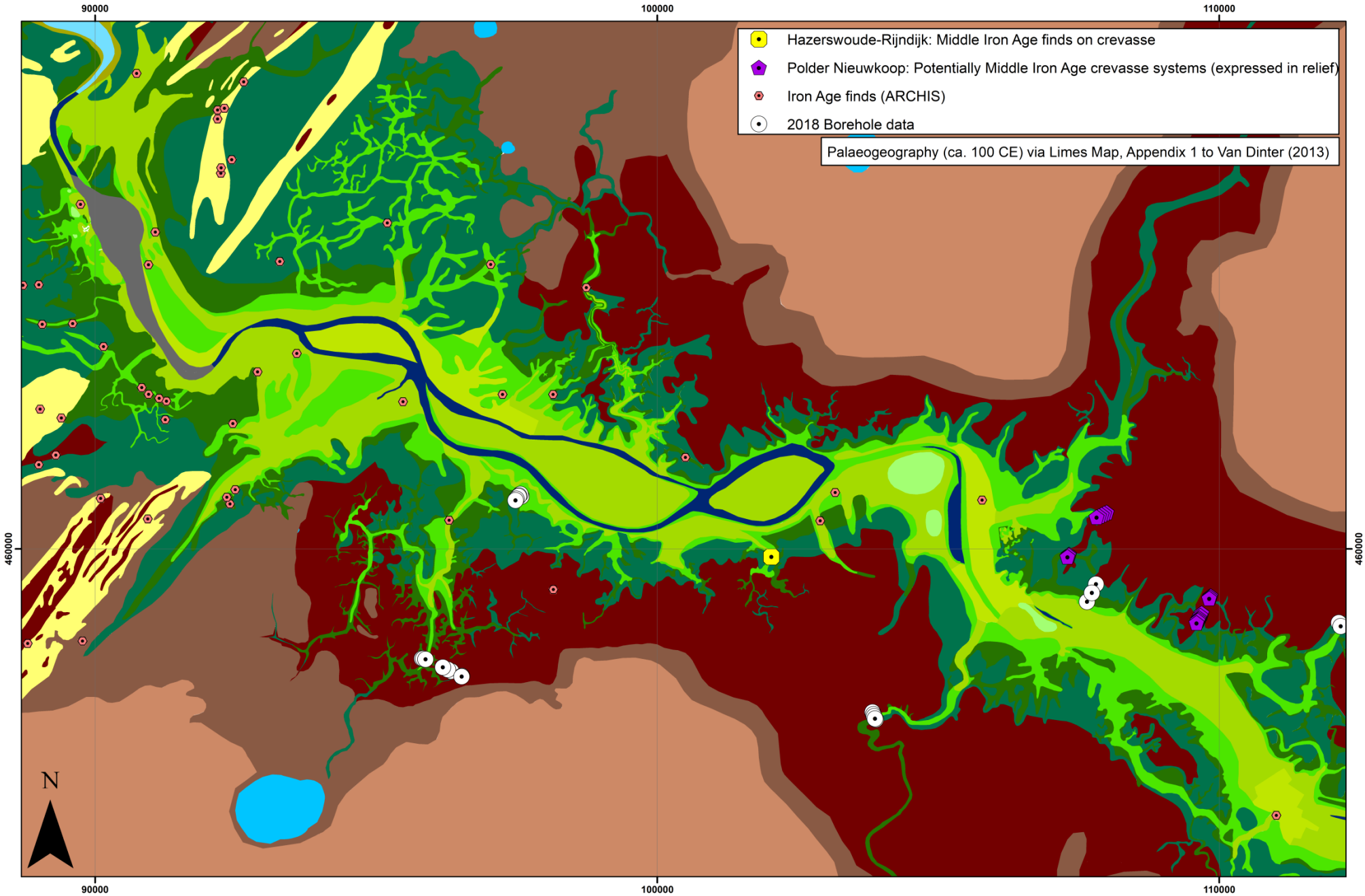

Figure 24: Middle Iron Age archaeological sites in the vicinity of crevasses along the Old Rhine.

4.2.3. Early medieval (Merovingian) remains and sites

Figure 25 shows the palaeogeographic map of the Old Rhine with the selection of Early Medieval (450 to 1050 CE or 1500 to 900 cal. years BP) archaeological finds from the 2015 ARCHIS database extract and two settlements along active crevasse. Less morphodyamic activity took place in the channel belt-flood basin continuum during the abandonment phase of the Old Rhine (see section 2.4) and therefore the configuration of landscape elements during the early Middle Ages is assumed to have not differed much from the configuration during the preceding Roman Ages.

Considering the extensive single-channel crevasses in this thesis, only on the Zwiet have archaeological remains been found, namely four ceramic remains from the later early middle Ages (*i.e* 725 to 900 CE or 1225 to 1050 cal. years BP, see the orange dot in figure 25. These finds indicate that the Zwiet by this time had presumably largely been abandoned, but due to its higher elevation compared to the surrounding flood basin (which possibly had been increased relatively due to differential compaction of the crevasse deposits compared to the adjacent peats) it still formed an attractive place for human activity. The fact that at the same location Early- to Middle-Roman Age remains (ceramics, revetments and features) have been found, and Middle Iron Age remains have been preserved at a more distal location (see section 4.2.2), shows that this location of the crevasse channel formed a suitable place for anthropogenic activity for a prolonged period in the past.

Downstream from the Zwiet, Early Medieval archaeological remains in the vicinity of and on (former) crevasses have been found at two locations (see figure 25). Both sites, at Leiderdorp (Dijkstra *et al*., 2016, the light purple dot in figure 25) and at Oegstgeest (Hemminga & Hamburg, 2006, the pink dot in figure 25) are surrounded by archaeological remains from the 2015 ARCHIS extract from the Early Middle Ages too.

At Leiderdorp, the Leitha crevasse, originating from pre-Roman Age times, was identified during extensive geoarchaeological research into the Leithon settlement (Dijkstra *et al*., 2016). A palaeosol overlying the oldest crevasse deposits is hypothesized to have been formed during the (Late-) Iron Age under calm, low-energetic conditions. This suggests that the oldest crevasse channel activity in the area originates from pre-Iron Age times. During the following Merovingian period (ca. 450 – 750 CE, although no definite ages are given by Dijkstra *et al*., 2016) a shallower successive crevasse channel migrated initially in southern and later in northern direction. The average estimated width of the channel in its final phase was ca. 10 – 12 m, quite similar to the width of the (final stage of the) four crevasse channels considered during the fieldwork. The depth is assumed to be around 1 m, based on aquatic flora remains which were found. Interestingly, Dijkstra *et al*. (2016) note that the channel must have still experienced regular (possibly daily) water level fluctuations due to the tides based on the analysis of pollen, molluscs, and macrobotanical remains. This crevasse channel became abandoned near the end of the Merovingian period, but around 800 CE a new channel formed (possibly a reactivation). Contrastingly, the analysis of molluscs showed that there were no regular water level fluctuations in the channel anymore and that thus the reach of the tides had significantly decreased compared to the preceding centuries. Another, younger reactivation is hypothesized to be initiated by a major storm surge in 838 CE (Dijkstra *et al.* 2016).

Even more downstream, at Oegstgeest (pink dot in figure 25) three small crevasse channels (ca. 20 m broad channel belts and minimum depth of 2 m below the surface) were identified in test excavation trenches, two of which were still active during Merovingian times, dated roughly between 550 – 650 CE, based on ceramics, ^{14}C-, and dendrochronological datings from archaeological remains from the adjacent

settlement (Hemminga & Hamburg, 2006). The third crevasse is older than 550 CE, based on the fact that revetments along its banks together with bundles of branches on the bottom of its channel were put in place in order to counteract the filling-in of the channel. Given their very proximal location to the Old Rhine channel belt, they could have belonged to the same crevasse splay.

Early medieval archaeology 450-1500 CE (1500-450 cal. years BP) along the Old Rhine

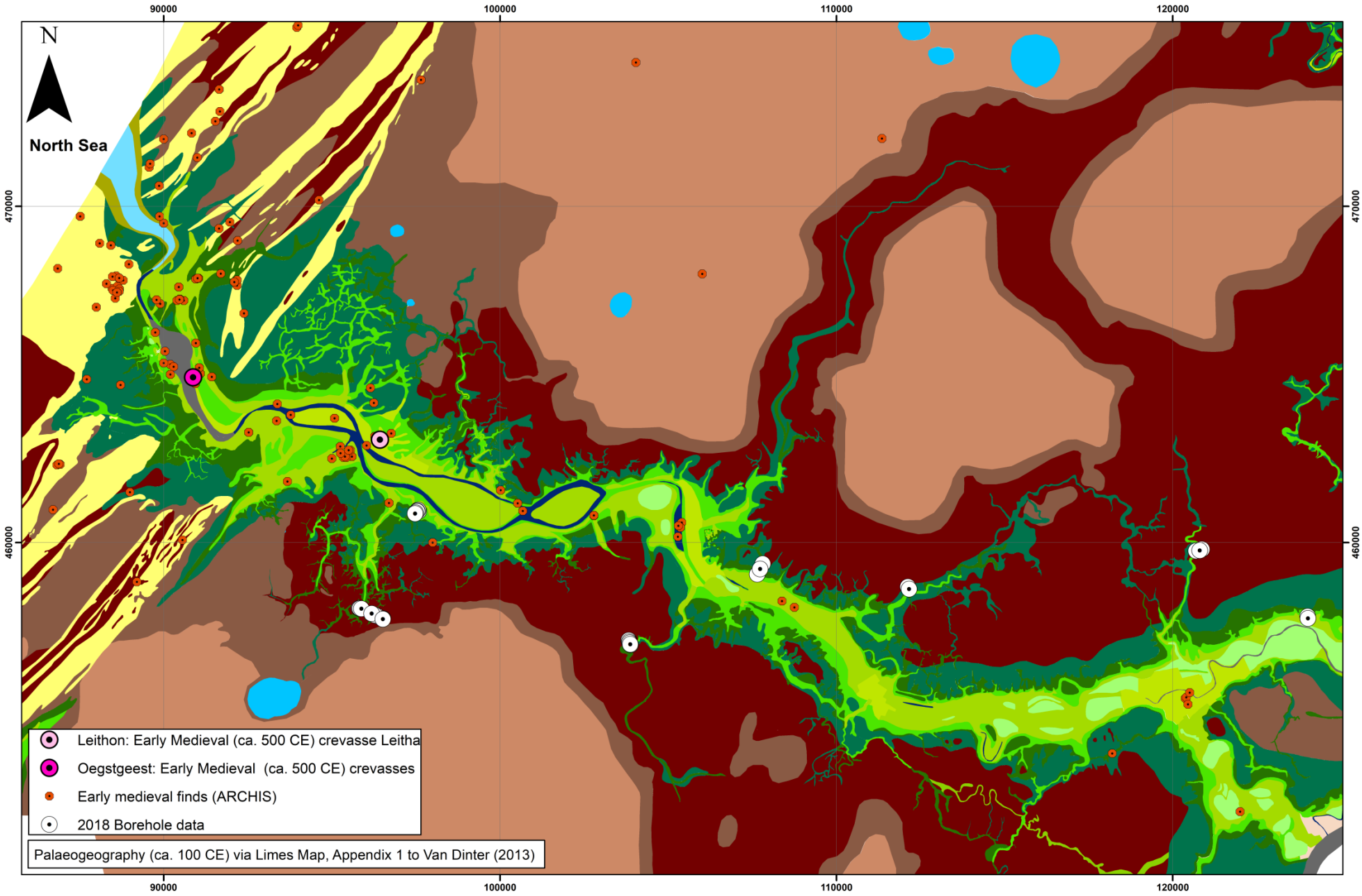

Figure 25: Early medieval archaeology in the Old Rhine area.

4.3 Implications of local crevasse developments for insight into the system-scale evolution

In this section, first the stratigraphy of the four crevasses and their stratigraphic context as described in section 4.1 will be compared to each other. Likewise, a comparison of the planform shape and extent into the flood basin between the four crevasses will be made. Thereafter, the similarities and differences between the four crevasses will be linked to the archaeological remains found on crevasse deposits as described in section 4.2, to infer specific phases of crevasse formation and development. Both the stratigraphic correlation as well as the archaeological remains, thus provide valuable information regarding the minimum and maximum ages of not only the four crevasses reviewed here, but also of similar crevasses along the Old Rhine.

4.3.1 Comparison of crevasse stratigraphy

The deposits of all four crevasses – from upstream to most downstream location the Grecht, the Meije, the Alphen Zuid, and the Zwiet respectively – lay on top of Holland peat deposits (see the lithogenetic cross-sections). The thickness of the underlying peats, however, differs. There is a clear downstream decrease in the thickness of the peats. Underneath the Grecht and the Meije crevasse deposits the peats are a few metres thick, whereas underneath the Alphen Zuid and Zwiet crevasse facies they are only a few decimetres and ca. a metre thick respectively. Moreover, in the cross-sections of the Grecht and the Meije, tidal deposits belonging to the Naaldwijk formation (Wormer member) are absent, whilst thick tidal facies underlying the Holland peats are encountered at the bottom of the cross-sections of the Alphen Zuid and Zwiet. This indicates that the area across which extensive tidal sediments were deposited prior to the closing of the Western-Netherlands coast due to beach barrier formation (see section 2.4) had its inland margin located roughly between the Alphen Zuid crevasse and the Meije, which was already found in earlier research (*e.g.* Zagwijn, 1986).

The natural levee and floodplain deposits of the crevasses are mostly of comparable dimensions and composition. The natural levees are all loamy to silty clayey with a fining upwards trend and contain detritus and fine sand laminations, and occasionally shell gritt and fragments and plant remains. The natural levee of the Meije lies beyond the margin of the constructed cross-section. The natural levee of the Zwiet differs slightly, since it is sandier, and has more abundant laminations at a regular interval, whereas the above-mentioned detritus and fine sand laminations are scarcer. Concerning the flood basins, the overall trends are similar and as expected in each cross-section. The amount of silt present in the floodplains decreases with increased distance from the natural levees of the crevasses. Contrastingly, the organic content of the deposits increases up to ca. 25 m from the natural levees, after which it is assumed to remain roughly constant. Reed and wood remains were identified in parts of all floodplain deposits too.

Another similarity between the four crevasses is that their flood basin deposits are all overlain by younger (former) Holland peats, indicating that peat formation probably started at roughly the same moment at all crevasse locations. Furthermore, the top layer of each cross-section consists of ca. 30-40 centimetres of anthropogenically disturbed silty clays.

There are two important differences between the four crevasses. The thickness of the peat deposits overlying the crevasse deposits decreases in downstream direction along the Old Rhine. In the cross-section of the Grecht, the peat deposits rapidly wedge out from the proximal towards the distal flood basin, where

they are ca. 2 m thick. In the cross-section of the Meije they are at maximum ca. 1 m thick, at the Alphen Zuid crevasse ca. 0.5 m maximally and the youngest peats of the Zwiet cross-section are only 0.1 to 0.2 m thick. These differences could be attributed to varying rates of peat compaction and oxidation at different locations or to different rates of peat growth. A second difference, specifically between the Zwiet and three other more upstream located crevasses, is the presence of two phases of crevasse levee deposits, with an intermittent peat layer in between them. No major differences in channel in-fill deposits were identified.

4.3.2 Variation in planform shape and extent

There is no clear difference in the maximum preserved extent of the crevasses, which is between ca. 6 and 8 kilometres for the four crevasses. Contrastingly, the planform shape of Zwiet crevasse differs considerably from the three other crevasses. As can be seen in *e.g.* figure 25, the Zwiet has a distinctly more dendritic, 'cauliflower-like' network of interconnected channels of variable size near its distal margin. The Grecht, Meije and Alphen Zuid crevasses, on the other hand, are characterized by a single main crevasse channel with no significant minor (side-)channels branching off (at least not preserved in the present-day relief). One of those smaller side-channels of the Zwiet has been investigated during the fieldwork campaign and is thought to be a contemporaneous tidal creek, based on its logged sedimentary characteristics (Appendix D).

4.3.3 Three crevasse phases

Three crevasse phases of the Old Rhine can be identified by combining the results from the parallels in lithostratigraphy of the crevasses (section 4.1 and sections 4.3.1 & 4.2.2) with a rough crevasse age framework inferred from the archaeological remains in or on crevasse deposits (section 4.2).

The oldest and first crevasse phase is characterized by small crevasse splay complexes like the buried crevasses with Neolithic archaeological remains (section 4.2.1). Based on the stratigraphy of these crevasses and the aforementioned archaeological remains these crevasses must have been formed at least before ca. 4500 cal. years BP. The first phase is therefore hypothesized to have lasted from ca. 5500 to 4500 cal. years BP. It would then fall within the range of levee phase 1, for which no lifespan is specified by Roelofs (2019), but which is related to the upstream Werkhoven system, active from 6454 to 4049 cal. years BP (Cohen *et al.*, 2012).

The second crevasse phase is characterized by the formation and development of the extensive single-channel crevasses. Based on the stratigraphy of these systems and the presence of Middle Iron Age finds on the Zwiet and on similar (reactivated) crevasses along the Old Rhine (section 4.2.2), these crevasses must have been formed at least before ca. 2500 cal. years BP. From this *t.a.q.* age and insights from the changes in boundary conditions, it is hypothesized that this phase lasted from ca. 3800 to 2800 cal. years BP. This means that it is roughly contemporaneous with levee phase 2 from ca. 4000 till 2800 cal. years BP, as identified by Roelofs (2019) based on earlier research by Stouthamer (2005), and related to the Houten channel belt system.

The third and last crevasse phase of the Old Rhine is in essence a phase of renewed clastic input into most crevasses. The anthropogenically-disturbed silty clay layer at the top of each crevasse cross section is thought to be deposited during this third crevasse phase. It can be seen as a temporary reactivation phase of these extensive single-channel crevasses, which is related to the increase in suspended sediment load in the

Old Rhine from around 2500 cal. years BP onwards (Erkens, 2009; section 2.5.2). Therefore, the third crevasse (reactivation) phase is hypothesized to have occurred between ca. 2500 and 1500 cal. years BP.

An in depth discussion about the causes and mechanisms behind the beginning and termination of each phase follows in the next chapter.

5. Discussion

In this chapter the palaeogeographic reconstruction of the four crevasses along the Old Rhine through time, as described in chapter 4, will be linked to the changes in up- and downstream boundary conditions of the Old Rhine as summarized in figure 26 and described in section 2.5. By doing so, it is aimed to infer which processes and mechanisms are dominant in intitial crevasse formation, maturation, and ultimately decrease of activity and abandonment. Thereafter, the effects of initial conditions on crevasses are discussed. Then the implications of these findings for the palaeogeography and archaeology of the Old Rhine and the potential of crevasses for natural land-building projects in deltas are described. Finally some recommendations for future research are given.

5.1 Effects of up- and downstream boundary conditions

This section discusses the effect of changes in tidal processes and storm surges (downstream boundary conditions) and fluctuations in (extreme) flood frequency and suspended sediment supply (upstream boundary conditions) on crevasse formation and development.

5.1.1 Downstream boundary conditions: tides & storm surges

Tides

In section 2.3 it was hypothesized that tidal processes positively affect the abundance of crevasses along the tidal-fluvial reach of a lowland river systems and that they increase the period of morphodynamic activity and hence promote crevasse development and maturation.

The influence of regular tidal flushing and backwater-effects on the crevasses along the Old Rhine was already recognized by authors in the distant (*cf.* Berendsen, 1982; Stouthamer and Berendsen, 2001) and more recent past (*cf.* Diependaele & Drenth, 2010; Van Dinter, 2013; De Haas *et al*., 2018a). Berendsen (1982) coined the term perimarine crevasses, which are crevasses of which the formation is enhanced by tides-induced water level fluctuations. The aforementioned authors all observed a spatial trend in tidal influence: it increases towards the estuary mouth. They all based this on the increase in abundancy of crevasse splays and their more dendritic planform shape towards the estuary mouth as recognizable in the preserved last stages of crevasses along the Old Rhine.

The logged composition of crevasse facies confirms the already observed spatial trend of increasing tidal influence in downstream direction. The natural levee facies of the Zwiet and the Alphen Zuid crevasses, the two most downstream located crevasses clearly contain tidally bundled laminations, whereas these are absent in the natural levees of the Meije and the Grecht. It is also confirmed by the fact that the Zwiet crevasse has a distinctly more dendritic planform shape the three more upstream located crevasses.

However, this observed importance of tidal processes was never correlated to the spatial-temporal development of the Old Rhine system nor has it been attempted to reconstruct their relative magnitude throughout the lifespan of the system.

During the first crevasse phase (from ca. 5500 to 4500 cal. years BP), the Western-Netherlands coast was still progradating in western direction (see figure 6 and 7 in section 2.4). Hence, the reach of the tidal backwater effect and thus regular flushing of crevasses was farther inland (*i.e.* compared to the present-day

coastline) at the start of this phase than at the end. Therefore, it is expected that there is a downstream trend in the age of crevasses formed during this phase. Most of the more inland crevasses should probably be centuries older than more seaward-located ones. The magnitude of the tidal prism entering the estuary is not expected to have differed much during this phase, since the estuary dimension and course didn't change significantly (see figure 6 and 7), nor did the tidal range, which remained ca. 1.5 m (Van der Molen & De Swart, 2001b; Hijma & Cohen, 2011; De Haas *et al*., 2018a; see section 2.5.1).

The impact of the tidal backwater effect on crevasses seems to be most evident if the situation during second crevasse phase (form ca. 3800 to 2800 cal. years BP) is compared to the situation during the consecutive centuries. During the second crevasse phase, the formation and maturation of extensive crevasses takes place, whereas after its end no new crevasses are formed and morphodynamic activity in the extensive crevasses diminishes. The end of the second crevasse phase coincides with an on-going process of gradual decrease in magnitude of the tidal prism and in magnitude and reach of the tidal backwater effect.

The third crevasse phase (from ca. 2500 to 1500 cal. years BP), during which most of the extensive crevasses are reactivated seems to be unaffected by and unrelated to changes in the tides, as it took place during a period of ongoing decrease of the magnitude and reach of the tidal backwater effect.

The filling in of the estuary mouth and the change of its course during and after the end of the second crevasse phase led to a decrease in estuary mouth and channel dimensions, reducing the tidal prism entering the system which in turn negatively affected the reach and magnitude of the tidal backwater-effect (see section 2.5.1). Additionally, progadation of the tidal flood wave was hampered by the increasingly sinuous ('swan-neck') shape of the estuary (see section 2.4). Frequent (semi-diurnally) tidal flushing of their inlets decreased significantly and backwater induced water level fluctuations propagated less far up their course. Therefore, the throats of the crevasses, especially the extensive ones which progradated kilometres long into the peatlands, gradually filled in as a result of which less water and sediments could enter the other parts of the crevasse in the flood basin and morphodynamic activity of the entire crevasse decreased. This process of infilling of the crevasse throats probably started earliest at the most inland-located crevasses, as the decrease in tidal backwater effect was most marked there first.

The development of new crevasses was hindered too, as quick crevasse healing was not inhibited anymore by regular tidal flushing, which kept newly formed natural levee breaches (*i.e.* crevasse throats) open. Thus there is a clear difference in establishment of new crevasses during the first and second crevasse phase and after the end of the second crevasse phase.

The reactivation of the crevasses during the third crevasse phase is unrelated to tidal processes. Hence, it has to be related to other processes and factors, which will be examined below.

The present study thus adds a temporal component to the observed spatial trend of tidal influence along the Old Rhine by the identification of three distinct crevasse phases. Comparison of the two led to new insights into the effect the tide-induced backwater effect on crevasses. The hypothesis formulated in section 2.3 is confirmed.

Regular flushing of the crevasse throat induced by the tidal backwater effect is indeed important for preventing quick crevasse healing and thus facilitating crevasse formation and maturation. Tidal flushing, however, does not cause a natural levee to breach, thereby initiating crevasse formation. It has a long-term effect on crevasse development. If it is absent, crevasses seem to be more likely to be quickly abandoned,

leading to a lower number of crevasses being formed and less maturation of crevasses. This confirms the observation Roelofs (2019) that numerical modelling scenarios in Delft3D with increased tidal range led to an increase in abundancy and size of crevasses in the back-barrier system (see section 2.2).

Since the age estimation of the four crevasses is so far solely based on insights from stratigraphic correlation and archaeological remains from associated Old Rhine crevasses, it is too coarse to differentiate between the timing of the start of abandonment of the four crevasses in this thesis. Because the configuration of the Old Rhine estuary (*i.e.* its dimensions and course) is currently assumed to have changed gradually, the extent of tidal influence should have decreased slowly too. If the tides are indeed most important for preventing the crevasse throats from filling in, then it is expected that the process of gradual abandonment started earliest at the Grecht and latest (and perhaps to a lesser extent) at the Zwiet. The difference in timing could range from several decades to one or two centuries at maximum for consecutive crevasse along the Old Rhine, depending on the rate of the decrease of the tidal backwater effect and local conditions at the crevasse throat and in the flood basin. Traces of Early Medieval human habitation both at Oegstgeest and at Leithon along infilling crevasses (see section 4.2.3), provide some insight in this respect. They indicate that some very downstream-located crevasses were still in the abandonment phase in the last centuries of the Old Rhine's activity, whereas most of the more upstream-located crevasses were already abandoned by this time. The results of the ^{14}C-dated deposits will provide a more detailed overview. Future more detailed insights into the change in configuration of the Old Rhine estuary, concerning both the spatial as well as temporal resolution, will benefit the understanding of the differences in abandonment of the crevasses too.

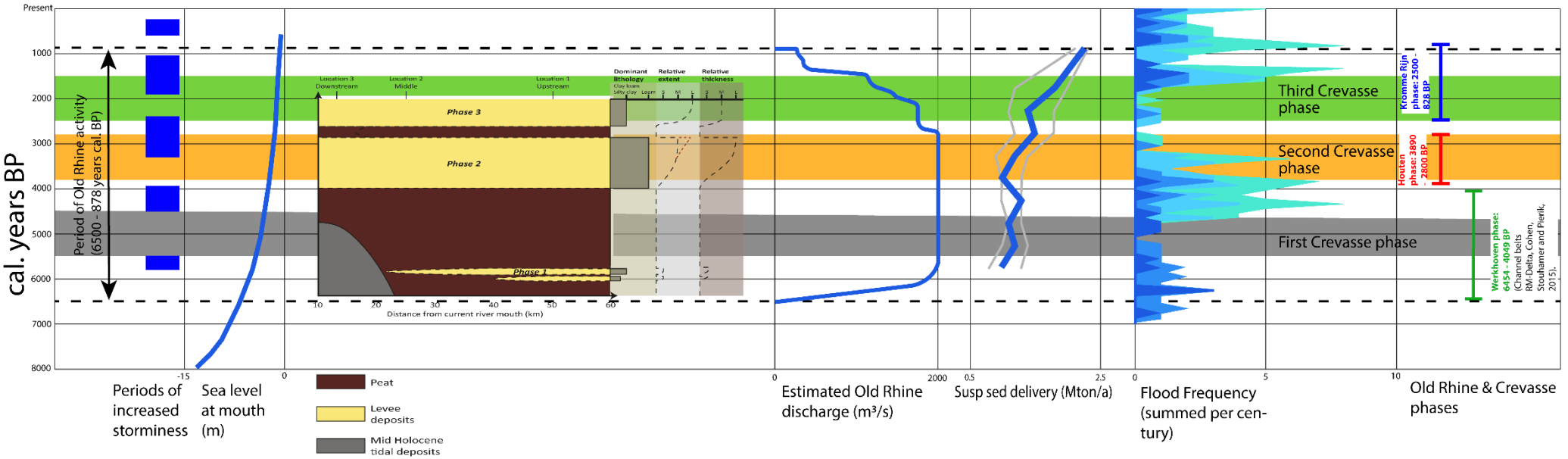

Figure 26: Boundary Conditions of the Old Rhine system, Old Rhine channel belt, natural levee and crevasse phases. **Boundary conditions** – (see figure 8); **Old Rhine activity** – (see figure 8); **Channel belt phases** – (Cohen *et al*., 2012; Stouthamer, 2005); **Natural levee phases and dimensions** – (Roelofs, 2019); **Crevasse phases** - (this study).

Storm surges

In addition to the changes in tidal influence, the frequency of North Sea storm surges is another potentially important changing downstream boundary condition. Storm surges can propagate relatively far upstream in the tidal-fluvial realm of river systems. During roman times (ca. 2000 cal. years BP), saline storm surge water could reach up to at least 15 kilometres upstream from the Old Rhine estuary mouth, as indicated by palaeo-ecological research (Van Amen & Brinkkemper, 2009; Van Dinter, 2013). Especially the more severe ones can thus have a large impact on crevasses. The timing of the four identified periods of increased storminess in the northern Europe coastal regions within the lifespan of the Old Rhine system (Holocene Storm Periods, see section *2.5.1*) does not correlate well with the timing of the overbank or the crevasse phases (see figure 26). It has to be noted, of course, that this is not the reconstructed degree of storminess for the Western-Netherlands coast specifically. It is likely that (most) storm surges which were relevant for the Old Rhine were not included in the record of Sorrel et al. (2012), which distorts the comparison of the crevasse phases with the periods of increased storminess.

Both the first and the third crevasse phase are within periods of relatively calm storm conditions. Only during the latter half of the second crevasse phase (from ca. 3300 to 2800 cal. years BP) there is an increase in storminess as Holocene Strom Period III is from ca. 3300 to 2400 cal. years BP (Sorrel *et al.* 2012 and figure 26). Therefore, storm surges might have had a positive effect on crevasse enlargement, and ongoing progradation and maturation. Besides, storm surges had the potential to effectively block river discharge at the estuary mouth, thereby raising the water levels at the downstream margin of the Old Rhine and consequently enhancing the reach and magnitude of the back water effect in the Old Rhine (Van Dinter, 2013; De Haas *et al.*, 2018a; Roelofs, 2019). Thicker than usual sand laminations present in the logged crevasse natural levee facies (at locations close to the estuary mouth) could be correlated to a major storm surge event. It is unlikely that a major flood event transports such relatively coarse sediments to the distal parts of the crevasse channels and flood basins, since most of its coarser-sized sediments are deposited at more upstream locations near the Rhine-Meuse delta apex under regular flow conditions and more proximal to the Old Rhine channel belt under (extreme) flood conditions. On the other hand, sufficient volumes of sand would have been available just west of the estuary mouth as part of the ebb-tidal delta, which were prone to erosion and subsequent extensive transportation during (large) storm surge events.

5.1.2 Upstream boundary conditions: flood events, discharge and suspended sediment supply

Floods & River Discharge

The most important changing upstream boundary condition is the flood frequency. In section 2.3 it was hypothesized that an increase in the frequency of flood events of different magnitudes leads to an increase in the number of crevasses and is the driving factor in crevasse progradation and development. In the literature review (section 2.2.1) it was mentioned that flood events cause the formation and promote the evolution of crevasses (Knighton & Nanson, 1993; Slingerland & Smith, 2004; Toonen *et al.*, 2016).

Below, the timing of periods of high flood frequency from the flood record by Toonen (2013) (see section 2.5, figure 8, and figure 26) is compared to the crevasse phases to assess whether more crevasse formation and progradation took place.

Periods of high flood frequency which coincide with crevasse phases are: *i)* from 5000 to 3000 cal. years BP, during which most of the second crevasse phase (from ca. 3800 to 2800 cal. years BP) takes place and *ii)* from 1700 cal. years BP until present, during which the last part of the third crevasse phase (from ca. 2500 to 1500 cal. years BP) takes place (Toonen, 2013; Cohen *et al*., 2016) see figure 26).

The second half of the first period of high flood frequency is concurrent with the second crevasse phase during which extensive crevasses develop. Within this period there is a ca. 100-year period around 3300 cal. years BP with relatively many extreme floods (Cohen *et al*., 2016; 44). The abandonment of the major crevasses during this phase (2800 cal. years BP) follows shortly after the end of this high flood frequency period.

Between roughly 3000 and 2000 cal. years BP, the most extreme floods are absent (or not recorded) and minor flood events are rare. Crevasse formation and maturation strongly decreased or was even absent at all. The Middle Iron Age (ca. 2500 cal. years BP) archaeological remains on crevasse deposits are from this relatively calm period, during which the already developed crevasses formed attractive locations for human habitation and were not yet fully covered in peat (see section 4.2).

The decrease in frequency of flood events concurs roughly with the onset of gradual loss of discharge in the Old Rhine due to a series of upstream avulsions (figure 26, section 2.5.2). There is no causal link between the decrease in flood frequency and discharge. Their more or less simultaneous timing seems to be purely coincidental. Besides, it has to be noted that the discharge remaining constant during most of the Old Rhine's lifespan is only an assumption, about which there is still a lot of uncertainty.

The loss of discharge had a negative effect on the influence of tidal processes as it contributed to the change in configuration of the Old Rhine estuary (see section 2.4). It led to an increase of the influence of longshore currents relative to the outflow of river and tides, which eventually caused the mouth of the estuary to shift northwards. As a result, the shape of the estuary's course changed from a rather straight broad funnel to a narrow increasingly sinuous ('swan-neck') course, which led to a decrease of the tidal prism ins the estuary.

During the second period of high flood frequency from ca. 1750 cal. years BP until present no widespread formation of new crevasses or progradation of established crevasses took place.

The roughly simultaneous end of the second crevasse phase and the end high flood frequency period indicates the importance of frequent (extreme) flood events for crevasse formation and progradation – in this specific case in combination with regular flushing by tidal waves and tide induced backwater-effects.

The important facilitating role of tidal flushing is indicated by absence of crevasse formation and development during the period of increased flood frequency from 1700 cal. years BP onwards. The difference between the first period of high flood frequency and the second is the strong decrease in the tidal prism and tidal flushing of the crevasses induced by the tidal backwater effect during the latter. Regular tidal flushing of the crevasse throat is vital to prevent quick abandonment of newly formed crevasses, as already stated in section 5.1.1. Hence, new crevasses could be formed during the second period of high flood frequency, but these are either poorly preserved or very limited in extent (and consequently not recognized along the Old Rhine if present).

Flood events are important for the formation and maturation of crevasses on two time-scales. First, they initiate the breach of the natural levees and the formation of proximal crevasse splays on an event time-scale. Second, subsequent flood events are the prime cause of crevasse progradation during the following decades and centuries. Tidal flushing does not cause a natural levee to breach, but prevents rapid filling in of the breach, which is especially important if the next flood event follows after several decades during which the breach would almost completely fill in. Storm surges probably have a comparable effect on crevasse formation and maturation as they can also cause the initial levee breach and progradation of established extensive crevasses.

The findings regarding the effect of flood events confirm earlier findings by Knighton & Nanson (1993) and Slingerland & Smith (2004) that floods cause crevasse formation and promote progradation. This study adds a new insight in the effect of tidal flushing of crevasse throats. Tidal flushing is a conditional factor facilitating crevasse maturation by preventing filling in of the crevasse throat. Tides are diurnal or semi-diurnal and thus have a continuous effect on crevasses. Large flood events and storm surges, on the other hand, are extreme events taking place irregularly, which cause most morphodynamic activity: the initial levee breach and crevasse progradation.

Suspended sediment supply

The increase in suspended sediment supply from ca. 2500 cal. years BP onwards due to anthropogenic deforestation in the upstream parts of the Rhine river catchment area can be correlated to the deposition of generally finer sediments on top of the peat deposits overlying crevasse flood basin sediments and channel in-filling sediments respectively.

The reactivation of the four crevasses during the third crevasse phase (see figure 26 and section 4.3) is probably caused by a combination of the increase in flood events and the continuous increase in suspended sediment load. It started due to the increase in suspended sediment form ca. 2500 cal. years BP onwards and was later intensified by the increase in flood frequency. In the crevasse cross-sections it is characterized by a thin (silty) clay layer on top of the peats overlying the crevasse facies from the second crevasse phase. It falls within the third overbank phase of the Old Rhine as identified by Roelofs (2019) and linked to the Kromme Rijn channel belt phase identified by Stouthamer (2005) (see figure 26). The extensive crevasses, such as the four crevasses analysed in this thesis, were most probably in different stages of abandonment, which moreover differed spatially along the course of each individual crevasse too. The more upstream located crevasses presumably acted as in-filling peat drainage channels since the decrease in tidal influence, frequency and Old Rhine discharge (see the next section). This seems especially true for the Meije crevasse, which is still conveying discharge until present-day (albeit no peat drainage water anymore). On the other hand, the more downstream, seaward located crevasses received clastic input and were regularly tidally flushed for a longer time (*e.g.* the Leitha and Oegstgeest crevasses described in section 4.2.3 and the Zwiet). Therefore, the degree to which each crevasse was reactivated will have differed too. The reactivation will have mostly been limited to deposition of fine sediments during major flood events, during which the crevasse channels acted as suitable depressions in the flood basin peatlands rerouting excess river waters to the distal flood basin parts.

The third crevasse phase roughly coincides with the timing of the first clastic input into the ‘tidal peat drainage channels’ (*e.g.* the Vlaarding, Harg, Schie and Rotte) along the New Meuse Estuary to the South which is dated around 2100 cal. years BP (Cohen *et al.*, 2012). It also falls within the period when many

avulsions in the more upstream parts of the Delta occur (Stouthamer & Berendsen, 2001; Cohen *et al*., 2016; Van Dinter *et al*., 2017; Pierik *et al*., 2018). The authors mention that older main channels became increasingly prone to avulsion as different branches and crevasses along their course had an increased and more efficient deposition on their natural levees due to the increase in suspended sediment. This increased sediment loading caused accelerated peatland subsidence as a result of which the flood basin gradient increased as well, up to a point where it had an advantage over the average gradient of the Old Rhine. Thus the avulsion potential was severely increased.

5.2 Effects of initial flood basin conditions

Apart from changes in boundary conditions of the Old Rhine which affect crevasses, the initial flood basin conditions have an effect on crevasse evolution too. This section discusses the effects of the presence of peatlands with raised bog domes and peat drainage channels in the flood basins on the evolution of crevasses. It is postulated that some of the more extensive crevasses along the Old Rhine were formed as hybrid crevasse-peat drainage systems.

Flood basin peatlands development

As described in section 2.4.3, since 5700 cal. years BP peat formation took place in the West-Netherlands former back-barrier basin behind the beach barriers which closed the Holland coast (Vos, 2015; Pons, 1992). The peat developed from eutrophic reed peats to forest peats. Unfortunately, there are no detailed reconstructions of the development of the spread of different peatland types before Roman times. Nonetheless, the raised sphagnum bogs and their peat drainage channels were most probably already established after ca. 2000 years since peat formation had started, around the beginning of the second crevasse phase 3800 cal. years BP (see section 2.4.3). Moreover, the configuration of the different types of peatlands within the peat areas of the flood basin of the Old Rhine is not expected to have differed much from the situation around 100 CE as reconstructed by Van Dinter (2013). The total area of raised bogs might have been overestimated in this reconstruction. Only the extent and height of the raised bogs, as well as the type of peatland at a local scale might have differed.

Peat is generally more erosion resistant than *e.g.* aeolian cover sand deposits and thus hampers crevasse channel progradation and lateral migration (see section 2.2.2). The presence of a pre-existing network of shallow peat drainage channels as depressions in between raised bog domes provided ample potential locations for the ‘avulsion by annexation’ type of crevasse development as mentioned by Slingerland and Smith (2004) (section 2.2.1). With this background knowledge in mind, the peat drainage channels, formed efficient channels for interception of excess crevasse discharge from a nearby progradating crevasse channel during a river flood event or storm surge. Since other relict channels were absent in the peatlands, the peat drainage channels formed the only potential channels to be captured by the crevasses. Therefore, at least the three most upstream located crevasses studied in this thesis (*i.e.* the Grecht, Meije, and Alphen Zuid) are presumed to have adopted the course of pre-existing peat drainage channels, turning these into hybrid crevasse-peat drainage channels. The roughly similar distances between these three crevasses favours this hypothesis, since the pre-existing peat drainage channels are expected to have been located at comparabledistances from each other. The Zwiet is assumed to have not adopted the course of a pre-existing peat drainage channel. Because of its different, more dendritic planform shape and location close to the coast it is thought to have evolved from or taken over part of a tidal creek system.

The mechanism of peat drainage creek adoption is visualized in figure 27. The formation of natural levees along the hybrid crevasse-peat drainage channels led to compaction of the underlying peat, which became more erosion resistant and thus prevented lateral crevasse channel migration even more (*cf.* Pierik *et al.*, 2018). However, it cannot be reconstructed at which moment during crevasse progradation or at which location along the course of the peat drainage channel annexation took place per individual crevasse. After a peat drainage channel was intercepted by a crevasse channel, the latter conveyed at least a part if not all of the drainage from the raised bog domes formerly discharged by the peat drainage channels. Gradually the peat drainage channels transformed into hybrid-crevasse peat drainage channels due to a progressive increase in sediment influx from the Old Rhine. Consequently, the planform shape, course and extent of Grecht, Meije, Alphen Zuid and presumably other similar extensive crevasses were to a variable degree determined by the pre-existing courses of the peat drainage channels, which on their turn are strongly related to the peatland configuration and the general slope of the West-Netherlands Rhine-Meuse delta.

Most of the extensive crevasses along the Old Rhine therefore acted at least for part of their existence as hybrid crevasse-peat drainage systems (which was already hypothesized by de Haas et al, 2018a). As such, these cannot be classified within the standard classification scheme for crevasses as constructed by Smith et al. (1989) and modified by Farrell (2001) (see section 2.2).

The above-described process of peat drainage channel occupation can be compared to the mechanisms leading to connection between progradating crevasse channels and expanding tidal creek ingressions inferred by Pierik et al. (2018). In their study they describe the processes and feedback mechanisms of human-induced avulsion. Progradating crevasse channels of the Rhine from the Central Rhine Meuse delta connected with expanding tidal creek ingressions from the Old Meuse estuary in the peatlands in between the Old Rhine and Old Meuse estuary. The formation of the hybrid crevasse-peat drainage channels of the Old Rhine differs from the connection between the two above described expanding types of systems. In the case of the crevasses of the Old Rhine, only the crevasses were actively expanding their course and a connection between the crevasses and the peat drainage channel was established at a certain point along the course of the peat drainage channels, not at the distal ends of both systems (as is the case in the study by Pierik et al. (2018)). Nor were the hybrid crevasse/peat drainage channels likely to lead to a full-avulsion of the Old Rhine to either the North or the South. The distal (upstream) ends of the (former) peat drainage channels were located at the edges the raised bog domes, and hence there was no gradient advantage over the main course of the Old Rhine. Moreover, there was no other major river system present north of the Old Rhine which could be ‘captured’ by a potential avulsion.

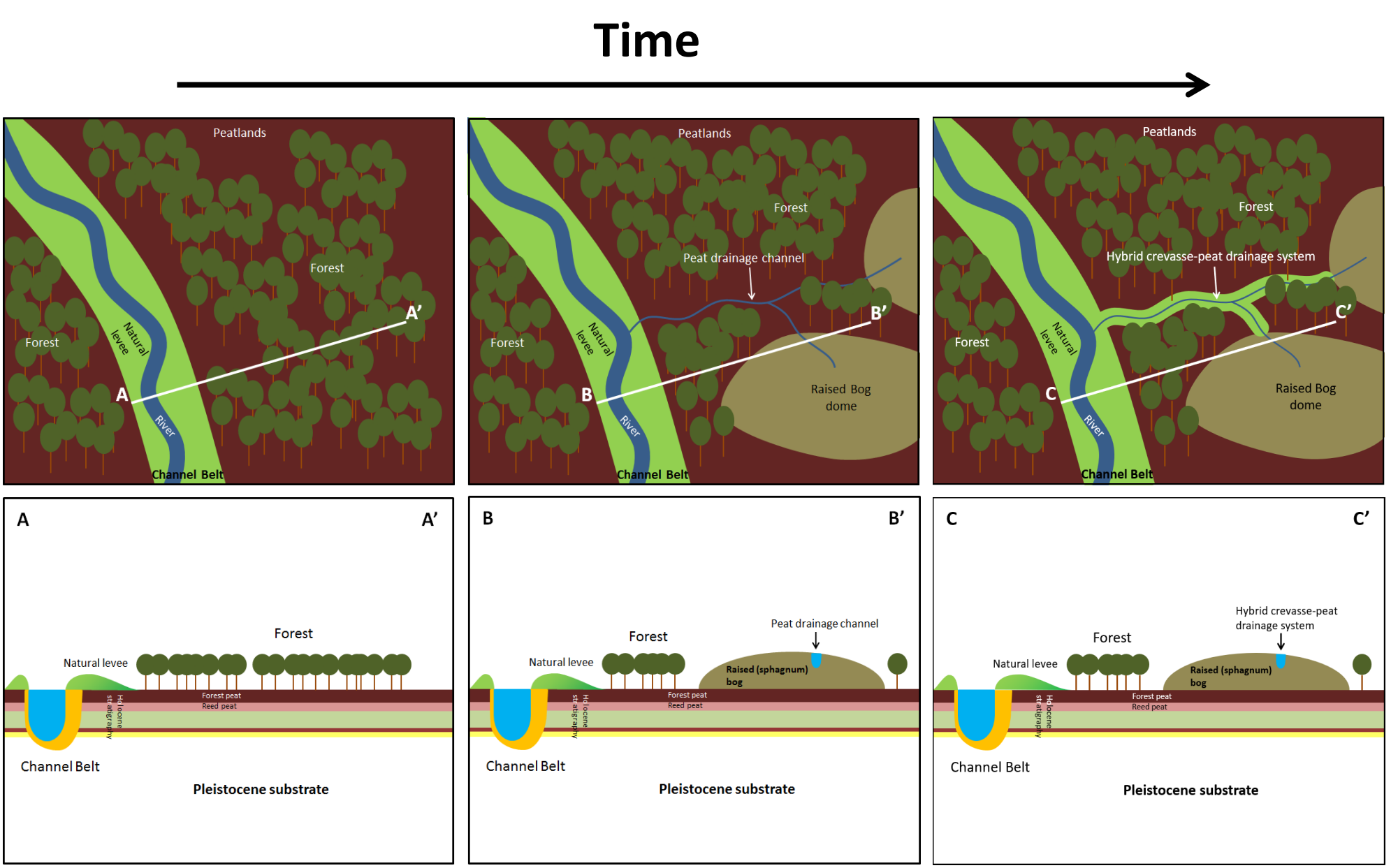

Figure 27: Schematized peat drainage channel take-over by a crevasse.

5.3 Implications

5.3.1 Implications for palaeogeography and archaeology

The coarse chronologic framework of three distinct crevasse phases in the Old Rhine system's history, as identified and analysed in section 4.3 and 5.1 & 5.2 respectively, together with the analysis of the archaeological remains present in the Old Rhine area in section 4.2 enables a refinement of the archaeological expectation of crevasses of the Old Rhine. Crevasses form attractive spots for human activity as they have a relatively high elevation compared to the surrounding flood basin clays and peatlands and can be quickly reached from the Old Rhine. Hence, better insight into the timing of the maturation of the crevasses leads to a better indication of when these systems became (most) suitable for human occupation.

Palaeogeographic maps can be updated with the current understanding of the different stages of the development of the crevasses along the Old Rhine. Coupled with the insights from the archaeology along the Old Rhine, this leads to a more refined expectation of the potential of traces of human activity from a certain period on a specific location. Moreover, the reconstructed spatio-temporal crevasse development makes it possible to get an idea about the taphonomy of archaeological remains from certain periods. Consequently, at particular locations it can be expected that remains are either very well, partly, or not at all preserved. Periods characterized by more morphodynamic activity (*e.g.* due to increased flood frequency or more storminess) provide either better (*i.e.* via increased sedimentation) or worse (*i.e.* via increased erosion) conditions for preservation of material culture. High sedimentation rates lead to rapid burying of archaeological artefacts and ecofacts, which effectively seals them of from oxygen and decreases the chance of damage due to erosion, increasing their potential for preservation. It is expected that in the case of the Old Rhine this led to more and better preservation of archaeological remains overall. On the other hand, periods of increased flood frequency or storminess can lead to worse conditions for human subsistence in the whole Old Rhine system, thereby potentially decreasing the human population in an area and consequently the number of archaeological remains (Groenewoudt *et al*., 2019). The remaining anthropogenic presence could, however, concentrate on the most attractive location(s) in the landscape, in this case the relatively highly crevasses (Van Dinter & Van Zijverden, 2010). Therefore, increased morphodynamic activity on crevasses can have both reinforcing and reducing effects on the archaeology of crevasses. The absence of archaeological remains from the Bronze Age period (section 4.2.1) as opposed to the relatively large number of Middle Iron Age finds could be related to this phenomenon, as the former mostly coincides with the last phase of a period of increased flood frequency (section 2.5.2 & 5.1.2), whilst the latter is set within a period of relatively few flood events. This is of course without taking any cultural processes or ecological changes into account.

Earlier studies into the archaeology of crevasses (*e.g.* Van Dinter & Van Zijverden, 2010) focused mainly on human activity on crevasse splays in the Rhine Meuse delta, at relatively close distance from the main river system channel belt. These proximal locations along the river channel belt are considered the prime locations where archaeology on crevasse (splay) deposits can be expected, given their easy, nearby access to the river channel for transport (Van Dinter & Van Zijverden, 2010). Along the Old Rhine, the same apparent pattern can be observed. The analysis in section 4.2 indicates that human activity was mostly present near the Old Rhine channel belt. However, there is a bias in the registered and reported archaeology from the former Old Rhine channel belt and flood basin. Given the fact that most urban and industrial areas are located along the Old Rhine channel, whereas the flood basins mostly consist of agricultural areas, the

vast majority of (large-scale) spatial development projects takes place in the urbanized areas and not in the agricultural meadows. Hence, it is likely that there is an underestimation (underappreciation?) of the expectation of archaeological remains on more distal crevasse deposits.

The third crevasse phase from ca. 2500 until ca. 1500 cal. years BP is significant for the conclusions drawn by Van Dinter (2013), which were later adopted by, amongst others, Van Ginkel & Vos (2018). She concluded that the location of Roman fortifications (part of the so-called *limes* border-defense system) along the Old Rhine was primarily based on the location of bifurcations and the throats of small tributary streams of the Old Rhine (see section 1.2). The Grecht and Meije crevasses concerned in this thesis are prime examples of such small tributary streams of which the entrances were guarded by forts (*i.e. castella*). They are assumed to have formed natural transport routes from the flood basins to the Old Rhine. During the reactivation phase of these systems they still mainly acted as peat drainage channels, discharging most of the excess water of the raised bogs in the flood basin peatlands. Regular tidal flushing of the throats of these systems had decreased or altogether ceased, resulting in silting up of their channels. A flood event or storm surge led to temporary renewed flushed and sedimentation in these systems. It is therefore likely that the increasingly shallow Grecht and Meije were unsuitable for large-scale (military) transport for most of the year or even for periods of consecutive years. Nonetheless, as they were still inundated during the Roman presence in the Old Rhine area, it is very likely that they were still conceived as a source of potential treat by the Romans.

Constrastingly, the Zwiet and the Alphen Zuid crevasses were located on the southern banks of the Old Rhine channel belt, within the borders of the Roman Empire. As such, they weren't considered as much of a potential threat as the Meije and the Grecht. On Van Dinter's (2013) map (Appendix A) it is assumed that watch towers were built both at the location of the Zwiet's as well as the Alphen Zuid's throat. Remains of these building have not been found yet, however. Watchtowers are smaller-scale fortifications than the *castella* near the Meije and the Grecht. There was no need to build *castella* at the Zwiet and Alphen Zuid because of the general lack of potential threat coming from these crevasses. A watchtower manned by only a small amount of soldiers was deemed sufficient to guard them. If need be, additional troops could be send rather quickly considering the presence of nearby *castella* and the limes road in between the fortifications along the Old Rhine. In the case of the Zwiet, the Matilo *castellum* (at present-day Leiden) was located just downstream, whilst the Albania (now Alphen aan den Rijn) and Nigrum Pullum (now Zwammerdam) *castella* were located downstream and upstream of the Alphen Zuid crevasse respectively.

In conclusion, the refined reconstruction of the development of the Old Rhine extensive crevasses in this thesis confirms Van Dinter's (2013) conclusions.

5.3.2 Implications for natural land-building projects in deltas

In section 1.2 it was stated that crevasses are relevant for natural land-building in low-lying deltas experiencing the negative effects of global climate change-induced relative sea level rise (*e.g.* the Mississippi delta). Hence, a better understanding of crevasse formation and maturation dynamics could aid in future sustainable delta management.

The outcomes of this thesis add to the understanding of crevasses in the fluvial-tidal realm of lowland river systems under changing upstream and downstream boundary conditions. They show that crevasses can progradate and mature due to frequent flood events, given that the crevasse throats are being kept open by

regular flushing due to a roughly constant tide-induced backwater effect. Storm surges could have a similar effect on crevasses as flood events. In section 2.2.2 it was mentioned that intermediate vegetation strenghts in the flood basin lead to the most sufficient trapping of sediments delivered to the flood basin by crevasses (Nienhuis *et al*., 2018).

In the Rhine-Meuse delta and other tidally influenced deltas around the world, implementation of natural land-building projects implies allowing both the sea as well as river flood events to influence large parts of low-lying land. Crevasses could provide sufficient amounts of sediment to flood basins to keep up with (relative) sea level rise if their throats are prevented from filling in by regularly tidally flushing and flood events and storm surges are allowed to freely flood the flood basins via their course. Nevertheless, given that these prerequisites are met, the potential of crevasses for natural land-building projects is still dependent on the fluvial-sediment budget of the river system and the presence of vegetation in the flood basin. Sedimentation by crevasses cannot keep up with relative sea level rise if the river system is starved of sediment (Roelofs, 2019), for example caused by upstream trapping of sediment by dams (*e.g.* Syvitski *et al*., 2005). When there is a vegetation deficit or if vegetation types which are sufficient in sediment trapping are absent, the sediment is not effectively trapped in specific zones but more spread out. Hence, sedimentation rates are then unlikely to match (relative) sea level rise rates.

As the Rhine-Meuse is currently largely fluvial-sediment starved, and floods are prevented from flooding the flood basins, this would require storm surges to be allowed to penetrate far inland to reach the crevasses and provide sediment for sustainable natural land-building. Whether this would provide sufficient enough sediment to the crevasses to match relative sea level rise rates cannot be concluded based on the outcomes of this thesis. Further research is needed to assess this. Allowing storm surges to flood the flood basins would imply a major revision of the Dutch policy in counteracting the negative effects of future relative sea level rise, in which the sea is still mostly seen as the natural ‘enemy’.

5.4 Recommendations and future research

The new insights in this thesis form the beginning of a qualitative understanding of crevasse formation and evolution in the tidal-fluvial realm of a river system. To come to a better, and perhaps more generic and quantitative understanding the following recommendations and suggestions for (directions of) future research are given below.

First, the ^{14}C-ages of crevasse formation and abandonment will either confirm or refute the hypothesized crevasse phases ages. Hence they will lead to a better coupling of crevasse formation and subsequent development to changes in boundary conditions and autogenic processes (section 5.1). A better reconstruction of peatland dynamics (spatially and temporally) will aid in validating when certain hybrid crevasse-peat drainage systems were formed (section 5.2.1).

Second, the analysis of the effects of boundary conditions will benefit from more accurate, Old Rhine specific reconstructions. The changes in tidal boundary conditions have been only estimated based on the configuration of the Old Rhine estuary. The channel width and configuration of the channel belt complex could not be determined with certainty based on the data that is available so far in the palaeogeographic reconstructions by De Haas et al. (2018a). Hence the changes in tidal boundary conditions can be better reconstructed when more accurate (spatio and temporal) palaeogeographic reconstructions of the Old Rhine become available in the future. Modelling of the propagation of the tidal wave and the reach of the backwater

effect in the Old Rhine estuary, as done in recent studies such as by Leuven (2019), can be a valuable asset in this regard too. A Holocene storm surge record specific for the Western-Netherlands coast or even the Old Rhine estuary will provide a more profound insight into the effect of marine storm events on the crevasses in the tidal-fluvial realm of the Old Rhine. When individual storm surge events are known, these could be linked to the formation of specific crevasses and the spatial variability of their effect along the Old Rhine could be assessed.

Recent and future insights into estuary dynamics regarding the effects of increased mud supply and vegetation (*e.g.* Braat *et al*., 2017; Lokhorst *et al*., 2018) and tidal bar dynamics (*e.g.* Leuven, 2019) on estuary dimensions and morphology will provide a better understanding in how these in turn affect the tidal backwater effect through time and consequently the crevasse evolution.

At last, it would be recommended to compare the Old Rhine case study to various other tidally-influenced rivers in other parts of the world by analyzing Google Earth and other satellite imagery, and by performing fieldwork and laboratory analyses as in this thesis. Studying the planform shape, extend, sedimentology, and age of crevasses of such river systems will aid the understanding of the general processes controlling crevasse formation and development in the tidal-fluvial realm. In the Netherlands, the Old Rhine might be compared to the (former) Meuse estuary to the south in the Rotterdam region and the former Oer-IJ estuary to the north.

6. Conclusions

The aim of this thesis is to gain a general and qualitative understanding of the effects of changes in fluvial and tidal boundary conditions, their interplay on crevasse evolution. The main findings are presented below.

- More crevasses are active and maturation of these systems is promoted when a strong tidal backwater effect is present.

The four extensive crevasses studied in this thesis were formed when there was a relatively constant tidal backwater effect. When this backwater effect decreased, morphodynamic activity in most crevasses ceased and less new crevasses were formed. Frequent tidal flushing of the crevasses induced by the tidal backwater-effect prevents rapid filling- in of the natural levee breach of the crevasse and hence enables prolonged morphodynamic activity in these systems. Crevasses closer to the estuary mouth are to a larger degree and to a longer extent affected by the tidal backwater effect than more inland-located crevasses.

- Flood events cause the breach of the natural levee which initiates crevasse formation. Subsequent flood events lead to crevasse maturation and cause most of the crevasse progradation

During periods of increased flood frequency more crevasses are formed and kilometres-long crevasses develop. This is facilitated by regular tidal flushing induced by the tidal backwater effect as described above. A decrease in the flood frequency hampers or leads to a cease in crevasse progradation.

- Peat drainage channels draining raised bogs in the flood basin form pre-existing depressions in the flood basin which can be intercepted by progradating crevasse channels. This enlarges the potential extend of a crevasses and can accelerate its progradation into the flood basin.

The Grecht, Meije, and the Alphen Zuid, the three most upstream located crevasses, have probably taken over pre-existing peat drainage channels. After morphodynamic activity decreased, the crevasses probably still acted as drainage channels.

- The chronological framework of crevasse phases in this thesis enables a more refined estimation of the archaeological expectation of crevasses along the Old Rhine.

The oldest archaeological remains can be expected on buried crevasses and date from the Middle to Late-Neolithic period (ca. 5300-2000 BCE). Bronze Age (ca. 2000-800 BCE) remains are virtually completely absent in crevasse deposits. Middle-Iron Age (ca. 500-12 BCE) and Roman Age (12 BCE-450 CE) remains have a high expectation on most of the crevasses still recognizable in the present landscape.

- Crevasses could provide sediment to counteract the negative effect s of relative sea level rise for vulnerable flood basins.

Implementation of such projects requires the presence of sufficient vegetation cover in the flood basins to efficiently trap sediments which are deposited there by allowing flood events and storm surges to flood the flood basins. Further research is needed to assess whether this would be feasible in the Netherlands and other deltas.

References

Allen, J.R.L. (1965). A review of the origin and characteristics of recent alluvial sediments. *Sedimentology 5*, 89–191.

Beets, D.J. & Van der Spek, A.J.F. (2000). The Holocene evolution of the barrier and the back-barrier basins of Belgium and the Netherlands as a function of late Weichselian morphology, relative sea-level rise and sediment supply. *Netherlands Journal of Geosciences, 79(1),* 3-16.

Berendsen, H. (1982). De genese van het landschap in het zuiden van de provincie Utrecht. *PhD thesis*, Utrecht University, Utrecht.

Berendsen, H., & Stouthamer, E. (2000). Late Weichselian and Holocene palaeogeography of the Rhine-Meuse delta, The Netherlands. *Palaeogeography, Palaeoclimatology, Palaeoecology*, *161*, 311–335.

Berendsen, H., & Stouthamer, E. (2002). Paleogeographic evolution and avulsion history of the Holocene Rhine–Meuse delta, The Netherlands. *Netherlands Journal of Geosciences, 81(1),* 97–112.

Berendsen, H.J.A. (2005). Fysisch-geografisch onderzoek. *Uitgeverij Van Gorcum,* Assen.

Bodewes, B. (2014). Numerical modelling of the geologically reconstructed Oer-IJ estuary. *MSc Thesis*, Utrecht University.

Braat, L., Van Kessel, T., Leuve, J. & Kleinhans, M. (2017). Effects of mud supply on large-scale estuary morphology and development over centuries to millennia. *Earth Surface Dynamics, 5*(4), 617-652.

Burns, C., Mountney, N., Hodgson, D., & Colombera, L. (2017). Anatomy and dimensions of fluvial crevasse-splay deposits: Examples from the Cretaceous Castlegate Sandstone and Neslen Formation, Utah, U.S.A. *Sedimentary Geology, 351*, 21-35.

Cohen, K.M., Stouthamer, E., Pierik, H.J. & Geurts, A.H. (2012). Rhine-Meuse Delta Studies' Digital Basemap for Delta Evolution and Palaeogeography. Department of Physical Geography. Utrecht University. Digital Dataset. http://persistent-identifier.nl/?identifier=urn:nbn:nl:ui:13-nqjn-zl

Cohen, K., Toonen, W., & Weerts, H. (2016). Overstromingen van de Rijn gedurende het Holoceen Relevantie van de grootste overstromingen voor archeologie van het Nederlandse rivierengebied. *Deltares report, 1209091-000,* Utrecht, the Netherlands.

De Bakker, H. & Schelling, J. (1966). A system of soil classification for the Nehterlands (The higher levels).

De Bakker, H. & J. Schelling. (1989). Systeem van Bodemclassificatie voor Nederland; de hogere niveaus. Second edition, edited by Brus, J. and C. van Wallenburg. *Wageningen: DLO Staring Centrum*.

De Haas, T., van der Valk, L., Cohen, K., Pierik, H., Weisscher, S., Hijma, M., Kleinhans, M. (2018a). Long-term evolution of the Old Rhine estuary: unraveling effects of changing boundary conditions and inherited landscape. *The Depositional Record*.

De Haas, T., Pierik, H., van der Spek, A., Cohen, K., van Maanen, B., & Kleinhans, M. (2018b). Holocene evolution of tidal systems in The Netherlands: Effects of rivers, coastal boundary conditions, eco-engineering species, inherited relief and human interference. *Earth-Science Reviews, 177*, 139-163. Elsevier B.V.

Diependaele, S. & Drenth, E. (2010). Archeologisch onderzoek langs de rijksweg N11 (Spookverlaat) ten behoeve van de aanleg van het windturbinepark Rijnwoude te Hazerswoude-Rijndijk (gem. Rijnwoude, prov. Zuid-Holland). Een Neolithische vindplaats langs de Oude Rijn. *ArcheoMedia-Report A06-286-R and A06-359-R*, Nieuwerkerk aan den IJssel, the Netherlands.

Dijkstra, M.F.P., Verhoeven, A.A.A. & Van Straten, K.C.J. (Eds.) (2016). Nieuw licht op Leithon Archeologisch onderzoek naar de vroegmiddeleeuwse bewoning in plangebied Leiderdorp-Plantage Themata 8. *Amsterdam, the Netherlands: Universiteit van Amsterdam / Diachron UvA bv.*

Dikau, R., Herget, J. & Hennrich, K. (2005). Land Use and Climate Impacts on Fluvial Systems during the Period of Agricultrure in the River Rhine Catchment (Rhinelucifs) – An introduction. *Erdkunde 59*, 177-183.

Erkens, H. (2009). Sediment dynamics in the Rhine catchment: Quantification of fluvial response to climate change and human impact. PhD-thesis, Utrecht University. *Netherlands Geographical Studies 388*, 278 pp.

Erkens, G., Van Der Meulen, M., & Middelkoop, H. (2016). Double trouble: Subsidence and CO 2 respiration due to 1,000 years of Dutch coastal peatlands cultivation. *Hydrogeology Journal, 24*(3), 551-568.

Esposito, C., Shen, Z., Törnqvist, T., Marshak, J., & White, C. (2017). Efficient retention of mud drives land building on the Mississippi Delta plain. *Earth Surface Dynamics, 5*(3), 387-397.

Ethridge, F.G., Skelly, R.L. & Bristow, C.S. (1999). Avulsion and crevassing in the sandy braided Niobrara River: complex response to baselevel rise and aggradation. In Smith & Rogers (Eds.), *Fluvial Sedimentology VI* (pp. 171–91). Special Publication of the International Association of Sedimentologists Oxford, UK: Blackwell 28.

Farrell, K. (2001). Geomorphology, facies architecture, and high-resolution, non-marine sequence stratigraphy in avulsion deposits, Cumberland Marshes, Saskatchewan.*Sedimentary Geology, 139*, 93-150.

Gouw, M. & Erkens, G. (2007). Architecture of the Holocene Rhine-Meuse delta (the Netherlands) - A result of changing external controls. *Netherlands Journal of Geosciences, 86(1)*, 23-54.

Groenewoudt, B., Van Lanen, R.J. & Pierik, H.J. (2019). Bevolkingsaantallen berekenen. Kan dat, op basis van archeologische gegevens? *Archeologie in Nederland, 1*(3), 36-41.

Gulliford, A., Flint, S., & Hodgson, D. (2017). Crevasse splay processes and deposits in an ancient distributive fluvial system: The lower Beaufort Group, South Africa. *Sedimentary Geology, 358*, 1-18.

Hajek, E., & Edmonds, D. (2014). Is river avulsion style controlled by floodplain morphodynamics? *Geology, 42*(3), 199-202.

Hajek, E., & Wolinsky, M. (2012). Simplified process modeling of river avulsion and alluvial architecture: Connecting models and field data. *Sedimentary Geology, 257-260*, 1-30.

Heiri, O., Lotter, A., & Lemcke, G. (2001). *Loss on ignition as a method for estimating organic and carbonate content in sediments: reproducibility and comparability of results.*

Hemminga, M. & Hamburg, T. (2006). Een Merovingische nederzetting op de oever van de Oude Rijn. *Archol-Report 69*, Leiden, the Netherlands.

Hijma, M., & Cohen, K. (2011). Holocene transgression of the Rhine river mouth area, The Netherlands/Southern North Sea: Palaeogeography and sequence stratigraphy. *Sedimentology, 58*(6), 1453-1485.

Hijma, M., Cohen, K., Hoffmann, G., Van Der Spek, A., Stouthamer, E., & Journal, N. (2009). *From river valley to estuary: the evolution of the Rhine mouth in the early to middle Holocene (western Netherlands, Rhine-Meuse delta).*

Hijma, M., van der Spek, A., & van Heteren, S. (2010). Development of a mid-Holocene estuarine basin, Rhine-Meuse mouth area, offshore The Netherlands. *Marine Geology, 271*(3-4), 198-211.

Hoffmann, T., Erkens, G., Cohen, K., Houben, P., Seidel, J., & Dikau, R. (2007). Holocene floodplain sediment storage and hillslope erosion within the Rhine catchment. *Holocene, 17*(1), 105-118.

Hoffmann, T., Erkens, G., Gerlach, R., Klostermann, J., & Lang, A. (2009). Trends and controls of Holocene floodplain sedimentation in the Rhine catchment. *Catena, 77*(2), 96-106.

Jones, L.S. & Schumm, S.A. (1999). Causes of avulsion: an overview. In Smith & Rogers (Eds.), *Fluvial Sedimentology VI* (pp. 171–178). Special Publication of the International Association of Sedimentologists Oxford, UK: Blackwell 28.

Kleinhans, M., Cohen, K., Hoekstra, J., & IJmker, J. (2011). Evolution of a bifurcation in a meandering river with adjustable channel widths, Rhine delta apex, The Netherlands. *Earth Surface Processes and Landforms, 36*(15), 2011-2027.

Kleinhans, M., Ferguson, R., Lane, S., & Hardy, R. (2013). Splitting rivers at their seams: Bifurcations and avulsion. *Earth Surface Processes and Landforms, 38*(1), 47-61.

Knighton, A.D. & Nanson, G.C. (1993). Anastomosis and the continuum of the channel pattern. *Earth Surface Processes and Landforms, 18,* 613–25.

Kroes, R.A.C. & Feiken, H. (2011). Plangebied Polder Nieuwkoop, Zuid- en Noordeinderpolder, gemeente Alphen aan den Rijn; archeologisch vooronderzoek: een beleidsadvieskaart. *RAAP-Report-2468*, Weesp, the Netherlands.

Leuven, J.R.F.W. (2019). Bar and channel patterns in estuaries. PhD-thesis, Utrecht University. *Utrecht Studies in Earth Sciences 180*, 276 pp.

Lokhorst, I., Braat. L., Leuven, J., Baar, A., Van Oorschot, M., Selaković, S. & Kleinhans, M. (2018). Morphological effects of vegetation on the tidal-fluvial transition in Holocene estuaries. *Earth Surface Dynamics, 6*(4), 883-901

Makaske, B. (2001). Anastomosing rivers: a review of their classification, origin and sedimentary products. *Earth-Science Reviews, 53*, 149-196.

Makaske, B., Berendsen, H., & van Ree, M. (2007). Middle Holocene Avulsion-Belt Deposits in the Central Rhine-Meuse Delta, The Netherlands. *Journal of Sedimentary Research, 77*(2), 110-123.

Millard, C., Hajek, E., & Edmonds, D. (2017). Evaluating Controls On Crevasse-Splay Size: Implications For Floodplain-Basin Filling. *Journal of Sedimentary Research, 87*(7), 722-739.

Nichols, G. (2009). Sedimentology and stratigraphy. *John Wiley & Sons*.

Nienhuis, J., Törnqvist, T., & Esposito, C. (2018). Crevasse Splays Versus Avulsions: A Recipe for Land Building With Levee Breaches. *Geophysical Research Letters, 45*(9), 4058-4067.

Pierik, H., Cohen, K., Vos, P., van der Spek, A., & Stouthamer, E. (2017). Late Holocene coastal-plain evolution of the Netherlands: the role of natural preconditions in human-induced sea ingressions. *Proceedings of the Geologists' Association, 128*(2), 180-197.

Pierik, H., Stouthamer, E., & Cohen, K. (2017). Natural levee evolution in the Rhine-Meuse delta, the Netherlands, during the first millennium CE. *Geomorphology, 295*, 215-234.

Pierik, H., Stouthamer, E., Schuring, T., & Cohen, K. (2018). Human-caused avulsion in the Rhine-Meuse delta before historic embankment (The Netherlands). *Geology, 46*(11), 935-938.

Pons, L.J. (1992). Holocene peat formation in the lower parts of The Netherlands. In: Verhoeven, J.T.A. (Ed.) (pp. 7–79). Fens and Bogs in The Netherlands: Vegetation, History, Nutrient Dynamics and Conservation. Kluwer.

Schuring, T. (2016). Development of new river channels and river maturation in the Rhine-Meuse delta, during the late Roman Period and Early Middle Ages, AD 300-1000 - using a conceptual river phase model for integration of existing and new (multidisciplinary) datasets for river maturation in longitudinal and lateral direction on a centennial temporal resolution. *MSc Thesis*, Utrecht University.

Roelofs, L. (2019). Levee morphology and evolution in the fluvial-tidal realm. *MSc Thesis*, Utrecht University.

Shen, Z., Törnqvist, T., Mauz, B., Chamberlain, E., Nijhuis, A. & Sandoval, L. (2015). Episodic overbank deposition as a dominant mechanism of floodplain and delta-plain aggradation. *Geology, 43*(10), 875-878.

Slingerland, R. & Smith, N.D. (1998). Necessary conditions for a meandering-river avulsion *Geology, 26*, 435-438.

Slingerland, R., & Smith, N.D. (2004). River Avulsions and Their Deposits. *Annual Review of Earth and Planetary Sciences, 32*(1), 257-285.

Smith, N.D., Cross, T.A., Dufficy, J.P. & Clough, R. (1989). Anatomy of an avulsion. *Sedimentology, 36*, 1-23.

Smith, N.D., Slingerland, R.L., Perez-Arlucea, M., & Morozova, G.S. (1998). The 1870s avulsion of the Saskatchewan River. *Canadian Journal of Earth Sciences*, 35, 453–466.

Sorrel, P., Debret, M., Billeaud, I., Jaccard, S., McManus, J. & Tessier, B. (2012). Persistent non-solar forcing of Holocene storm dynamics in coastal sedimentary archives. *Nature Geoscience, 5(12)*, 892-896.

Stouthamer E. (2001a). Holocene avulsions in the Rhine-Meuse delta, The Netherlands. *PhD thesis*, Utrecht University, The Netherlands. 209 pp.

Stouthamer, E. (2001b). Sedimentary products of avulsions in the Holocene Rhine–Meuse Delta, The Netherlands. *Sedimentary Geology, 145(1-2),*73–92.

Stouthamer, E. (2005). Reoccupation of channel belts and its influence on alluvial architecture in the Holocene Rhine–Meuse delta, The Netherlands. *River Deltas: Concepts, Models and Examples*.

Stouthamer, E. & Berendsen, H. (2001). Avulsion frequency, avulsion duration, and interavulsion period of Holocene channel belts in the Rhine–Meuse delta, the Netherlands. *Journal of Sedimentary Research, 71*(4), 589–598.

Stouthamer, E., Cohen, K., & Gouw, M. J. (2011). Avulsion and its implications for fluvial-deltaic architecture: insights from the Holocene Rhine-Meuse delta. *SEPM Special Publication, 97*, 215–232.

Stouthamer, E., Cohen, K.M.C., & Hoek, W.Z.H. (2015). De vorming van het land: geologie en geomorfologie. *Perspectief uitgevers*.

Syvitski, J.P.M., Vörösmarty, C.J., Kettner, A.J. & Green, P. (2005). Impact of Humans on the Flux of Terrestrial Sediment to the Global Coastal Ocean. *Science 308*, 376-380.

TNO, Geological Survey of the Netherlands. (2013). Lithostratigrafic Nomenclature of the shallow subsurface, version 2013. Retrieved 28-09-2018, from https://www.dinoloket.nl/nomenclator-ondiep.

Toonen, W. (2013). A Holocene flood record of the Lower Rhine. PhD-thesis, Utrecht University. *Utrecht Studies in Earth Sciences 41*, 204 pp.

Toonen, W., Kleinhans, M., & Cohen, K. (2012). Sedimentary architecture of abandoned channel fills. *Earth Surface Processes and Landforms, 37*(4), 459-472.

Toonen, W., Middelkoop, H., Konijnendijk, T., Macklin, M., & Cohen, K. (2016). The influence of hydroclimatic variability on flood frequency in the Lower Rhine. *Earth Surface Processes and Landforms, 41*(9), 1266-1275.

Toonen, W., van Asselen, S., Stouthamer, E., & Smith, N. (2016). Depositional development of the Muskeg Lake crevasse splay in the Cumberland Marshes (Canada). *Earth Surface Processes and Landforms, 41*(1), 117-129.

Toonen, W., Foulds, S., Macklin, M., & Lewin, J. (2017). Events, episodes, and phases: Signal from noise in flood-sediment archives. *Geology, 45*(4), 331-334.

Törnqvist, T. & Bridge, J. (2002). Spatial variation of overbank aggradation rate and its influence on avulsion frequency. *Sedimentology, 49(5)*, 891-905.

Van Amen, I. & Brinkkemper, O. (2009). De plantenresten uit Romeinse sporen. In: Polak, M. & De Groot, T. (eds): *Vondsten langs de Limes*. Rapportage Archeologische Monumentenzorg 167 (Amersfoort): 32-68.

Van Asselen, S., Erkens, G., Stouthamer, E., Woolderink, H., Geeraert, R., & Hefting, M. (2018, 9 15). The relative contribution of peat compaction and oxidation to subsidence in built-up areas in the Rhine-Meuse delta, The Netherlands. *Science of the Total Environment, 636*, 177-191.

Van Dasselaar, M. & Depuydt, S. (2009). Archeologisch onderzoek Prinsenschouw te Hazerswoude-Rijndijk (gemeente Rijnwoude) Bureauonderzoek en inventariserend veldonderzoek met boringen. *ArcheoMedia-Report A08-408-I/1*, Capelle aan den IJssel, the Netherlands.

Van Der Molen, J., & De Swart, H. (2001). Holocene wave conditions and wave-induced sand transport in the southern North Sea. *Continental Shelf Research, 21*(16-17), 1723-1749.

Van Dinter, M. (2013). The Roman limes in the Netherlands: how a delta landscape determined the location of the military structures. *Netherlands Journal of Geosciences, 92(1)*, 11-32.

Van Dinter, M., & Van Zijverden, W. (2010). Settlement and land use on crevasse splay deposits; geoarchaeological research in the Rhine-Meuse Delta, the Netherlands. *Geologie en Mijnbouw/Netherlands Journal of Geosciences. 89*, pp. 21-34. Stichting Netherlands Journal of Geosciences.

Van Dinter, M., Cohen, K., Hoek, W., Stouthamer, E., Jansma, E., & Middelkoop, H. (2017). Late Holocene lowland fluvial archives and geoarchaeology: Utrecht's case study of Rhine river abandonment under Roman and Medieval settlement. *Quaternary Science Reviews, 166*, 227-265.

Van Heteren, S., Van Der Spek, A., & Van Der Valk, B. (2011). Evidence and Implications of Middle- To Late- Holocene Shoreface Steepening Offshore the Western Netherlands. *World Scientific Pub Co Pte Lt*. 188-201.

Verboom-Jansen, M. & Wullink, A.J. (2011). Een archeologisch bureau-onderzoek en inventariserend veldonderzoek door middel van boringen ter plaatse van monumentterrein 8.798, ten noorden van Hazerswoude-Rijndijk, gemeente Rijnwoude (ZH). *ARC-Report 2010-267*, Geldermalsen, the Netherlands.

Vos, P. (2015). Origin of the Dutch coastal landscape: long-term landscape evolution of the Netherlands during the Holocene, described and visualized in national, regional and local palaeogeographical map series. PhD thesis, Utrecht University.

Wynia, H., Arkema, M. & Pruis, R. (2018). Grind, greppels en een Romeinse brug. *Archeologie in Nederland, 1*(5), 52-53.

Zagwijn, W.H. (1986). Nederland in het Holoceen. *Rijks Geologische Dienst*, Haarlem.

Appendices

Appendix A

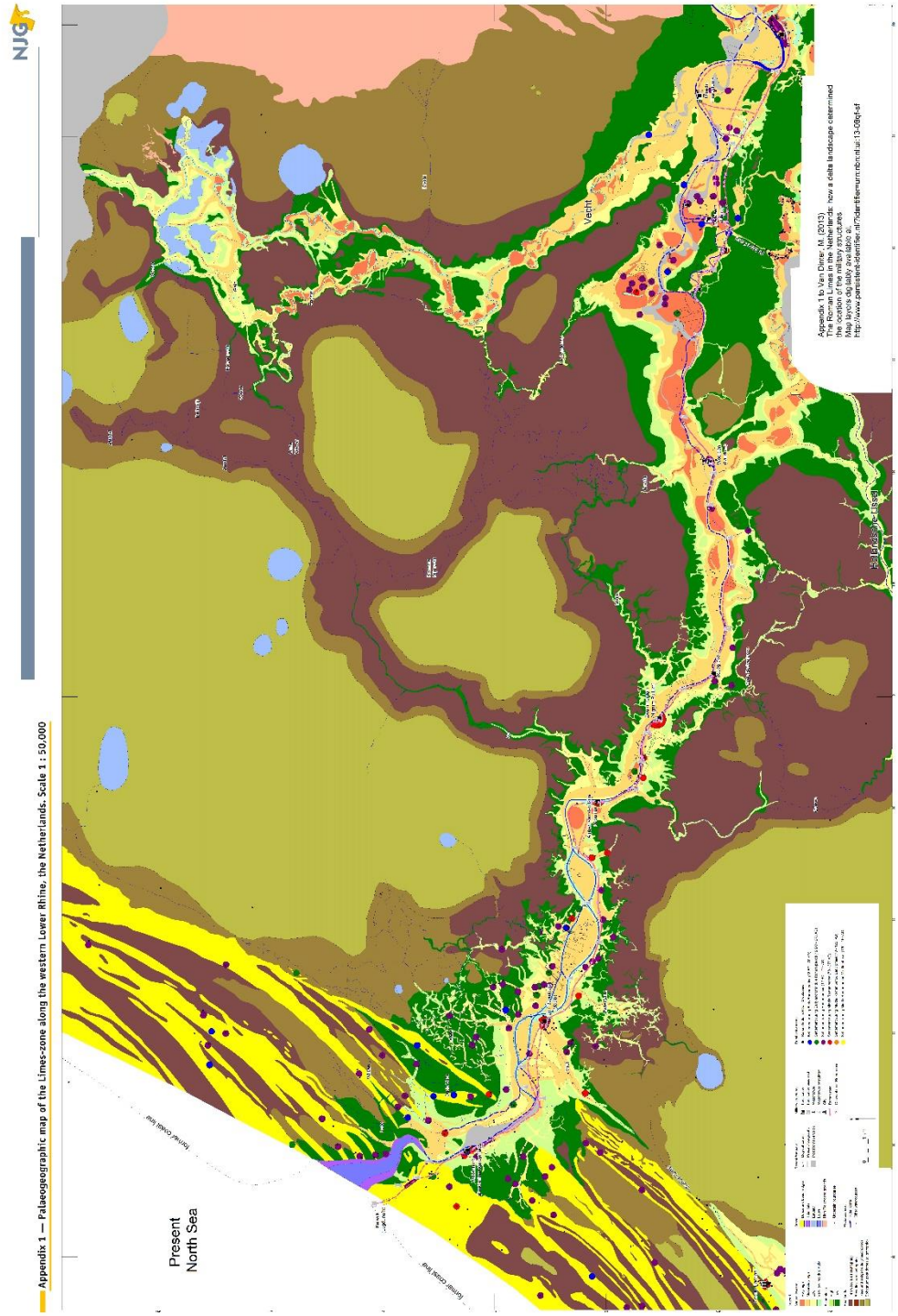

Appendix 1 adopted from Van Dinter (2013): Palaeogeographic map of the limes-zone along the Western Lower Rhine, the Netherlands, 1:50,000.

Appendix B

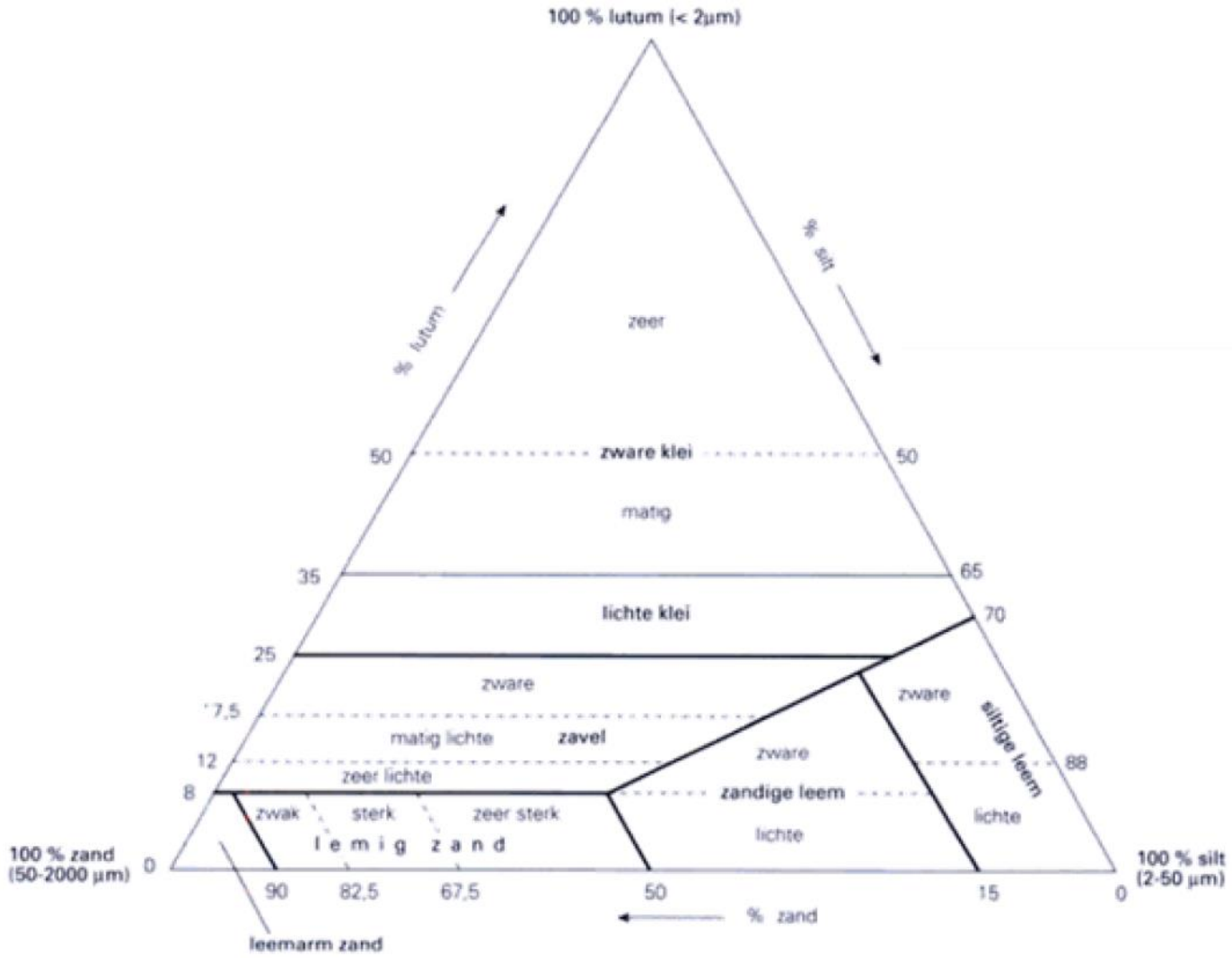

Adopted lithological classification scheme based on De Bakker & Schelling (1966), adjusted by Berendsen (2005) (the same scheme is used in De Bakker & Schelling's (1989) classification).

Appendix C

CONVERSIETABEL UU-LLG CODERINGEN **LLG-NL codes vs. LLG-USDA codes**

UU-LLG (B&S 2001)				LLG USDA		
TEXTUUR	ORG	Omschrijving	M50 / %GR	TEXTURE	ORG	Description
None	**V3**	Veen		*None*	**P**	Peat
None	**V2**	Kleiig Veen		*None*	**PM**	Peat Muck
None	**V1**	Venige Klei		*None*	**M**	Muck
...	**H2**	Sterk Humeus		...	**M2**	Very Mucky / Very Humic
...	**H1**	Humeus		...	**M1**	Mucky / Humic
...	**H0**	Iets Humeus			**M0**	Little Mucky / Little Humic
None	ZV	Zandig Veen			SP	Sandy Peat
None	VZ	Venig Zand			PS	Peaty Sand
ZK	...	Zeer Zware Klei		**C**	...	Clay
MK	...	Matig Zware klei		**SiC**	...	Silty Clay
LK	...	Lichte klei		**SiCL**	...	Silty Clay Loam
ZZL	...	Zware zavel		**SiL**	...	Clay Loam
MZL	...	Matig lichte Zavel		**SiL**	...	Loam
LZL	...	zeer Lichte Zavel		**SL**	...	Sandy Loam
ZSL	...	Zware siltige leem		**SiL**	...	Silt Loam
SL	...	Siltige leem		SiL	...	Silt Loam
LSL	...	Lichte siltige leem		**Si**	...	Silt
ZL	...	Zware zandige Leem L		SiL	...	Silt Loam
L	...	Zandige leem		SiL	...	Silt Loam
LL	...	Lichte zandige leem		SiL	...	Silt Loam
Z-ZK	...	Zandige Zeer Zware Klei		C	...	Clay
Z-MK	...	Zandige Matig Zware Klei		**SC**	...	Sandy Clay
Z-LK	...	Zandige Lichte Klei		**SCL**	...	Sandy Clay Loam
Z-ZZL	...	Zandige Zware Zavel		SL	...	Sandy Loam
Z-MZL	...	Zandige Matig lichte Zavel		SL	...	Sandy Loam
Z-LZL	...	Zandige zeer Lichte Zavel		**LS**	...	Loamy Sand
Z-L	...	Zandige Leem		SiL	...	Silt Loam
ULZ	...	Zeer sterk lemig zand		SL	...	Sandy Loam
MLZ	...	Sterk lemig zand		SL	...	Sandy Loam
LZ	...	Lemig zand		LS	...	Loamy sand
ILZ	...	Zwak lemig zand		LS	...	Loamy sand
Z	...	Zand		**S**	...	Sand
UFZ	...	Uiterst fijn zand	50–105 *µm*	**vfS**	...	Extremely fine sand
ZFZ	...	Zeer fijn zand	105-150	**vfS**	...	Very fine sand
FZ	...	Matig Fijn Zand	150-210	**fS**	...	Fine sand
MZ	...	Matig Grof Zand	210-420	**mS**	...	Medium sand
GZ	...	Grof tot Zeer Grof Zand	420-2000	**cS**	...	Coarse/ very coarse sand
ZFG		Zeer fijn grind	2-5 *mm*	**fG**		Very fine gravel
FG		Fijn Grind	5-16	**G**		Fine gravel
GG		Grof Grind	16-64	**cG**		Coarse gravel
ST		Steen	64-100	**ST**		Stone
KEI		Kei	100-500			Rock / Cobble
BLOK		Blok	> 500			Block / Boulder
IGHZ		Iets Grindhoudend Zand	3-10 *%GR*	S		Slightly gravelly sand
MGHZ		Matig Grindhoudend Zand	10-25	S		Gravelly sand
SGHZ		Sterk Grindhoudend Zand	25-50	S		Strongly gravelly sand
SZHG		Sterk Zandhoudend Grind	50-75	G		Strongly sandy gravel
MZHG		Matig Zandhoudend Grind	75-90	G		Sandy gravel
IZHG		Iets Zandhoudend Grind	90-97	G		Slightly sandy gravel

Versie 1.5 – K.M. Cohen, M.P. Hijma, T.E. Törnqvist

Appendix D

201801001	Pierik, Roelofs, Moree	07-09-2019

Coordinaten	Hoogte	Diepte	KAARTEENHEID	Geomorfogenetische kaart:	
Xco	Z [m]	[cm]	Geologische kaart:	Grondwatertrap:	
Yc	-1.11	350	Begroeiingskaart:	Bodemkaart:	
o					
103874 456980					

Alphen Zuid, Rietveldsepad 17, Noordelijk oeverwal crevasse, hoogste punt ca. 10 m van sloot af (midden perceel. acc. = 3.1 m foto guts van 270 - 350 - cmv. Hoogte via AHN3. "00" weggelaten van XCO. Hoogte via AHN3 data.

Diepte	Textuur	Org	Plr	Kleur	Redox	Grind	M50	Ca	Fe	GW	M	LKL	Strat	Bijzonderheden
10	MK			dgrbr	o			0						geroerd, Echteld Crevasse kom
20	MK			dgrbr	o			0						geroerd
30	MK			dgrbr	o			0						geroerd
40	MK			dgrbr	o			1						geroerd, baksteengruis
50	MK			brgr	o			1						geroerd
60	MK			brgr	or			1						
70	MK			brgr	or			1						
80	MK			brgr	or			1						
90	MK			brgr	or			1						Echteld Crevasse oever
100	LK			brgr	or			1						
110	LK		hr	brgr	or									
120	ZZL		hr	brgr	or									# 1 mm Z laagjes
130	ZZL		hr	brgr	or									1 mm Z laagjes
140	ZZL		hr	brgr	or									1 mm Z laagjes
150	ZZL		hr	brgr	or					GW				1 mm Z laagjes
160	ZZL		hr	brgr	r									
170	MZL	H0	hr	dgr	r									
180	MZL	H0	plr	dgr	r									
190	ZZL	H0	plr	dgr	r									mm laagjes Z
200	ZZL	H0	plr	dgr	r									mm laagjes Z
210	ZZL	H0	plr	dgr	r			2						Schgr mm laagjes Z
220	ZZL	H0	plr	dgr	r			2						Schgr mm laagjes Z
230	ZZL	H0	plr	dgr	r			2						mm laagjes Z
240	ZZL	H0	plr	dgr	r			2						Detrit mm band
250	ZZL	H0	plr	dgr	r			2						Schel fragment, detrit mm band
260	ZZL	H0	plr	dgr	r			2						Schel fragment, detrit mm band
270	ZZL	H0	plr	dgr	r			2						Detrit mm band
280	ZZL	H0	plr	dgr	r			1						
290	LK	H2	r	lbrgr	r			1						
300		V1	r	grbr	r			0						ca8cm overgang NiHo vanaf hier
310		V2	r	grbr	r			0						rietveen
320		V2	r	grbr	r			0						rietveen
330	ZZL	H2	r	dbrgr	r			0						rietveen, ca. 5 cm overgang
340	UFZ		r	gr	r		50-105	1						NaWo vanaf hier
350	UFZ		r	gr	r		50-105	1						

Einde boring: 201801001

201801002	Pierik, Roelofs, Moree	07-09-2019

Coordinaten	Hoogte	Diepte	KAARTEENHEID	Geomorfogenetische kaart:
Xco	Z [m]	[cm]	Geologische kaart:	Grondwatertrap:
Yc	-1.82	370	Begroeiingskaart:	Bodemkaart:
o				
103860 457022				

Alphen Zuid, Noordelijke kant van oever crevasse in de kom. Acc. 8.8 cm. AHN3 = Hoogte. Monster:RietveldCI: coor: 103859/457025 +- 3.5 m van 77 cm tot 164 -cmv; RietveldCII: zelfde coor. monster van 145 tot 245 -cmvHoogteAHN3

Diepte	Textuur	Org	Plr	Kleur	Redox	Grind	M50	Ca	Fe	GW	M	LKL	Strat	Bijzonderheden
10	Z-MK			dbr	or			0	1					Geroerd met Z bijmeng Echt Kom
20	Z-MK			dbr	or			0	1					Geroerd met Z bijmeng Echt Kom
30	MK			dbr	or			0	1					Geroerd met Z bijmeng Echt Kom
40	MK			dbr	or			0	1					
50		V1		dbr	or			0		GW				Geox NiHo V
60		V1		dbr	r			0	0					Geox NiHo V, gel overgang
70	MK	H1	r	grbr	r			0	0					Echteld
80	MK	H1	r	grbr	r			0	0					
90	MK	H1	r	grbr	r			0	0					Detr gelaag 2mm
100	MK	H2	r	dgrbr	r			0	0					Detr gelaag 2mm, takjes & riet
110	MK		r	dgrbr	r			0	0					Detr gelaag 2mm, takjes & riet
120					r				0					
130					r				0					
140	MK	H2	h	dgrbr	r			0	0					Hout (takken)
150		V1	h	br	r			0	0					1 cm hum K, NiHo
160		V1	h	br	r			0	0					1 cm hum K, NiHo, gel overgang
170	ZK	H2	plr	dgrbr	r			0	0					Overgang 3 - 5 cm naar Ech
180	ZK	H2	plr	dgrbr	r			0	0					
190		V2	r	br	r			0	0					NiHo, heel veel riet
200		V2	r	br	r			0	0					NiHo, heel veel riet
210					r			0	0					GM
220					r			0	0					GM
230		V2	r	br	r			0	0					NiHo
240	MZ		r	gr	r		210-420	1	0					Licht kleiige bijm. NaWo
250	LZ		r	blgr	r			2	0					NaWo
260	LZ		r	blgr	r			2	0					NaWo
270	LZ		r	blgr	r			2	0					NaWo
280	LZ		r	blgr	r			2	0					NaWo
290	LZ		r	blgr	r			2	0					NaWo
300					r				0					GM
310					r				0					GM
320					r				0					GM
330	MZL		r	blgr	r			2	0					NaWo, Kleiiger
340	LZ		r	blgr	r			2	0					NaWo
350	ZZL		r	lgr	r			2	0					NaWo, UFZ bandjes
360	ZZL		r	lgr	r			2	0					NaWo, UFZ bandje 2 cm
370	ZZL		r	lgr	r			2	0					NaWo, veel silt

Einde boring: 201801002

201801003	Pierik, Roelofs, Moree	07-09-2019

Coordinaten	Hoogte	Diepte	KAARTEENHEID	Geomorfogenetische kaart:	
Xco	Z [m]	[cm]	Geologische kaart:	Grondwatertrap:	
Yc	-1.6	630	Begroeiingskaart:	Bodemkaart:	
o					
103888 456968					

In midden, diepste deel van crevassegul ca. 4 m van oostsloot af. Monster RietveldA-I van bladresten uit restgeulopvulling op ca. 305 -cmv. Rietveld A-II schelpfragment (mossel?) uit bodem? restgeul op ca. 450 -cmv. acc=5.6m

Diepte	Textuur	Org	Plr	Kleur	Redox	Grind	M50	Ca	Fe	GW	M	LKL	Strat	Bijzonderheden
10	Z-MK			dgrbr	o				2					geroerd, Z bijmenging
20	Z-MK			dgrbr	o				2					geroerd, Z bijmenging
30	Z-MK			dgrbr	o				2					geroerd, Z bijmenging
40	MK	H2	plr	gr	o				2					brokkelig en slap
50	MK	H2	plr	gr	o				2					brokkelig&slap, vorm geox Veen
60	MK	H2	plr	gr	o				2					brokkelig en slap
70	MK	H2	plr	gr	o			1	2					brokkelig en slap
80	LK	H2	plr	gr	o			2	2					brokkeligslap, verspdetrlaag
90	LK		plr	gr	or			2	1					# matig slap
100	LK		plr	gr	or			2	1					Schgr matig slap
110	LK		plr	gr	r			2	0					matig slap
120	LK		plr	gr	r			2	0					matig slap
130	LK		h	gr	r			2	0					matig slap
140	LK		plr	gr	r			2	0					Schgr matig slap
150	LK		plr	gr	r			2	0					matig slap
160	LK		plr	gr	r			2	0					# matig slap
170	LK		plr	gr	r			2	0					# Schgr
180	LK		plr	gr	r			2	0					
190	LK		plr	gr	r			2	0					
200	LK		plr	gr	r			2	0					Zeer geleid overgang steviger
210	ZZL		plr	gr	r			2	0					steviger
220	ZZL		plr	gr	r			2	0					steviger
230	ZZL		plr	gr	r			2	0					steviger
240	ZZL		plr	gr	r			2	0					# gm
250	ZZL		plr	gr	r			2	0					#
260	ZZL		plr	gr	r			2	0					
270	ZZL		plr	gr	r			2	0					detr laagjes
280	ZZL		plr	gr	r			2	0					detr laagjes
290	ZZL		plr	gr	r			2	0					detr laagjes
300	ZZL		plr	gr	r			2	0					detr laagjes
310	ZZL		plr	gr	r			2	0		1			detr laagjes schgr
320				gr	r			2	0					# gm
330	ZZL		plr	gr	r			2	0					# schgr blaadjes
340	ZZL		h	gr	r			2	0					verslagen detr bandjes
350	ZZL	H0	h	brgr	r			2	0					
360	ZZL	H0	plr	brgr	r			2	0					
370	ZZL	H0	plr	brgr	r			2	0					
380	ZZL		plr	gr	r			2	0					
390	ZZL		plr	gr	r			2	0					
400	ZZL		plr	gr	r			2	0					#
410	ZZL		plr	gr	r			2	0					# schgr
420	ZZL		plr	gr	r			2	0					SchgrSchgr
430	MZL		plr	gr	r			2	0					Schgr
440	MZL			gr	r			2	0					
450	MZL		r	gr	r			2	0		2			Schelpfrag

460	MZL		plr	dgr	r			2	0					houtstuk
470	MZL		plr	dgr	r			2	0					
480	MZL		plr	dgr	r			2	0					#
490	MZL		plr	gr	r			2	0					#
500	MZL		h	gr	r			2	0					
510	MZL		h	gr	r			2	0					versp hout
520	ZFZ			gr	r		105-150	2	0					geliedielijke overgang
530	ZFZ			gr	r		105-150	2	0					
540	ZFZ		plr	dbrgr	r		105-150	2	0					veel detr. bandjes
550	ZFZ		plr	dbrgr	r		105-150	2	0					veel detr. bandjes
560	ZFZ		plr	dbrgr	r		105-150	2	0					# ca 50 % detr. bandjes
570	ZFZ		plr	dbrgr	r		105-150	2	0					# veel detr. bandjes
580	ZFZ		plr	dbrgr	r		105-150	2	0					veel detr. bandjes
590	ZFZ		plr	dbrgr	r		105-150	2	0					veel detr. bandjes
600	LK			gr	r			2	0					abrupte overgang
610	FZ		h	dgr	r		150-210	2	0					schgr
620	FZ		r	dgr	r		150-210	2	0					schelpfragment
630	MZ			dgr	r		210-420	2	0					# einde boring

Einde boring: 201801003

201801004	Pierik, Roelofs, Moree	07-09-2019

Coordinaten	Hoogte	Diepte	KAARTEENHEID	Geomorfogenetische kaart:
Xco	Z [m]	[cm]	Geologische kaart:	Grondwatertrap:
Yc	-1.95	110	Begroeiingskaart:	Bodemkaart:
o				
103848 457057				

Verder "kom" in. geen acc genoteerd. Hoogte via AHN3 data.

Diepte	Textuur	Org	Plr	Kleur	Redox	Grind	M50	Ca	Fe	GW	M	LKL	Strat	Bijzonderheden
10	Z-MK			dbr	o									Z bijmenging
20	Z-MK			dbr	o									Z bijmenging
30	Z-MK			dbr	o									Z bijmenging
40		V1		dbr										geox veen brokkelig
50		V1		dbr										#
60		V1		dbr										
70	ZK	H1		dbr										
80	ZK			dbrgr										
90	ZK	H1		dbrgr										
100														gm
110														#gm

Einde boring: 201801004

201801005	Pierik, Roelofs, Moree	07-09-2019

Coordinaten	Hoogte	Diepte	KAARTEENHEID	Geomorfogenetische kaart:
Xco	Z [m]	[cm]	Geologische kaart:	Grondwatertrap:
Yc	-1.92	110	Begroeiingskaart:	Bodemkaart:
o				
103832 457096				

Acc=2.1 m. Zelfde als 'waarneming' langs sloot, ca. 5 m daarvanaf. Monster RietveldB-I: 44 - 144 -cmv =veen op crevasse klei om min ouderdom crevasse te bepalen. Hoogte via AHN3.

Diepte	Textuur	Org	Plr	Kleur	Redox	Grind	M50	Ca	Fe	GW	M	LKL	Strat	Bijzonderheden
10	Z-MK			dgrbr										
20	Z-MK			dgrbr										
30	Z-MK			dgrbr										
40		V1		dbr										vergaan veen
50		V1		dbr										vergaan veen
60		V1		dbr										vergaan veen
70		V1		dbr										vergaan veen
80		V1		dbr										vergaan veen
90	ZK	H1		dgr										
100	ZK	H1		dgr										
110	ZK	H1		dgr										#

Einde boring: 201801005

201801006	Pierik, Roelofs, Moree	10-09-2019

Coordinaten	Hoogte	Diepte	KAARTEENHEID	Geomorfogenetische kaart:
Xco	Z [m]	[cm]	Geologische kaart:	Grondwatertrap:
Yc	-1.09	500	Begroeiingskaart:	Bodemkaart:
o				
120804 459770				

Crevasse 2 bij Kanis. Boer Verduijn-Geuze. Op Westelijke oeverwal van de crevasse. Schgr = schelpengruis. Detr. = detritus

Diepte	Textuur	Org	Plr	Kleur	Redox	Grind	M50	Ca	Fe	GW	M	LKL	Strat	Bijzonderheden
10	ZK			dbr	o			0						ger, zwart brokken verbrand
20	ZK			dbr	o			0						ger, zwart brokken verbrand
30	ZK			dbr	o			0						geroerd
40	ZK			dbr	o			0	1					geroerd
50	ZK			dbr	o			0	1					
60	MK			brgr	or			1	1					houtskool
70	MK			brgr	or			2	1					mangaan vlekjes
80	LK			brgr	or			2	1					mangaan vlekjes, heel siltig
90	LK			brgr	or			2	1					schgr
100	ZZL		plr	brgr	or			2	1					
110	ZZL		plr	brgr	or			2	1					verkoold plr= concreties?
120	ZZL		plr	lbrgr	or			2	1					verkoold plr= concreties?
130	MZL		r	lbrgr	or			2	1					# veel silt
140	MZL		r	lbrgr	or			2	1					riet verticaal
150	ZZL		r	gr	r			2	0					riet verticaal, verkoold spul
160	ZZL		plr	gr	r			2	0					ca. 3mm UFZ bandjes
170	ZZL		plr	gr	r			2	0					ca. 3mm UFZ bandjes
180	ZZL		r	gr	r			2	0					verkoold riet
190	ZZL		r	gr	r			2	0					verticaal riet, 3 mm UFZ bandj
200	LK		plr	gr	r			2	0					# verticaal riet
210	MZL		plr	gr	r			2	0					3 mm UFZ bandjes
220	MZL		plr	gr	r			2	0					K bandje
230	ULZ		r	gr	r			2	0					rel weiig plr.
240	ZZL		r	gr	r			2	0					
250	MZL		plr	gr	r			2	0					heel siltig, iets zandiger
260	ZZL		plr	gr	r			2	0					#
270	LK		plr	gr	r			2	0					2 cm UFZ bandje
280	LK			gr	r			2	0					2 cm UFZ bandje (dikker)
290	LK			gr	r			2	0					2 cm UFZ (dikker) hum band
300	ZZL			gr	r			2	0					Humeus bandje
310	LZ		plr	gr	r			2	0					wordt zandiger
320	LK		plr	gr	r			2	0					detr. bandjes
330	ZZL		plr	gr	r			2	0					
340	ZZL		plr	gr	r			2	0					# verspoeld plr
350	ZZL			gr	r			2	0					schgr, hum, K en Z bandjes
360	ZZL			gr	r			2	0					schgr, hum, K en Z bandjes
370	ZZL			gr	r			2	0					schgr, hum, K en Z bandjes
380	ZZL			gr	r			2	0					schgr, hum, K en Z bandjes
390	ZZL			gr	r			2	0					schgr, hum, K en Z bandjes
400	ZZL			gr	r			2	0					schgr, hum, K en Z bandjes
410	ZZL			gr	r			2	0					schgr, hum, K en Z bandjes
420	MZL			gr	r				0					# Veel detr K bandj en Z bandj
430	LK			gr	r				0					Veel detr K bandj en Z bandj
440	MZL	H0	plr	brgr	r				0					Veel detr K bandj en Z bandj
450	LK			gr	r				0					Veel detr K bandj en Z bandj
460	ZFZ			gr	r		105-150		0					Veel detr K bandj en Z bandj
470	ZFZ			gr	r		105-150		0					Veel detr K bandj en Z bandj
480	ZFZ			gr	r		105-150		0					Veel detr K bandj en Z bandj

490	MZL			gr	r				0					Veel detr K bandj en Z bandj
500	MZL		plr	gr	r				0					# takje, einde boring

201801007	Pierik, Roelofs, Moree	10-09-2019

Coordinaten	Hoogte	Diepte	KAARTEENHEID	Geomorfogenetische kaart:	
Xco	Z [m]	[cm]	Geologische kaart:	Grondwatertrap:	
Yc	-1.58	540	Begroeiingskaart:	Bodemkaart:	
o					
120864 459802					

Acc. ca. 6.6 m. Oostelijke oever (kleiner en lager) overgang naar kom. Schgr = Schelpgruis. Versp = verspoeld. Hum = humeus. Gel over = geleidelijke overgang. Glgr/gr = glgr vs gr geband.KanisA-I:48-148 -cmv;A-II:380-457 -cmv

Diepte	Textuur	Org	Plr	Kleur	Redox	Grind	M50	Ca	Fe	GW	M	LKL	Strat	Bijzonderheden
10	Z-MK			brgr										Bakst, geroerd
20	Z-MK			brgr										Bakst, geroerd
30	Z-MK			brgr	o				1					Bakst, geroerd
40	Z-MK			brgr	o				1					
50		V1	r	dbr	or									Sterk veraard. Hout
60		V2	r	dbr	r									Hout
70		V2	r	br	r									Hout
80		V2	r	br	r			0						Hout
90	MK	H2		br	r			0						Overgang geleidelijk
100	MK			gr	r			0						# Slap
110	ZK			gr	r			0						Slap
120	ZK			gr	r			0						Slap
130	ZK			gr	r			0						Slap
140	ZK	H0		brgr	r			0						Slap
150	ZK	H0		brgr	r			0						Slap
160	ZK	H0		brgr	r			0						Slap
170	ZK			gr	r			0						# Slap
180	ZK			gr	r			2						#Steviger verspplr takjesschgr
190	MK			gr	r			2						versp plr takjes
200	MK			gr	r			2						versp plr
210	MK			gr	r			2						weinig plr
220	MK			gr	r			2						weinig plr sterk gebandglgr/gr
230	MK			gr	r			2						weinig plr sterk gebandglgr/gr
240	MK			gr	r			2						sterk geband glgr/gr vergaan h
250	MK	H0		gr	r			2						# sterk geband glgr/gr veel h
260	MK	H0		gr	r			2						# +veel hout
270	MK	H0		gr	r			2						veel hout
280	MK	H0		gr	r			2						veel hout
290	MK			gr	r			2						hout
300	MK			gr	r			2						hum bandjes en schgr.
310	MK			gr	r			2						
320	MK	H2		dgrbr	r			1						#
330	MK	H0		grbr	r			1						#
340	MK			brgr	r			1						
350	MK			brgr	r			1						
360	MK			brgr	r			1						
370	MK	H1		brgr	r			1						
380				br	r									hout

390	MK	H1		brgr	r			0						
400	MK	H0		brgr	r			0						# 5 cm geen sample
410														GM
420		V1		brgr	r			0						
430		V1		brgr	r			0						veel hout
440	ZK	H0		gr	r			0						geband
450		V2		br	r			0						matig compact, hout
460		V2		br	r			0						matig compact, hout
470		V2		br	r			0						matig compact, hout
480		V2		br	r			0						# matig compact, hout
490		V2		br	r			0						# compacter, gel over, geband
500	ZK	H2		grbr	r			0						
510	ZK	H2		grbr	r			0						
520	ZK	H2		grbr	r			0						
530		V2		br	r			0						Super compact
540														# GM, einde boring.

Einde boring: 201801007

201801008	Pierik, Roelofs, Moree	07-09-2019

Coordinaten	Hoogte	Diepte	KAARTEENHEID	Geomorfogenetische kaart:
Xco	Z [m]	[cm]	Geologische kaart:	Grondwatertrap:
Yc	-1.7	750	Begroeiingskaart:	Bodemkaart:
o				
120692 459758				

acc. = 2.9 m. Direct (ca. 3 m) vanaf reigerstraat pad naar boerderij Verduijn-Geuze. Ca. 100 m vanaf westover Grecht Crevasse. Ger = geroerd, Z Bijm = Zand bijmenging. h = hout.

Diepte	Textuur	Org	Plr	Kleur	Redox	Grind	M50	Ca	Fe	GW	M	LKL	Strat	Bijzonderheden
10	Z-MK			dbr	o				0					Ger, Z bijm
20	Z-MK			dbr	o				0					
30	Z-MK			dbr	or				1					baksteengruis
40	Z-MK			dbr	or				1					
50		V1	plr	dbr	r				0					"VVV" = geox V, riet, takjes
60		V1	plr	dbr	r				0	GW				"VVV" = geox V, riet, takjes
70		V2	plr	dbr	r			0	0					# Zegge(veen)
80		V2	plr	br	r			0	0					Zegge(veen)
90		V2	plr	br	r			0	0					Zegge(veen)
100		V2	plr	br	r			0	0					Zegge(veen), riet en h
110		V2	plr	br	r			0	0					Zegge(veen), riet en h
120		V2	plr	br	r			0	0					Zegge(veen)
130		V2	plr	br	r			0	0					Zegge(veen)
140		V2	plr	br	r			0	0					# Zegge(veen)
150		V2	plr	br	r			0	0					#
160		V2	plr	br	r			0	0					
170		V2	plr	br	r			0	0					Takje, riet, slap
180		V2	plr	br	r			0	0					heel slap riet- en bosveen
190		V2	plr	br	r			0	0					bosveen
200		V2	plr	br	r			0	0					riet
210		V2	plr	br	r			0	0					geleid overg Zegge
220		V1	plr	grbr	r			0	0					# reit, veel K
230		V1	plr	grbr	r			0	0					riet
240		V1	plr	grbr	r			0	0					riet
250	ZK	H2	plr	brgr	r			1	0					riet
260	ZK	H1	plr	brgr	r			1	0					riet
270		V1	plr	grbr	r			0	0					hout, takje, riet
280		V1	plr	grbr	r			0	0					veel hout
290		V1	plr	grbr	r			0	0					veel hout
300		V1	plr	grbr	r			0	0					# riet
310		V1	plr	grbr	r			0	0					# hout, takjes
320		V1	plr	grbr	r			0	0					hout, takjes
330		V1	plr	grbr	r			0	0					hout, takjes
340		V1	plr	grbr	r			0	0					hout, takjes
350		V1	plr	grbr	r			0	0					hout, takjes
360		V1	plr	grbr	r			0	0					hout, takjes
370		V1	plr	grbr	r			0	0					stuk solide hout
380														# GM
390		V1	plr	grbr	r			0	0					# hout, beetje riet
400		V1	plr	grbr	r			0	0					hout
410		V1	plr	grbr	r			0	0					hout, +riet, takjes
420		V2	plr	grbr	r			0	0					hout, +riet, takjes
430		V2	plr	grbr	r			0	0					rietveen, minder hout
440		V2	plr	grbr	r			0	0					rietV minder h 1cm Kband riet+
450		V2	plr	grbr	r			0	0					Rietveen
460														# GM
470	ZK	H2	r	grbr	r			1	0					# veel riet
480	ZK	H2	r	grbr	r			0	0					veel riet

490	ZK	H2	r	grbr	r			0	0					veel riet
500		V1	r	br	r			0	0					
510		V2	plr	zw	r			0	0					slap, takje
520		V2	plr	dbr	r			0	0					slap, takje
530		V2	plr	zw	r			0	0					heel veel riet
540		V2	plr	zw	r			0	0					# heel veel riet
550		V2	plr	dbr	r			0	0					#
560		V2	plr	dbr	r			0	0					
570		V2	plr	dbr	r			0	0					els (rood)
580		V2	plr	dbr	r			0	0					els (rood)
590		V2	h	dbr	r			0	0					els (rood)
600		V2	h	dbr	r			0	0					els (rood)
610		V2	h	dbr	r			0	0					els (rood)
620		V2	h	dbr	r			0	0					#
630		V2	r	dbr	r			0	0					# els rood
640		V2	r	dbr	r			0	0					hout, K band 1/2 mm
650		V2	h	dbr	r			0	0					hout, riet
660		V2	h	dbr	r			0	0					hout, riet
670		V2	h	dbr	r			0	0					# hout, riet
680														# GM
690														GM
700		V2	h	br	r			0	0					riet
710		V2	h	br	r			0	0					riet
720	FZ				r		150-210	0	0					Bodemvorm A-Hor (Boxtel?)
730	FZ				r		150-210	0	0					
740														GM
750														# GM

Einde boring: 201801008

201801009	Pierik, Roelofs, Moree	11-09-2019

Coordinaten	Hoogte	Diepte	KAARTEENHEID	Geomorfogenetische kaart:	
Xco	Z [m]	[cm]	Geologische kaart:	Grondwatertrap:	
Yc	-1.45	620	Begroeiingskaart:	Bodemkaart:	
o					
107733 459219					

Alphen aan den Rijn, halverwege kom (200-300 m vanaf de weg)
Kerkvaartspad 40, perceel met wandelpad

Diepte	Textuur	Org	Plr	Kleur	Redox	Grind	M50	Ca	Fe	GW	M	LKL	Strat	Bijzonderheden
10	Z-LK			br	o			0	1					ger. bijmenging zand
20	Z-LK			br	o			0	1					ger. bijmenging zand
30	Z-LK			br	o			0	1					ger. bijmenging zand
40	Z-LK			brgr	or			0	1					ger. bijmenging zand
50	Z-LK			brgr	or			0	1					
60	Z-LK		h	brgr	or			0	1	GW				
70								0	0		x			GM, kern gestoken voor
80	ZK	H2	h	brgr	r			0	0		x			overgang KR fase naar
90	ZK	H2	h	brgr	r			0	0		x			veen eronder
100	ZK	H2	h	brgr	r			0	0		x			
110		V1	h h	grbr	r			0	0		x			
120		V1	h h	grbr	r			0	0		x			
130		V1	hr	grbr	r			0	0		x			
140		V1	plr	grbr	r			0	0		x			# takje
150		V1	plr	gr gr	r			0	0					
160	MK		rh	gr gr	r			0	0					Graduele overgang naar V1
170	MK		rh	gr	r			1	0					
180	LK			lgr	r			1	0					
190	LK				r			1	0					
200	LK				r			1	0					
210								1	0					GM
220								1	0					# GM
230	LK	H0	rh	gr	r			1	0					Veel planten resten
240	LK	H0	rh	gr	r			1	0					^
250	MK		plr	gr	r			1	0					|
260	MK		plr	gr	r			1	0					|
270	MK		plr	gr	r			1	0					|
280	MK		plr	gr	r			1	0					|
290	MK		plr	gr	r			2	0					Weinig planten resten
300									0					# GM
310	ZZL		plr	gr	r			2	0					Laminatie kleur (humeus?)
320	ZZL		plr	gr	r			2	0					Slap, laminatie
330	ZZL		plr	gr	r			2	0					Laminatie kleur (humeus?)
340	ZZL		plr	gr	r			2	0					Laminatie kleur (humeus?)
350	ZZL		plr	gr	r			2	0					Takjes, laminaties
360	ZZL		plr	gr	r			2	0					laminaties kleur (humeus?)
370	ZZL		plr	gr	r			2	0					laminaties kleur (humeus?)
380	ZZL		plr	gr	r			2	0					# schelp gruis
390	ZZL		plr	dgr	r			2	0					schelp gruis
400	LK		plr	dgr	r			2	0					schelp gruis
410	ZZL		plr	dgr	r			2	0					schelp (slakje)
420	ZZL		plr	dgr	r			2	0					schelp gruis
430	ZZL		plr	dgr	r			0	0					ZZL wordt grover naar beneden
440	ZZL		plr	dgr	r			0	0					
450		V1		br	r			0	0					
460		V2		br	r			0	0					#
470		V2	r	br	r			0	0					Zegge???
480		V2	r	br	r			0	0					

490		V1	r	br	r			1	0					
500	MK	H2	r	grbr	r			2	0					Meer compact dan bovenstrooms
510	MK		r	gr	r			2	0					slapper
520	LK		r	gr	r			2	0					schelp gruis
530	LK		r	lgr	r			2	0					schelp gruis
540	LK	H1	r	lgr	r			1	0					#
550	LK	H1	r	brgr	r			0	0					humeuze bandjes
560	LK	H2	r	brgr	r			1	0					
570	ZZL		r	gr	r			2	0					
580	LZ		r	gr	r			2	0					Schelp gruis, snelle overgang
590	LZ		plr	gr	r			2	0					hor. riet (event??)
600	LZ		plr	gr	r			2	0					klei bandjes
610	LZ		plr	gr	r			2	0					material wordt grover
620	LZ		plr	gr	r			2	0					roots

Einde boring: 201801009

201801010	Pierik, Roelofs, Boechat-Albernaz	11-09-2019

Coordinaten	Hoogte	Diepte	KAARTEENHEID	Geomorfogenetische kaart:	
Xco	Z [m]	[cm]	Geologische kaart:	Grondwatertrap:	
Yc	-1.2	430	Begroeiingskaart:	Bodemkaart:	
o					
107648 459062					

Oever 1, kerkvaarderspad Alphen aan den Rijn
Boring +/- 100 m van de weg
Acc GPS = 7 m

Diepte	Textuur	Org	Plr	Kleur	Redox	Grind	M50	Ca	Fe	GW	M	LKL	Strat	Bijzonderheden
10	ZK			brgr	o o			0	0					
20	ZK			brgr	o o			0	0					
30	ZK			brgr	or			0	1					
40	ZK			brgr	or			0	1		x			Houtskool, sed samples
50	ZK			gr gr	or			1	1		x			sed samples
60	LK			gr gr	or			1	1		x			sed samples
70	LK			brgr	or			1	1		x			sed samples, mng spots
80	LK		plr	brgr	r			1	0		x			sed samples
90	LK		plr					1	0		x			sed samples
100	LK	H2	h					0	0	GW				
110	LK	H1	r	brgr	r			0	0					#
120	LK	H1	r	brgr	r			0	0					sed samples
130	ZZL	H0	plr	lbrgr	r			0	0		x			
140	ZZL	H0	r	gr	r			2	0					
150	ZZL	H0	r	gr	r			2	0					verticaal riet
160	ZZL	H0	plr	gr	r			2	0					
170	ZZL	H0	plr	gr	r			2	0					
180	ZZL	H0	plr	gr	r			2	0					
190	ZZL	H0	plr	gr	r			2	0		x			# sed samples
200	ZZL	H0	r	gr	r			2	0					#
210	ZZL	H0	r	gr	r			2	0		x			sed samples
220	ZZL	H0	h	gr	r			2	0					
230	ZZL	H0	r	gr	r			2	0					
240	LK		plr	gr	r			2	0		x			sed samples
250	ZZL		plr	gr	r			2	0		-x			begin kern
260	ZZL		plr	gr	r			0	0		x			# hout
270	ZZL	H1	h	brgr	r			0	0		x			
280	ZZL	H1	h	brgr	r			0	0		x			
290	ZZL	H1	h	brgr	r			0	0		x			
300	ZZL	H2	h	brgr	r			0	0		x			
310	ZZL	H2	h	brgr	r			0	0		x			
320		V1	r	br br	r			0	0		x			/ 5 geleidelijke overgang
330		V2	h	br br	r			0	0		x			
340		V2	r	blgr	r			0	0		x			# clay layer 1 cm
350		V1	plr	blgr	r			0	0		x			#
360	ZZL		plr	blgr	r			2	0					/4 geleidelijke overgang
370	ZZL			blgr	r			2	0					minder humeus
380	ZZL		r	blgr	r			2	0					^
390	ZZL		r		r			2	0					|
400	ZZL				r			2	0					|
410	ZZL		r	blgr	r			2	0					|
420	ZZL		r	blgr	r			2	0					|
430	ZZL		r	blgr	r			2	0					meer humeus

Einde boring: 201801010

201801011	Pierik, Roelofs, Moree	12-09-2019

Coordinaten	Hoogte	Diepte	KAARTEENHEID	Geomorfogenetische kaart:
Xco	Z [m]	[cm]	Geologische kaart:	Grondwatertrap:
Yc	-1.5	470	Begroeiingskaart:	Bodemkaart:
o				
107808 459373				

Kerkvaarderspad 40, Alphen aan den Rijn Ver het weiland in (400-600 m vanaf de weg) Acc. GPS = 5.9 m

Diepte	Textuur	Org	Plr	Kleur	Redox	Grind	M50	Ca	Fe	GW	M	LKL	Strat	Bijzonderheden
10	LK			brgr	o			0	1					zand. bijm.
20	LK			brgr	o			0	1					zand. bijm.
30	LK			brgr	o			0	1					
40	LK			brgr	o			0	1					
50	LK			dbrgr	or			0	1					tikje humeus
60	MK	H2		grbr	or			0	0					
70	MK	H2		grbr	r			0	0					baksteentjes, decomposed peat
80		V2	h	br	r			0	0					
90		V2	h	br	r			0	0					
100		V2	h	br	r			0	0					
110		V2	h	br	r			0	0					
120		V2	h	br	r			0	0					
130		V2	h	br	r			0	0					
140		V2	h	br	r			0	0					
150		V2	h	br	r			0	0					#
160		V2	h	br	r			0	0					Clayey peat with a lot of wood
170		V2	h	br	r			0	0					Clayey peat with a lot of wood
180		V2	h	br	r			0	0					Clayey peat with a lot of wood
190		V1	h	grbr	r			0	0					Clayey peat with a lot of wood
200		V2	h	br	r			0	0					Clayey peat with a lot of wood
210		V2	h	br	r			0	0					Clayey peat with a lot of wood
220		V2	h	br	r			0	0					Clayey peat with a lot of wood
230		V2	h	br	r			0	0					#
240		V2	h	br	r			0	0					
250		V2	h	dbr	r			0	0					Maybe a bit of oxidation
260		V2	h	br	r			0	0					
270		V2	h	br	r			0	0					
280		V2	r	br	r			0	0					
290		V2	r	br	r			0	0					Slap, riet, sharp contact
300														GM
310														# GM
320	LK		r	blgr	r			2	0					siltig, schelp gruis, sticky
330	LK		r	blgr	r			2	0					siltig, schelp gruis, sticky
340	LK		r	blgr	r			2	0					siltig, schelp gruis, sticky
350	LK		r	blgr	r			2	0					siltig, schelp gruis, sticky
360	LK		r	blgr	r			2	0					siltig, schelp gruis, sticky
370	LK		r	blgr	r			2	0					siltig, schelp gruis, sticky
380	LK		r	blgr	r			2	0					siltig, schelp gruis, sticky
390	LK		r	blgr	r			2	0					siltig, schelp gruis, sticky
400	LK		r	blgr	r			2	0					# siltig, schelp gruis, sticky
410	LK			blgr	r			2	0					siltig, schelp gruis, sticky
420	LK			blgr	r			2	0					siltig, schelp gruis, sticky
430	LK			blgr	r			2	0					siltig, schelp gruis, sticky
440	LK			blgr	r			2	0					siltig, schelp gruis, sticky
450	LK			blgr	r			2	0					siltig, schelp gruis, sticky
460	LK			blgr	r			2	0					siltig, schelp gruis, sticky
470	LK			blgr	r			2	0					# siltig, schelp gruis, sticky

Einde boring: 201801011

201801012	Pierik & Moree	12-09-2019

Coordinaten	Hoogte	Diepte	KAARTEENHEID	Geomorfogenetische kaart:
Xco	Z [m]	[cm]	Geologische kaart:	Grondwatertrap:
Yc	-1.6	470	Begroeiingskaart:	Bodemkaart:
o				
120742 459767				

Broing op ca. 2/3 van afstand westelijke oeverwal naar boring 201801007 in kom.Vanaf 340 -cmv: Getijdekreekje in NaWo? Hoger gelegen in landschap en daarom veel dunner NiHo veenlaag(je) gevolgd door dikker(e) crevasse oever?

Diepte	Textuur	Org	Plr	Kleur	Redox	Grind	M50	Ca	Fe	GW	M	LKL	Strat	Bijzonderheden
10	ZK	H1		dbrgr	or			0						
20	ZK	H1		dbrgr	or			0						
30	ZK	H1		dbrgr	or			0						
40	ZK	H1		dbrgr	or			0	2					
50	ZK	H2		dbrgr	r			0	0					geox veen?
60		V2	r	dbr	r			0	0					# hout, takjes
70		V2	r	br	r			0	0					hout, takjes
80		V2	r	br	r			0	0					hout, takjes
90		V2	h	br	r			0	0					hout, takjes
100		V2	h	br	r			0	0					hout, takjes
110		V2	h	br	r			0	0					hout, takjes
120		V2	h	br	r			0	0					hout, takjes
130		V1	r	grbr	r			0	0					# hout, takjes
140	MK	H0	plr	gr	r			0	0					#hout, riet
150	MK	H0	plr	gr	r			0	0					hout, riet
160	MK	H0	plr	brgr	r			0	0					hout, riet
170		V1	plr	brgr	r			0	0					
180	ZK	H1	h	brgr	r			0	0					
190	ZK	H2	h	brgr	r			0	0					slap
200	MK	H2	h	brgr	r			0	0					slap
210														# GM
220	MK	H1		dgr	r			0	0					#
230	MK	H2		dgr	r			0	0					
240														# GM, hout
250	ZK	H1	plr	dgr	r			0	0					# hout, blad
260	ZK	H1		dgr	r			0	0					
270	ZK	H1		dgr	r			0	0					
280	ZK	H1		dgr	r			0	0					
290	ZK	H1		dgr	r			0	0					
300	ZK	H1		dgr	r			0	0					takjes
310	ZK	H1		dgr	r			0	0					blad, takje
320	ZK	H1		dgr	r			0	0					#
330		V1		br	r			0	0					# Slap
340	MK		r	blgr	r			1	0					Slap riet, org vanaf hier NaWo
350	MK		r	blgr	r			1	0					Slap
360	MK		r	blgr	r			1	0					Slap
370	MK		r	blgr	r			1	0					Slap
380	MK		r	blgr	r			2	0					Slap
390	MK		r	blgr	r			2	0					Slap
400	MK		r	blgr	r			2	0					# Slap
410	LK		r	blgr	r			2	0					# geband detritus
420	LK		r	blgr	r			2	0					geband detritus
430	LK		r	blgr	r			2	0					geband detritus
440	LK		r	blgr	r			1	0					geband detritus
450	LK		r	blgr	r			1	0					geband detritus
460	LK		r	blgr	r			1	0					UFZ bandjes
470														# GM, einde boring.

Einde boring: 201801012

201801013	Pierik, Roelofs, Moree	12-09-2019

Coordinaten	Hoogte	Diepte	KAARTEENHEID	Geomorfogenetische kaart:	
Xco	Z [m]	[cm]	Geologische kaart:	Grondwatertrap:	
Yc	-0.47	370	Begroeiingskaart:	Bodemkaart:	
o					
124019 457749					

Houtdijk 17, Woerden
Op oever dicht bij sloot&huis (tussen boring 019&018 van Stouthamer profiel) Acc. 3.5

Diepte	Textuur	Org	Plr	Kleur	Redox	Grind	M50	Ca	Fe	GW	M	LKL	Strat	Bijzonderheden
10	Z-MK			dbrgr				0	0					ger
20	Z-MK			dbrgr				0	0					ger
30	Z-MK			dbrgr				0	1					ger
40	MK			brgr				0	1					
50	MK			brgr				0	1					
60	MK			brgr				0	1					
70	MK			brgr				1	1		x			
80	MK			brgr				0	1					
90	MK			brgr				1	1					
100	MK	H0	plr	dbrgr				1	1					
110	ZK	H2	plr	dbrgr				2	1					
120	ZK		r	gr				2	1					
130	ZZL		plr	gr				2	1					vert. wortel
140	ZZL		plr	gr				2	0					
150	MZL		plr	gr				2	0	GW				
160	MZL			gr				2	0					
170	MZL			gr				2	0					licht geband mm zand
180	MZL			gr				2	0					schelp gr
190	MZL		h	gr				2	0					zand laagje
200	LK			gr				2	0					
210	ZZL			gr				2	0					#
220	ZZL			gr				2	0					Zandband cm
230	LZ			gr				2	0		x			UFZ
240	MZL			gr				2	0		x			
250	MZL			gr				2	0					zeer sterk geband zand mm
260	MZL			gr				2	0					zeer sterk geband zand mm
270	MZL			gr				2	0					detritus bandje, zand band mm
280	ZZL		plr	gr				2	0					detritus bandje, verslagen r/h
290	LK		plr	gr				2	0					#
300	ZZL		plr	gr				2	0					detritus
310	ZZL		h	gr				2	0					houtje, sterk geband
320	LK		plr	gr				2	0					sterk geband
330	MK	H1	plr	gr				1	0		x			r&h, h bandje, schelp gr
340	MK	H1	plr	gr				1	0					H bandje zwart, r, schelp gr
350	MK	H1	plr	gr				1	0					
360		V1	plr	grbr				0	0					geleidelijke overgang naar 360
370		V1	plr	grbr				0	0					#

Einde boring: 201801013

201801014	Roelofs, Weisscher, Sonnemans	12-09-2019

Coordinaten	Hoogte	Diepte	KAARTEENHEID	Geomorfogenetische kaart:	
Xco	Z [m]	[cm]	Geologische kaart:	Grondwatertrap:	
Yc	-1.56	320	Begroeiingskaart:	Bodemkaart:	
o					
120828 459780					

Acc. = 2.8 m. Kanis, in de restgeul van de crevasse. Sch = Schelp? KS genoteerd?

Diepte	Textuur	Org	Plr	Kleur	Redox	Grind	M50	Ca	Fe	GW	M	LKL	Strat	Bijzonderheden
10	MK			brgr	o			2	1					Geroerd
20	MK			brgr	o			2	1					Geroerd
30	MK			brgr	o			2	1					Geroerd
40	LK	H0	plr	brgr	o			1	1					Geroerd
50	LK	H1	plr	grbr	o			0	1					Vergaan veen
60		V1	plr	dbr	o			0						Vergaan veen
70		V1	plr	dbr	o			0		GW				Vergaan veen
80		V2	plr	dbr	o			0						Vergaan veen
90		V2	r	dbr	o			0						Vergaan veen
100		V2	r	dbr	or			0						
110		V2	h	br	r			0						blad
120		V2	h	br	r			0						blad
130		V2	r	br	r			0						
140		V1	r	grbr	r			0						
150	LK	H2	r	grbr	r			1						Schgr
160	LK		h	grbr	r			1						Schgr, schelpjes plat, riet(?)
170	LK		h	grbr	r			1						# Schgr, iets slap
180	LK		r	gr	r			2						# Schgr, slap, schelp
190	Z-LZL		r	gr	r			2						
200	LZ			gr	r			2						Licht geband, M50 = 50-105 Z
210	LZ			gr	r			2						Licht geband, Schelp, 50-105 Z
220	LZ			gr	r			2						Bandjes, M50 = 50-105
230	LZ			gr	r			2						meer K bandjes, M50 = 50-105
240	MK			gr	r			2						# geen Z, veel silt
250	MK		r	gr	r			2						#
260	MK		r	gr	r			2						onderkant geband Z
270	LZ			gr	r			2						geband
280	LZ			gr	r			2						geband
290	LZ			gr	r			2						geband
300	LZ			gr	r			2						geband
310	Z-MZL			gr	r			2						geband
320														# GM, Einde Boring.

Einde boring: 201801014

201801015	Roelofs, Moree, Weisscher	12-09-2019

Coordinaten	Hoogte	Diepte	KAARTEENHEID	Geomorfogenetische kaart:	
Xco	Z [m]	[cm]	Geologische kaart:	Grondwatertrap:	
Yc	-0.78	560	Begroeiingskaart:	Bodemkaart:	
o					
124011 457810					

Houtdijk 17, Woerden
Boring 18 uit profiel Stouthamer Op de hoek van het bosje

Diepte	Textuur	Org	Plr	Kleur	Redox	Grind	M50	Ca	Fe	GW	M	LKL	Strat	Bijzonderheden
10	ZK			gr	o			0	1					
20	ZK			gr	o			0	1					
30	ZK			gr	o			0	1					
40	MK			gr	o			0	1					
50	MK		r	gr	o			0	1					
60	MK		plr	gr	or			0	2					
70	MK		plr	gr	or			0	2					
80	MK	H2	plr	grbr	r			0	0					geleidelijke overgang
90	MK	H2	plr	grbr	r			0	0					riet, takjes
100	MK	H2	hr	grbr	r			0	0					verkoold hout, takjes
110		V1	hr	br	r			0	0					hout stuk
120		V1	hr	br	r			0	0					
130		V1	hr		r			0	0					#
140	MK		plr	gr	r			2	0					stuk hout
150	MK		plr	gr	r			2	0					versp riet
160	MK		plr	gr	r			2	0					versp riet
170	LK	H0	plr	gr	r			2	0					hum, detri. bandjes (mm)
180	LK		plr	gr	r			2	0					sch. gr
190	LK		plr	gr	r			2	0					slap
200														# GM
210	LK		plr	gr	r			2	0					# Slap detr. bandje
220	LK		plr	gr	r			2	0					detr. band, schgr, versp h r
230	LK		plr	gr	r			2	0					detr. band, schgr, versp h r
240	LK		plr	gr	r			2	0					detr. band, schgr, versp h r
250	LK		plr	gr	r			2	0					dikker detr. bandjes, schgr
260	LK		plr	gr	r			2	0					versp h, schgr
270	LK		plr	gr	r			2	0					dikker detr. bandjes, schgr
280	LK		plr	gr	r			2	0					#
290	LK	H1	plr	br	r			0	0					#schgr, versp plr, gel. overga
300		V2	hr	br	r			0	0					bosveen,houtriet, compact
310		V2	hr	br	r			0	0					
320	LK	H2	hr	grbr	r			0	0					stevig
330	LK	H1	hr	grbr	r			0	0					
340	LK	H1	hr	grbr	r			0	0					
350	LK	H1	hr	grbr	r			0	0					
360		V2	plr	br	r			0	0					# hout, compact
370		V2	plr	br	r			0	0					#
380		V2	plr	br	r			0	0					
390		V2	plr	br	r			0	0					
400		V2	plr	br	r			0	0					
410		V3	plr	br	r			0	0					Hout
420		V3	plr	br	r			0	0					Hout
430		V3	plr	br	r			0	0					Hout
440		V3	plr	br	r			0	0					#Hout
450		V3	plr	br	r			0	0					#Hout
460		V3	plr	br	r			0	0					Hout
470		V3	plr	br	r			0	0					Hout
480		V3	plr	br	r			0	0					Hout

490		V3	plr	br	r			0	0					Hout
500		V3	plr	br	r			0	0					Hout
510		V3	plr	br	r			0	0					Riet
520		V3	plr	br	r			0	0					Riet
530		V3	plr	br	r			0	0					#Riet
540		V3	plr	br	r			0	0					#Riet
550		V3	plr	br	r			0	0					Riet
560		V3	plr	br	r			0	0					Riet

Einde boring: 201801015

201801016	Roelofs, Boechat-Albernaz	13-09-2019

Coordinaten	Hoogte	Diepte	KAARTEENHEID	Geomorfogenetische kaart:	
Xco	Z [m]	[cm]	Geologische kaart:	Grondwatertrap:	
Yc	-1.1	370	Begroeiingskaart:	Bodemkaart:	
o					
97480 460864					

Hazerswoude, Houtdijk 5a, Trees
Naast grote sloot voor perceel Heineken (meest distale boring) Acc.
GPS=3.7 m

Diepte	Textuur	Org	Plr	Kleur	Redox	Grind	M50	Ca	Fe	GW	M	LKL	Strat	Bijzonderheden
10	ZZL		plr	brgr	o			0	1					ger, zandige bijmeng
20	ZZL		plr	brgr	o			0	1					
30	LK		plr	brgr	o			0	1					
40	LK		plr	brgr	o			0	1					
50	LK		plr	brgr	or			0	1					
60	LK		plr	brgr	or			0	1					
70	LK		plr	brgr	r			0	0	GW				
80	LK	H1	r	brgr	r			0	0					
90	LK	H1	r	brgr	r			0	0					
100	LK	H0	r	brgr	r			0	0					
110	LK	H0	r	brgr	r			0	0					
120	LK	H0	plr	brgr	r			0	0					
130	LK	H1	h	brgr	r			0	0					
140	LK	H1	h	brgr	r			0	0					#
150	ZK	H1	h	grbr	r			0	0					grad. overgang /5
160		V1	hr	br	r			0	0					
170		V1	r	br	r			0	0					
180		V2	h	br	r			0	0					
190		V2	r	br	r			0	0					klei bandjes tussen het pure v
200		V2	r	br	r			0	0					klei bandjes tussen het pure v
210		V1	r	br	r			0	0					
220		V1	r	br	r			0	0					# bandjes, hor r
230	LK	H2	r	br	r			1	0					
240	MK		r	blgr	r			1	0					
250	MK		r	blgr	r			1	0					Zandlaagje 0.4 mm
260	MK		r	blgr	r			2	0					
270	MK		r	blgr	r			2	0					
280	LK		r	blgr	r			2	0					Sticky, stiffer
290	ZZL		r	blgr	r			2	0					Schelp gr
300	ZZL		r	blgr	r			2	0					#Schelp gr
310	ZZL		r	blgr	r			2	0					
320	MZL		r	blgr	r			2	0					
330	LZL		r	blgr	r			2	0					
340	LZ		r	blgr	r			2	0					
350	LZ		r	blgr	r			2	0					Humic band
360	UFZ		r	blgr	r		50-105	2	0					
370	LZ		r	blgr	r			2	0					# klei bandje

Einde boring: 201801016

201801017	Pierik, Moree, McMahon	13-09-2019

Coordinaten	Hoogte	Diepte	KAARTEENHEID	Geomorfogenetische kaart:	
Xco	Z [m]	[cm]	Geologische kaart:	Grondwatertrap:	
Yc	-1.15	460	Begroeiingskaart:	Bodemkaart:	
o					
97496 460891					

Hazerswoude, Houtdijk 5a, bij Trees
Oeverwal dicht bij limesweg (meer proximaal dan 20180116) Acc.
GPS = 7.9 m

Diepte	Textuur	Org	Plr	Kleur	Redox	Grind	M50	Ca	Fe	GW	M	LKL	Strat	Bijzonderheden
10	ZZL			dbrgr	o			0						geroerd
20	ZZL			dbrgr	o			0						
30	LK			gr	or			0	1					
40	LK			gr	or			0	1					
50	LK			gr	or			0	1					
60	LK			gr	or			0	1	GW				
70				gr	or			0	1					# GM
80	LK		plr	gr	or			0	1					
90	LK		plr	gr	r			0	0					
100	LK		plr	gr	r			0	0					takjes
110	LK		r	gr	r			0	0					takjes
120	LK		r	gr	r			0	0					takjes
130	LK		plr	gr	r			0	0					
140	LK		plr	gr	r			0	0					#
150	LK		plr	gr	r			0	0					#
160	ZK	H1	plr	dgr	r			0	0					
170	ZK	H1	plr	dgr	r			0	0					
180	ZK	H1	h	dgr	r			0	0					hout stuk
190		V1	h	grbr	r			0	0					riet & hout stuk
200		V2	r	grbr	r			0	0					riet
210		V1	r	grbr	r			0	0					riet
220		V1	r	grbr	r			0	0					# riet
230		V1	r	dbr	r			0	0					#
240		V1	r	dbr	r			0	0					
250	LK		r	zw	r			0	0					
260	LK		r	blgr	r			2	0					
270	LK		r	blgr	r			2	0					mm z band H0
280	LK		r	blgr	r			2	0					
290	LK		r	blgr	r			2	0					
300	LK		r	blgr	r			2	0					#
310	ZZL		r	blgr	r			2	0					#
320	ZZL		r	blgr	r			2	0					
330	ZZL		r	blgr	r			2	0					
340	ZZL		r	blgr	r			2	0					
350	MZL		r	blgr	r			2	0					
360	LZ		r	blgr	r			2	0					
370	LZ		r	blgr	r			2	0					
380	LZ		r	blgr	r			2	0					#
390	LZ		r	blgr	r			2	0					#
400	LZ		r	gr	r			2	0					
410	LZ		r	gr	r			2	0					
420	MZL		r	gr	r			2	0					
430	MZL		r	gr	r			2	0					
440	MZL		r	gr	r			2	0					
450	ZZL		r	gr	r			2	0					
460	LK		r	gr	r			2	0					#

Einde boring: 201801017

201801018	Pierik, Moree, McMahon	13-09-2019

Coordinaten		Hoogte	Diepte	KAARTEENHEID	Geomorfogenetische kaart:
Xco		Z [m]	[cm]	Geologische kaart:	Grondwatertrap:
	Yc	-1.3	50	Begroeiingskaart:	Bodemkaart:
o					
97536	460935				

Hazerswoude, Houtdijk 5a, bij Trees Op
50 cm op iets wat Limeseg lijkt (?) Acc.
GPS = 3.4 m

Diepte	Textuur	Org	Plr	Kleur	Redox	Grind	M50	Ca	Fe	GW	M	LKL	Strat	Bijzonderheden
10	MZL			dbrgr										Geroerd
20	MZL			dbrgr										
30	MZL			dbrgr										
40	MZL			dbrgr										Grindje, LIMES???
50	MZL			dbrgr										

Einde boring: 201801018

201801019	Pierik, Moree, McMahon	13-09-2019

Coordinaten	Hoogte	Diepte	KAARTEENHEID	Geomorfogenetische kaart:
Xco	Z [m]	[cm]	Geologische kaart:	Grondwatertrap:
Yc	-1.26	330	Begroeiingskaart:	Bodemkaart:
o				
97542 460947				

Hazerswoude, Houtdijk 5a, bij Trees
In zandige oeverwal, net ten Noorden van Limes Acc
GPS = ? m

Diepte	Textuur	Org	Plr	Kleur	Redox	Grind	M50	Ca	Fe	GW	M	LKL	Strat	Bijzonderheden
10	MZL			dbrgr	or			1	2					ger
20	MZL			dbrgr	or			1	2					ger
30	MZL			gr	or			2	2		Sedi			
40	MZL			gr	or			2	2					
50	MZL			gr	or			2	2					
60	MZL			gr	or			2	2					
70	MZL			gr	or			2	2					
80	MZL			gr	or			2	2					
90	MZL			gr	or			2	2					
100	MZL			gr	r			2	0	GW	Sedi			
110	MZL		plr	gr	r			2	0					# zeer gelaagd, met zand mm/cm
120	MZL		plr	gr	r			2	0					zeer gelaagd met zand mm/cm
130	MZL		plr	gr	r			2	0					zeer gelaagd met zand mm/cm
140	MZL		plr	gr	r			2	0					zeer gelaagd met zand mm/cm
150	LZL		plr	gr	r			2	0					zeer gelaagd met zand mm/cm
160	LZL			gr	r			2	0		Sedi			zeer gelaagd met zand mm/cm
170	LZL			gr	r			2	0					# zeer gelaagd met zand mm/cm
180	LZL			gr	r			2	0					#
190	LZL			gr	r			2	0					
200	LZL			gr	r			2	0					
210	LZL			gr	r			2	0					
220	LZ			gr	r			2	0					Z=MZ210-300, bed/kronkelwaard?
230	LZ			gr	r			2	0					detr. band
240	LZ			gr	r			2	0					
250	LZ			gr	r			2	0					#
260														# GM
270														GM, zand gevoeld
280														GM, zand gevoeld
290														GM, zand gevoeld
300														GM, zand gevoeld
310														GM, zand gevoeld
320														GM, zand gevoeld
330														GM, zand gevoeld

Einde boring: 201801019

201801020	Roelofs, Boechat-Albernaz	13-09-2019

Coordinaten	Hoogte	Diepte	KAARTEENHEID	Geomorfogenetische kaart:	
Xco	Z [m]	[cm]	Geologische kaart:	Grondwatertrap:	
Yc	-1.1	140	Begroeiingskaart:	Bodemkaart:	
o					
97566 460973					

Hazerswoude, Houtdijk 5a, bij Trees, Meest proximale locatie, op de stroomrug? Acc GPS = 8.7 m

Diepte	Textuur	Org	Plr	Kleur	Redox	Grind	M50	Ca	Fe	GW	M	LKL	Strat	Bijzonderheden
10	LK			brgr	o			2	1					ger
20	LK			brgr	o			2	1					minder zandig
30	ZZL			brgr	o			2	1					|
40	ZZL			gr	o			2	1					|
50	ZZL			gr	o			2	1					|
60	MZL			gr	o			2	1					meer zandig
70								2	1					# GM
80	MZL			gr	or			2	1					
90	MZL			gr	or			2	1					klei laagje
100	MZL			gr	or			2	1					
110	FZ			gr	or		150-210	2	0					
120	LZL			gr	or			2	0					
130	ZZL			gr	or			2	0					
140	LZL			gr	or			2	0					#

Einde boring: 201801020

201801021	Pierik, Roelofs, Moree, et al.	13-09-2019

Coordinaten	Hoogte	Diepte	KAARTEENHEID	Geomorfogenetische kaart:
Xco	Z [m]	[cm]	Geologische kaart:	Grondwatertrap:
Yc	-0.67	130	Begroeiingskaart:	Bodemkaart:
o				
97585 460936				

Hazerwoude, Houtdijk 5a, bij Trees
Op weiland voor huis Trees, om te kijken wat er precies afgegraven is bij boring 016 tm 020 Acc
GPS= 10.7m

Diepte	Textuur	Org	Plr	Kleur	Redox	Grind	M50	Ca	Fe	GW	M	LKL	Strat	Bijzonderheden
10	Z-LK			brgr					1					ger, baksteen, heel droog
20	Z-LK			brgr					1					ger, baksteen, heel droog
30	Z-LK			brgr					1					ger, baksteen, heel droog
40	Z-LK			brgr					1					
50	ZZL			brgr					1					
60	ZZL			brgr					1					
70	MZL			gr					1					
80	MZL			gr					1					
90	LZL			gr					1					beetje gelaagd
100	LZL			gr					1					
110	MZL			gr					1					
120	MZL			gr					1					
130	MZL			gr					1					

Einde boring: 201801021

201801022	Moree & Veldhuijzen	14-09-2019

Coordinaten		Hoogte	Diepte	KAARTEENHEID	Geomorfogenetische kaart:
Xco	Yco	Z [m]	[cm]	Geologische kaart:	Grondwatertrap:
112161	458623	-1.15	640	Begroeiingskaart:	Bodemkaart:

Ca. 30 m van huidige rivier Meije, ca. 1/3 of 2/5 van uitgesmeerde oeverwal. Boer Theo Kemp vertrouwde ons toe dat zeker het distale deel vh weiland geëgaliseerd is met oeverwal. ca. 30 - 40 cm top verstoord dus. acc 7.5 m.

Diepte	Textuur	Org	Plr	Kleur	Redox	Grind	M50	Ca	Fe	GW	M	LKL	Strat	Bijzonderheden
10	MK			brgr	o			0	2					Baksteengruis, geroerd
20	MK			brgr	o			0	2					Baksteengruis, geroerd
30	MK			brgr	o			0	2					Baksteengruis, geroerd
40	MK			brgr	o			0	2					
50	MK			brgr	o			0	2					
60	MK			gr	o			0	2					
70	LK			gr	o			0	2					
80	LK			gr	o			0	2					
90	ZZL			gr	o			0	2					
100	ZZL			gr	or			1	2					
110	ZZL			gr	or			1	2					
120	ZZL			gr	or			2	2	GW				
130	MZL		plr	gr	r			2	0					#
140	MZL		plr	gr	r			2	0					
150	MZL		plr	dgr	r			2	0					Versp plr, hum bandjes
160	ZZL		h	dgr	r			2	0					Versp plr, hum bandjes, takjes
170	MZL		plr	dgr	r			2	0					Versp plr, hum bandjes
180	MZL			dgr	r			2	0					
190	MZL			dgr	r			2	0					
200														# GM
210	MZL			gr	r			2	0					#
220	ZZL		plr	gr	r			2	0					Schgr, lemig UFZ 22 bandjes
230	ZZL		plr	gr	r			2	0					verspoeld plr takje
240	LK		h	gr	r			2	0					Schgr, verspoeld plr takje
250	LK		plr	gr	r			2	0					Schgr
260	LK		plr	gr	r			2	0					
270	LK		plr	gr	r			2	0					
280	LK		plr	gr	r			2	0					# meer plr geband?
290	LK		plr	gr	r			2	0					# Slap, versp materiaal
300	LK		r	gr	r			2	0					Slap, schgr, versp materiaal
310	LK		plr	gr	r			2	0					Schgr
320	LK		r	gr	r			2	0					Versp plr band
330	LK		plr	gr	r			2	0					Versp plr, hout stuk
340	LK		plr	gr	r			2	0					Schelp frag, versp plr
350														GM verm zandig
360														# GM verm zandig
370	LK		plr	gr	r			2	0					# Schgr
380	MK	H1	plr	dbrgr	r			1	0					hout
390	MK	H1	plr	dbrgr	r			1	0					hout
400	MK	H1	plr	gr	r			1	0					
410	MK	H0	plr	gr	r			1	0					versp venig (V2?) bandje
420	MK	H0	plr	gr	r			1	0					hout
430	MK	H1	plr	brgr	r			1	0					
440	MK	H1	plr	brgr	r			0	0					# takjes
450	MK	H1	plr	brgr	r			0	0					#hout
460	MK	H2	h	brgr	r			0	0					groot stuk hout
470	MK	H2	h	grbr	r			0	0					groot stuk hout
480	MK	H2	h	grbr	r			0	0					groot stuk hout
490		V1	h	br	r			0	0					Bosveen?
500	ZK	H2	h	grbr	r			0	0					

510	ZK	H1	h	brgr	r			0	0					
520	ZK	H1	h	brgr	r			0	0					#
530	ZK	H1	plr	brgr	r			0	0					# takjes, hout=geen stukken
540	ZK	H1	plr	brgr	r			0	0					takjes, hout=geen stukken
550	ZK	H2	plr	grbr	r			0	0					takjes, hout=geen stukken
560	ZK	H2	plr	grbr	r			0	0					#
570		V1	plr	br	r			0	0					# Compact
580		V1	plr	br	r			0	0					Compact
590		V1	plr	br	r			0	0					# Compact
600		V1	plr	br	r			0	0					# Hout stukken + riet
610		V1	plr	br	r			0	0					Hout stukken + riet
620		V1	plr	br	r			0	0					Hout stukken + riet
630		V1	plr	br	r			0	0					Hout stukken + riet
640		V1	plr	br	r			0	0					# Hout stukken + riet EB

Einde boring: 201801022

201801023	Roelofs & Born	14-09-2019

Coordinaten	Hoogte	Diepte	KAARTEENHEID	Geomorfogenetische kaart:
Xco	Z [m]	[cm]	Geologische kaart:	Grondwatertrap:
Yc	-1.82	770	Begroeiingskaart:	Bodemkaart:
o				
112128 458688				

Acc. 7.1 m. Op overgang van uitgesmeerde oever (dus oorspronkelijk een eindje in natuurlijke kom) naar huidige kom. K = klei Z = Zand. Hum = humeus

Diepte	Textuur	Org	Plr	Kleur	Redox	Grind	M50	Ca	Fe	GW	M	LKL	Strat	Bijzonderheden
10	Z-LK			brgr	o			0	1					Geroerd, Z bijmenging
20	Z-LK			brgr	o			0	1					Geroerd, Z bijmenging
30	LK			brgr	o			0	1					
40	LK			brgr	o			0	1					
50	LK			gr	o			0	1					Baksteengruis, Fe conc.
60	MK			gr	o			0	1					compact
70	MK			gr	o			0	1					
80	ZK	H1	h	brgr	o			0	0					
90		V1		dbr	o			0	0					VVV = vergaan veen
100		V1		dbr	o			0	0					
110		V1		dbr	o			0	0	GW				
120		V1		dbrgr				0	0					# Heel kleiig, kan ook H2 zijn
130		V1		dbrgr				0	0					Heel kleiig, kan ook H2 zijn
140		V1		dbrgr	r			0	0					Heel kleiig, kan ook H2 zijn
150		V1		dbrgr	r			0	0					Heel kleiig, kan ook H2 zijn
160		V1	h	dbrgr	r			0	0					Vergaan Veen
170														# GM
180	ZK	H2	h	brgr	r			1	0					#
190	ZK	H2	h	brgr	r			0	0					
200	ZK	H2	h	brgr	r			0	0					
210	ZK	H2	h	brgr	r			1	0					
220	ZK	H2	h	brgr	r			1	0					
230	ZK	H2	h	brgr	r			1	0					
240	ZK	H2	h	brgr	r			1	0					
250														# GM
260	ZK	H1	h	brgr	r			1	0					#
270	ZK	H1	h	brgr	r			1	0					
280	ZK	H1	h	brgr	r			0	0					
290	ZK	H1	h	grbr	r			0	0					/2 overgang kleur
300	ZK	H1	h	grbr	r			1	0					meer kleiig naar boven in guts
310	ZK		h	grbr	r			1	0					
320	ZK		h	grbr	r			0	0					
330	ZK	H2	h	grbr	r			0	0					# meer humeus (naar onderen)
340	LK	H2	h	grbr	r			0	0					#
350		V1	h	br	r			0	0					
360	ZK	H2	h	grbr	r			0	0					
370	ZK	H2	r	grbr	r			0	0					hor. riet band
380		V1	h	br	r			0	0					riet
390		V2	plr	br	r			0	0					
400		V2	r	br	r			0	0					kever
410		V2	plr	br	r			0	0					#
420		V1	r	br	r			0	0					#
430		V1	r	br	r			0	0					hout
440		V1	h	br	r			0	0					riet, els hout (rood)
450		V1	h	br	r			0	0					
460		V1	h	br	r			0	0					
470		V2	r	br	r			0	0					
480		V2	h	br	r			0	0					

490														# GM
500		V2	r	br	r			0	0					#
510		V2	r	br	r			0	0					minder riet naar bovenkant gut
520		V2	r	br	r			0	0					
530		V2	r	br	r			0	0					
540		V2	r	br	r			0	0					
550		V2	r	br	r			0	0					
560		V2	r	br	r			0	0					
570		V2	r	br	r			0	0					# meer riet naar onderkant gut
580		V2	r	br	r			0	0					#
590		V2	r	br	r			0	0					K bandje /3
600	MK		r	gr	r			0	0					Siltig, abrupte overgang
610	ZK	H2		brgr	r			0	0					r bandje
620	ZK	H1	r	brgr	r			0	0					hum bandjes mm
630		V1	r	grbr	r			0	0					
640		V1	r	grbr	r			0	0					# GM
650														# Klei
660		V1	r	br	r			0	0					
670		V2	r	br	r			0	0					
680		V3	r	dbr	r			0	0					Heel compact
690		V3	h	dbr	r			0	0					Heel compact
700		V3	h	br	r			0	0					Heel compact
710		V2	r	br	r			0	0					
720		V1	r	br	r			0	0					#
730		V2	r	br	r			0	0					#
740		V2	r	br	r			0	0					
750		V2	r	br	r			0	0					K bandje 3 mm
760		V3	r	br	r			0	0					
770														# GM, Einde Boring

Einde boring: 201801023

201801024	Moree & Veldhuijzen	14-09-2019

Coordinaten	Hoogte	Diepte	KAARTEENHEID	Geomorfogenetische kaart:	
Xco	Z [m]	[cm]	Geologische kaart:	Grondwatertrap:	
Yc	-1.27	540	Begroeiingskaart:	Bodemkaart:	
o					
112151 458643					

Acc. 4.6 m. ca. 25 m noorderlijker dan boring 20180122 "maar kom in"/distalere gedeelte oever. Versp. = verspoeld

Diepte	Textuur	Org	Plr	Kleur	Redox	Grind	M50	Ca	Fe	GW	M	LKL	Strat	Bijzonderheden
10	MK			gr				0	2					geroerd, baksteengruis
20	MK			gr				0	2					geroerd, baksteengruis
30	MK			gr				0	2					geroerd, baksteengruis
40	MK			gr				0	2					geroerd, baksteengruis
50	MK			gr				0	2					
60	MK			gr				1	2					
70	MK			gr				1	2					
80	MK			gr				1	2					
90	LK			gr				1	2					
100	LK			gr				1	2					
110	LK			gr				0	2					#
120	LK			gr				0	2					
130	LK		plr	dgr				0	0	GW				Slap
140	LK	H1	h	dbr				0	0					Slap prut, verp plr
150	LK	H1	h	dbr				0	0					versp plr
160	LK		plr	gr				1	0					# abrupt overg(erosief?) H1-LK
170														# GM hout
180														GM hout
190	LK	H0	plr	gr				0	0					
200														GM hout
210	MK		h	gr				1	0					Schgr
220	MK		plr	gr				1	0					Schgr
230	MK	H0	plr	gr				1	0					Schgr, plr band
240	MK	H0	plr	gr				1	0					#
250	LK		plr	gr				1	0					# versp plr
260	LK		plr	gr				1	0					Schgr, versp plr
270	LK		plr	gr				1	0					Schgr, versp plr
280	LK		plr	gr				1	0					Schgr, versp plr
290	LK		plr	gr				2	0					Versp plr, takje
300	LK		plr	gr				2	0					Schgr, versp plr
310	LK		plr	gr				2	0					Schgr, versp plr
320	LK		plr	gr				2	0					# Schgr, versp plr
330	LK		plr	gr				2	0					# Schgr
340	LK		plr	gr				2	0					Schgr
350	LK		plr	gr				2	0					Schgr
360	LK		plr	gr				2	0					Schgr, schelpfragment
370	LK	H1	plr	brgr				0	0					
380	LK	H1	plr	brgr				0	0					
390	LK		plr	gr				0	0					Schgr
400														# GM
410	ZZL		plr	gr				0	0					#
420	ZZL		plr	gr				0	0					
430	ZZL		plr	gr				0	0					Schgr
440	ZZL		plr	gr				0	0					
450	LK	H2	plr	grbr				0	0					
460		V1	plr	br				0	0					hout
470		V1	plr	br				0	0					hout
480		V1	plr	br				0	0					# hout

490		V1	plr	br				0	0					#
500		V1	plr	br				0	0					
510	ZK	H2	plr	grbr				0	0					hout
520	ZK	H2	plr	grbr				0	0					hout
530		V1	plr	br				0	0					hout
540		V1	plr	br				0	0					# hout, einde boring.

Einde boring: 201801024

201801025	Roelofs & Born	14-09-2019

Coordinaten	Hoogte	Diepte	KAARTEENHEID	Geomorfogenetische kaart:	
Xco	Z [m]	[cm]	Geologische kaart:	Grondwatertrap:	
Yc	-1.67	490	Begroeiingskaart:	Bodemkaart:	
o					
112137 458671					

Acc. = 7.6 m. Tussen boring 20180123 en 20180124 in op raai. Kern: MeijeA-I van 315 tot 398 cm onder maaiveld om bodem oever/kom op top veen te bemonsteren (= maximale ouderdom (begin van) klastische fase van Meije).

Diepte	Textuur	Org	Plr	Kleur	Redox	Grind	M50	Ca	Fe	GW	M	LKL	Strat	Bijzonderheden
10	Z-LK			brgr	o			0	1					
20	Z-LK			brgr	o			0	1					
30	Z-LK			brgr	o			0	1					
40	Z-LK			brgr	o			0	1					
50	ZK			gr	o			0	1					
60	ZK			gr	o			0	1					
70	MK			gr	o			0	1					
80	MK			gr	o			0	1					
90	MK	H2	h	dbrgr	r			0	0					humeuzer
100	ZK	H2	h	dbrgr	r			0	0					
110	ZK	H2	h	dbrgr	r			0	0					#
120	ZK	H2	h	grbr	r			0	0					
130	ZK	H2	h	grbr	r			0	0					
140	MK	H1	h	grbr	r			0	0					
150	MK	H1	h	grbr	r			0	0					
160	MK	H1	h	grbr	r			0	0					
170	MK	H1	h	grbr	r			0	0					humeuze bandjes
180	MK	H1	h	grbr	r			0	0					# denneappeltje
190	ZK	H1		lbrgr	r			2	0					
200	ZK	H1		lbrgr	r			2	0					
210	ZK	H0	plr	lbrgr	r			2	0					
220	ZK	H0		brgr	r			0	0					
230	MK			gr	r			2	0					slakkenhuisje
240	MK			gr	r			1	0					slakkenhuisje
250	MK			gr	r			0	0					
260														# GM
270	ZK	H0		lbrgr	r			2	0					
280	ZK	H0		lbrgr	r			1	0					
290	ZK	H0		lbrgr	r			2	0					
300	ZK	H0		lbrgr	r			1	0					
310	ZK	H0		lbrgr	r			1	0					Schgr, humeus bandje
320	ZK	H0		lbrgr	r			1	0		1			
330	ZK	H0		gr	r			1	0		1			4 cm hout
340											1			# GM
350	ZK	H1		brgr	r			0	0		1			
360	ZK	H2		brgr	r			0	0		1			
370	ZK	H2		grbr	r			0	0		1			Kleiig bandje 2 mm.
380		V1		br	r			0	0		1			
390		V1		br	r			0	0		1			
400		V2		br	r			0	0		1			
410		V2		br	r			0	0					
420		V2		br	r			0	0					#
430		V2		br	r			0	0					
440		V2		br	r			0	0					Klei bandje
450		V1		br	r			0	0					
460		V2		br	r			0	0					
470		V2		br	r			0	0					Zeer veel hout
480		V2		br	r			0	0					

490		V2		br	r			0	0				# Einde Boring

Einde boring: 201801025

201801029	Moree & Boechat-Albernaz	18-09-2019

Coordinaten	Hoogte	Diepte	KAARTEENHEID	Geomorfogenetische kaart:
Xco	Z [m]	[cm]	Geologische kaart:	Grondwatertrap:
Yc	-2.1	370	Begroeiingskaart:	Bodemkaart:
o				
96522 457729				

acc. 2.6 m. Dichtbij de Veldhoeve, ca. 40/50 m van stal op overgang van westoever van getijdekreekje naar kom. Detr. = Detritus. Z. = Zand

Diepte	Textuur	Org	Plr	Kleur	Redox	Grind	M50	Ca	Fe	GW	M	LKL	Strat	Bijzonderheden
10	Z-MK			brgr	o			0	1					Z bijmenging, geroerd
20	Z-MK			brgr	o			0	1					Z bijmenging, geroerd
30	Z-MK			brgr	o			0	1					Z bijmenging, geroerd
40	Z-MK			brgr	o			0	1					Z bijmenging, geroerd
50	MK			gr	or			0	1					
60	MK			gr	or			0	1					
70	MK			gr	or			0	1					
80	MK		h	gr	or			0	0	GW				#
90	MK	H0	h	gr	r			0	0					
100	MK	H0	h	gr	r			0	0					
110	MK	H1	h	grbr	r			0	0					
120	MK	H2	h	lgrbr	r			0	0					
130	MK	H2	h	lgrbr	r			0	0					
140														GM Hout
150														# GM
160		V1	h	br	r			0	0					# Slap
170		V3	r	br	r			0	0					Slap
180		V3	r	br	r			0	0					Slap, Zegge(?)
190		V3	r	br	r			0	0					Slap, Kleiiger
200		V3	r	br	r			0	0					Slap, laminatie
210		V2	r	dbr	r			0	0					Slap
220		V2	r	dbr	r			0	0					Slap, takjes
230		V2	r	dbr	r			0	0					# Slap, takjes
240		V2	r	br	r			0	0					# Slap
250		V2	plr	br	r			0	0					Slap
260	ZK	H2	r	lgrbr	r			1	0					Zeer slap, geleid overg 5 cm.
270	ZK		r	gr	r			2	0					Zeer slap
280	ZK		r	gr	r			2	0					Zeer slap
290	ZK		r	gr	r			2	0					Zeer slap, enkele detr bandjes
300	ZK		r	gr	r			2	0					Zeer slap, enkele detr bandjes
310	ZK		r	gr	r			2	0					# Zeer slap
320	ZK		plr	gr	r			2	0					# Zeer slap
330	ZK		plr	gr	r			2	0					Zeer slap, Schgr
340	MK		plr	gr	r			2	0					Zeer slap, Schelp fragment
350	MK		plr	gr	r			2	0					Zeer slap, Schgr
360														GM
370														# GM, Einde Boring.

Einde boring: 201801029

201801030	Pierik, Roelofs, Candel	20-09-2019

Coordinaten	Hoogte	Diepte	KAARTEENHEID	Geomorfogenetische kaart:
Xco	Z [m]	[cm]	Geologische kaart:	Grondwatertrap:
Yc	-2.35	410	Begroeiingskaart:	Bodemkaart:
o				
96187 457895				

Acc. = 8.8 m. Boring ver van alle (getijde)kreken voor komstratigrafie op zoek naar twee fasen crevasses in het veen.

Diepte	Textuur	Org	Plr	Kleur	Redox	Grind	M50	Ca	Fe	GW	M	LKL	Strat	Bijzonderheden
10	Z-MK				o				1					Baksteen, geroerd
20	Z-MK				o				1					Baksteen, geroerd
30	Z-MK				o				1					Baksteen, geroerd
40		V2		dbr	or			0	0					Baksteengruis, veraard
50		V2		dbr	or			0	0					veraard
60		V2	h	dbr	or			0	0	GW				veraard
70		V2		dbr	or			0	0	GLG				veraard
80		V1	r	grbr	r			0	0					
90		V1		grbr	r			0	0					
100		V2		br	r			0	0					
110		V2	h	br	r			0	0					# takjes
120														#
130		V2	r	br	r			0	0					
140		V1	r	grbr	r			0	0					
150		V3	r	br	r			0	0					
160		V3	r	br	r			0	0					
170		V3	r	br	r			0	0					#
180		V3			r			0	0					
190		V3		zw	r			0	0					
200		V3		br	r			0	0					
210		V3		dbr	r			0	0					
220		V3		dbr	r			0	0					
230			r	brgr	r			0	0					Slap
240		V1	r	brgr	r			0	0					Slap, geleid overgang.
250	MK	H0	r	gr	r			0	0					Slap
260	LK		r	gr	r			2	0					Slap, brokkelig
270	LK		r	gr	r			2	0					Slap, brokkelig
280	LK		r	gr	r			2	0					Brokkelig
290	LK		r	gr	r			2	0					Stug, brokkelig
300	LK		r	gr	r			2	0					brokkelig
310	LK		r	gr	r			2	0					brokkelig
320	LK		r	gr	r			2	0					brokkelig
330	LK		r	gr	r			2	0					# stug, brokkelig
340	LK		r	gr	r			1	0					stug, brokkelig
350	LK		r	gr	r			2	0					stug, brokkelig
360	MK		r	gr	r			1	0					
370	MK		r	gr	r			1	0					
380	MK		r	gr	r			1	0					
390	MK		r	gr	r			1	0					
400	MK		r	gr	r			1	0					
410	MK		r	gr	r			1	0					# Einde Boring.

Einde boring: 201801030

201801031	Pierik, Roelofs, Candel	18-09-2019

Coordinaten	Hoogte	Diepte	KAARTEENHEID	Geomorfogenetische kaart:	
Xco	Z [m]	[cm]	Geologische kaart:	Grondwatertrap:	
Yc	-2.34	370	Begroeiingskaart:	Bodemkaart:	
o					
96277 457853					

Acc. 5 m. Tussenboring, oorspronkelijke (getijde)kreek was er niet ver vandaan (JM: aha, er niet ver vandaan). K = Klei.

Diepte	Textuur	Org	Plr	Kleur	Redox	Grind	M50	Ca	Fe	GW	M	LKL	Strat	Bijzonderheden
10	Z-MK			brgr										
20	Z-MK			brgr										
30	Z-MK			brgr										
40		V1	h	brgr				0						
50	LK	H2	h	brgr				0						geleidelijk veniger
60	LK	H2	h	brgr				0						geleidelijk veniger
70	LK	H2	h	brgr				0						geleidelijk veniger
80	LK	H2	h	brgr				0						geleidelijk veniger
90	LK	H2	h	brgr				0						geleidelijk veniger
100	LK	H2	h	brgr				0						/5 overgang
110		V1	h	grbr				0						
120								0						# GM
130		V2	r	br				0						Zegge (Mesotroof Veen)
140		V2	r	br				0						
150		V2	r	br				0						Zegge, hout (Mesotroof Veen)
160		V2		br				0						stuk hout
170		V1	r	br				0						Zegge, laklaag
180		V2	r	br				0						meer riet
190								0						GM
200								0						# GM
210		V2	r	br				0						Geleid overg. heel siltig
220		V1	r	grbr				0						Geleid overg. heel siltig
230	LK	H2	r	brgr				1						Geleid overg. heel siltig
240			r					1						GM
250			r					1						GM
260			r					1						GM
270			r					1						GM
280			r					1						# GM
290			r					1						GM
300			r					1						GM
310			r					1						# GM
320			r					1						GM+verstoordslapNaWo K metriet
330			r					1						GM+verstoordslapNaWo K metriet
340			r					1						GM+verstoordslapNaWo K metriet
350			r					1						GM+verstoordslapNaWo K metriet
360			r					1						GM+verstoordslapNaWo K metriet
370			r					1						# GM+verstoordslapNaWoKmetriet

Einde boring: 201801031

201801032	Moree & Boechat-Albernaz	18-09-2019

Coordinaten	Hoogte	Diepte	KAARTEENHEID	Geomorfogenetische kaart:	
Xco	Z [m]	[cm]	Geologische kaart:	Grondwatertrap:	
Yc	-2.05	370	Begroeiingskaart:	Bodemkaart:	
o					
96525 457740					

Acc. = 5.1 m. Op westelijke "oeverwalletje" (getijde)kreekje. Versp. = verspoeld.

Diepte	Textuur	Org	Plr	Kleur	Redox	Grind	M50	Ca	Fe	GW	M	LKL	Strat	Bijzonderheden
10	Z-MK			dbrgr										aardewerk, Z bijmenging
20	Z-MK			dbrgr										aardewerk, Z bijmenging
30	Z-MK			dbrgr										aardewerk, Z bijmenging
40	Z-MK			dbrgr										aardewerk, Z bijmenging
50	MK			gr										compact
60	MK			gr										# gegl. aardewerk
70	MK			gr										
80	MK			gr										
90	MK			gr										Zeer siltig (mica)
100	LK		plr	gr										Zeer siltig (mica)
110	LK		plr	gr										Zeer siltig (mica)
120	LK		plr	gr										Zeer siltig (mica)
130	LK		plr	gr										Zeer siltig (mica)
140	LK		plr	gr										# Zeer siltig (mica)
150	LK	H1		brgr										#
160	LK	H1	h	brgr										versp plr
170	LK	H0	h	gr										versp plr
180	LK	H0	h	gr										versp plr
190		V1	plr	dgrbr										geleid overgang, versp plr.
200		V2	plr	br										Zeggeveen
210		V2	h	dbr										Zeggeveen
220		V2	h	dbr										# Zeggeveen
230		V2	plr	dbr										# Zeggeveen
240		V2	plr	dbr										Zeggeveen
250		V2	plr	dbr										Zeggeveen
260		V2	plr	dbr										Zeggeveen
270		V2	plr	dbr										Zeggeveen
280		V2	plr	dbr										Zeggeveen
290		V1	plr	lgrbr										Scherper overgang ca. 3 cm.
300	MK		r	blgr										# Slap, NaWo vanaf hier.
310	MK		r	blgr										# Slap
320	MK		r	blgr										Slap
330	MK		r	blgr										Slap
340	MK		r	blgr										Slap, 1 mm detritus bandjes
350	MK		r	blgr										Slap, Schgr
360	MK		r	blgr										Slap, Schgr
370	MK		r	blgr										#Slap, Schgr, Einde Boring

Einde boring: 201801032

201801033	Pierik, Roelofs, Moree	19-09-2019

Coordinaten	Hoogte	Diepte	KAARTEENHEID	Geomorfogenetische kaart:
Xco	Z [m]	[cm]	Geologische kaart:	Grondwatertrap:
Yc	-1.95	330	Begroeiingskaart:	Bodemkaart:
o				
95881 458038				

Acc. 8.9 m. In restguel van Zwiet/Vliet crevasse. Monsters: ZoeterwoudeA-I = Schelpje op -240 cmv; II = Bladrestenklomp op -265-270- cmv; III = Kern van -97 tot - 185 cmv voor datering top restgeulopvulling.

Diepte	Textuur	Org	Plr	Kleur	Redox	Grind	M50	Ca	Fe	GW	M	LKL	Strat	Bijzonderheden
10	Z-LK			dgr	o			0						puin, baksteengruis
20	Z-LK			dgr	o			0						puin, baksteengruis
30	Z-LK			dgr	o			0						puin, baksteengruis
40	Z-LK			dgr	o			0						puin, baksteengruis
50	ZK	H2		zw	o			0						sterk geoxideerd veen
60	ZK	H2		zw	o			0						sterk geoxideerd veen
70	MK		h	gr	or			2	1					
80	MK		h	gr	or			2	1					schelpfragment
90	MK		h	gr	or			2	1					
100	MK		h	gr	or			2	1					
110	ZZL		h	gr	or			2	1					
120	ZZL		h	gr	r			2	0					# schgr, bladresten
130	ZZL		h	gr	r			2	0					bladresten
140	ZZL		h	gr	r			2	0					bladresten
150	LK		h	gr	r			2	0					geband bladresten
160	LK		h	gr	r			2	0					geband bladresten, schgr
170	LK		h	gr	r			2	0					# geband bladresten, mosrest
180	LK		plr	gr	r			2	0					# bladresten
190	LK		plr	gr	r			2	0					bladresten
200	LK		plr	gr	r			2	0					
210	LK		plr	gr	r			2	0					Schgr, Z bandje mm
220	LK		plr	gr	r			2	0					Schgr
230	LK		plr	gr	r			2	0					Z bandje mm
240	LK		plr	gr	r			2	0		1			Plat slakje "@"
250	LK		plr	gr	r			2	0					#
260	LK		plr	gr	r			2	0					#
270	LK		plr	dgr	r			2	0		2			Bladrestenklomp
280	LK	H0	plr	gr	r			2	0					
290	LK	H0	plr	gr	r			2	0					
300	LK	H0	plr	gr	r			2	0					Afwis detr./Z bandjes
310	LK	H0	plr	gr	r			2	0					
320	LK	H0	plr	gr	r			2	0					Takjes met grof Zand.
330														# GM, Einde Boring

Einde boring: 201801033

201801034	Pierik, Roelofs, Moree	19-09-2019

Coordinaten	Hoogte	Diepte	KAARTEENHEID	Geomorfogenetische kaart:
Xco	Z [m]	[cm]	Geologische kaart:	Grondwatertrap:
Yc	-1.93	470	Begroeiingskaart:	Bodemkaart:
o				
95841 458047				

Acc. 5.4 m. Op overgang westelijk Zwiet/Vliet oever naar kom. Dit perceel was vroeger boomkwekerij . Foto's van guts van 160 - 240 - cmv. Voor "rietgors" zie bodemkaart Zuid-Holland en toelichting (zie dropbox).

Diepte	Textuur	Org	Plr	Kleur	Redox	Grind	M50	Ca	Fe	GW	M	LKL	Strat	Bijzonderheden
10	Z-LK			gr	o			0						
20	Z-LK			gr	o			0						
30	Z-LK			gr	o			0						
40	Z-LK	H0		brgr	o			0						Baksteengruis
50		V1		zw	o			0						Geoxideerd Veen
60	LK	H0	plr	brgr	or			0						Vergaan plr
70	LK	H0	plr	brgr	or			1						Vergaan plr
80	LK	H1	plr	brgr	or			0		GW				Vergaan plr
90	LK	H1	plr	brgr	r			0						#
100	LK	H1	plr	brgr	r			0						
110	ZZL		plr	gr	r			1						
120	ZZL		plr	gr	r			2						
130	ZZL		plr	gr	r			2						
140	ZZL		r	gr	r			2						
150	LK		r	gr	r			2						
160	LK		r	gr	r			2						#
170	LK		r	gr	r			2						# Bladresten 1 mm zw band detr
180	LK		r	gr	r			2						
190	LK		r	gr	r			2						UFZ band 5 mm
200	LK		r	gr	r			2						UFZ bandje 2 mm siltig Z bandj
210	LK		r	gr	r			1						Detr. bandjes
220	LK		r	brgr	r			1						Detr. bandjes +abrupt/erosief?
230		V1	r	br	r			0						
240														# GM
250		V2	r	dbr	r			0						#
260		V2	r	dbr	r			0						
270		V2	r	dbr	r			0						Zegge
280		V2	plr	dbr	r			0						Zegge
290		V3	r	dbr	r			0						Zegge
300		V1	r	dbr	r			0						Zwart bandje versp(?) 1 cm
310	ZK	H2	r	dbr	r			1						
320	ZK	H2	r	grbr	r			1						#
330		V1	r	br	r			0						# Siltig verm. Gyttja
340		V1	r	br	r			0						Siltig verm. Gyttja
350	MK		r	blgr	r			0						Scherp over NaWoMK naar NiHoV1
360	LK		r	blgr	r			2						Rietgors milieu
370	LK		r	blgr	r			2						Rietgors milieu
380	LK		r	blgr	r			2						Rietgors milieu
390	LK		r	blgr	r			2						Rietgors milieu
400	LK		r	blgr	r			2						# Rietgors milieu
410	LK		r	blgr	r			2						#
420	LK		r	blgr	r			2						
430	LK		r	blgr	r			2						
440	ZZL		r	blgr	r			2						Schgr
450	ZZL		r	blgr	r			2						Schgr
460														GM
470														# GM, Einde Boring.

Einde boring: 201801034

201801035	Pierik, Roelofs, Moree	19-09-2019

Coordinaten	Hoogte	Diepte	KAARTEENHEID	Geomorfogenetische kaart:	
Xco	Z [m]	[cm]	Geologische kaart:	Grondwatertrap:	
Yc	-2.05	400	Begroeiingskaart:	Bodemkaart:	
o					
95817 458051					

Acc. = 5.0 m.10 m westelijker boring34. Monsters: ZoeterwoudeB-I: kern 91-144 -cmv; B-II: kern 144-226 -cmv en B-III: kern 113-213 -cmv. De humMK van 80 tot 140 -cmv is mogelijk V1 gezien bij kernsteken. foto 170-240-cmv

Diepte	Textuur	Org	Plr	Kleur	Redox	Grind	M50	Ca	Fe	GW	M	LKL	Strat	Bijzonderheden
10	Z-MK			dgr				0						
20	Z-MK			dgr				0						
30	Z-MK			dgr				0						
40		V1	plr	dbr				0	1					
50		V1	plr	dbr				0	1					
60	ZK	H2	plr	dbrgr				0	1					
70	ZK	H1	plr	brgr				0	1					
80	MK	H1	plr	brgr				0	0					
90	MK	H2	h	brgr				0	0					#
100	MK	H2	h	brgr				0	0		1			
110	MK	H2	h	brgr				0	0					Worteltjes
120	MK	H2	h	brgr				0	0		3			
130	MK	H2	h	brgr				0	0					
140	MK	H2	h	brgr				0	0					
150		V1	h	grbr				0	0		2			
160														# GM
170	LK	H0	h	brgr				1	0					# hout en takjes
180	LK	H0	h	brgr				2	0					hout en takjes
190	LK	H0	h	brgr				2	0					hout en takjes
200	LK	H1	h	brgr				2	0					/6
210		V2	r	br				0	0					5 cm V1 ertussen
220		V3	r	br				0	0					
230		V2	z	br				0	0					riet
240		V1	z	br				0	0					# riet, slap
250		V1	r	br				0	0					# K bandjes mm's
260		V1	r	br				0	0					K bandjes, mm's
270		V1	r	br				0	0					K bandjes, mm's
280		V1	r	br				0	0					MK band3cm Zw bandje 1cm lager
290		V1	r	br				0	0					
300		V1		grbr				0	0				Vg	Vg = Gyttja, groenig&homogeen
310		V1		grbr				0	0				Vg	Vg = Gyttja, groenig&homogeen
320		V1		grbr				0	0				Vg	# Vg = Gyttja, groenig&homogee
330	ZK		r	blgr				0	0					# 1 cm gyttja
340	ZK		r	blgr				2	0					1 mm Z band
350	ZK		r	blgr				2	0					detr. bandjes 1/2 mm
360	ZK		plr	blgr				2	0					detr. bandjes 1/2 mm
370	ZK		plr	blgr				2	0					detr. bandjes 1/2 mm
380	MK		plr	blgr				2	0					Schgr
390	MK		r	blgr				2	0					Schgr
400	MK		r	blgr				2	0					# Schgr, Einde Boring.

Einde boring: 201801035

201801036	Pierik & Roelofs	19-09-2019

Coordinaten	Hoogte	Diepte	KAARTEENHEID	Geomorfogenetische kaart:	
Xco	Z [m]	[cm]	Geologische kaart:	Grondwatertrap:	
Yc	-1.94	310	Begroeiingskaart:	Bodemkaart:	
o					
95824 458050					

Acc. 5.3 m. Tussen 35 en 34 in om overgang tussen veen en oever beter te begrijpen.

Diepte	Textuur	Org	Plr	Kleur	Redox	Grind	M50	Ca	Fe	GW	M	LKL	Strat	Bijzonderheden
10	Z-MK			dgr	o				0					
20	Z-MK			dgr	o				0					
30	Z-MK			dgr	o				0					
40		V1		dbr	o				0					
50		V1		dbr	o				0					
60	ZK	H2	h	brgr	or				1					
70	ZK	H2	h	brgr	or				1					
80	ZK	H2	h	brgr	r			1	0					#
90	ZK	H2	h	brgr	r			0	0					
100	ZK	H2	h	brgr	r			0	0					geleidelijke overgang.
110		V1	h	br	r			0	0					
120		V1	h	br	r			0	0					
130		V1	h	br	r			0	0					
140		V1	h	br	r			0	0					
150														# GM
160	ZK	H2	h	brgr	r			0	0					# rietje
170	LK	H2	h	brgr	r			0	0					
180	LK	H0	h	gr	r			2	0					
190	LK	H0	h	gr	r			2	0					
200	LK	H0	h	gr	r			2	0					
210	LK	H0	h	gr	r			2	0					
220	LK	H1	h	gr	r			2	0					
230		V1	h	br	r			0	0					#
240		V1	r	br	r			0	0					# geband met Klei
250		V1	r	br	r			0	0					geband met Klei
260		V2	r	br	r			0	0					
270		V2	r	br	r			0	0					1 cm Kleibandje
280		V2	z	br	r			0	0					geband Klei
290		V1	z	br	r			0	0					geband 1 cm Klei
300														GM
310														# GM

Einde boring: 201801036

201801037	Pierik, Roelofs, Moree	19-09-2019

Coordinaten	Hoogte	Diepte	KAARTEENHEID	Geomorfogenetische kaart:	
Xco	Z [m]	[cm]	Geologische kaart:	Grondwatertrap:	
Yc	-1.2	500	Begroeiingskaart:	Bodemkaart:	
o					
95865 458038					

Acc. = 6.7 m. Op westelijke oever Zwiet naast restgeul. Schgr. = Schelpengruis.

Diepte	Textuur	Org	Plr	Kleur	Redox	Grind	M50	Ca	Fe	GW	M	LKL	Strat	Bijzonderheden
10	Z-LK							0						
20	Z-LK							0						
30	Z-LK							0						
40	LZL				o			2						
50	LZL				o			2						
60	LZL				o			2						
70	LZL				o			2						
80	LZL				o			2						
90	LZL				o			2						
100	LZL				o			2						
110	LZL				o			2						Schgr
120	LZL				o			2						Schgr
130	LZL				o			2						Schgr
140	MZL		plr		or			2						Schgr, verslagen
150	MZL				or			2						Schgr
160	LZL		plr		or			2						Schgr
170	LZL				r			2		GW				Schgr
180	LZL				r			2						# Schgr
190	LZL		h		r			2						schgr
200	LZL		plr		r			2						schgr
210	LZL		plr		r			2						Zwart verpsoeld laagje
220	MZL		plr		r			2						
230	LZL		plr		r			2						AfwisK-Z bandjes 2mm
240	LZL		plr		r			2						AfwisK-Z bandjes2mmversp takje
250	ZZL		r		r			2						# AfwisK-Z bandjes 2 mm +Z
260	ZZL		plr		r			2						# AfwisK-Z bandjes 2 mm +Z
270	LK		plr		r			2						AfwisK-Z bandjes 2 mm +Z
280	LK		plr		r			2						AfwisK-Z bandjes 2 mm +K
290	LZ		plr		r			2						AfwisK-Z bandjes 2 mm +K
300	LZ		plr		r			2						AfwisK-Z bandjes 2 mm +K
310	LZ		plr		r			2						AfwisK-Z bandjes 2 mm +K
320	LZ		plr		r			2						AfwisK-Z bandjes 2 mm +K
330	LZ		plr		r			2						AfwisK-Z bandjes 2 mm +K
340	LZ		plr		r			2						# AfwisK-Z bandjes 2 mm +K
350	LK				r			2						# Z bandjes regelmatiginterval
360	LK				r			2						Regelmatiginterval (zie onder)
370	LK				r			2						
380	LK				r			2						
390	LK				r			2						
400	LK				r			2						
410	LK				r			2						
420	LK				r			2						#
430	LK				r			2						# 5 gebundelde sets van 10 cm
440	LK				r			2						5 gebundelde sets van 10 cm
450	LK				r			2						5 gebundelde sets van 10 cm
460	LK				r			2						5 gebundelde sets van 10 cm
470	LK				r			2						5 gebundelde sets van 10 cm
480	LK				r			2						5 gebundelde sets van 10 cm

490	LK				r			2						5 gebundelde sets van 10 cm
500	LK				r			2						# 5 gebundelde sets van 10 cm

201801038	Pierik, Roelofs, Moree	18-09-2019

Coordinaten		Hoogte	Diepte
Xco		Z [m]	[cm]
	Yc	-2.25	280
o			
96338	457826		

KAARTEENHEID	Geomorfogenetische kaart:	
Geologische kaart:	Grondwatertrap:	
Begroeiingskaart:	Bodemkaart:	

Acc. = 7.8 m. Aan de flank van de kleine (getijde)kreek (JM= op boorstaat als crevasse(??) omschreven) overgang naar kom 10 m van oever.

Diepte	Textuur	Org	Plr	Kleur	Redox	Grind	M50	Ca	Fe	GW	M	LKL	Strat	Bijzonderheden
10	Z-MK			dbr				0	0					
20	Z-MK			dbr				0	0					
30	ZK	H2		dbr				0	0					Overgang geox veen
40		V1		dbr				0	0					Sterk veraard veen
50	LK	H0	h	brgr				0	0					Stuk hout
60	LK	H0		brgr				0	0	GW				
70	MK	H1		brgr				0	0					
80	MK	H2		brgr				0	0					
90		V1	h	grbr				0	0					
100		V1	h	grbr				0	0					
110		V1	h	grbr				0	0					
120														# GM
130	MK	H1	h	grbr										
140	MK	H1	h	grbr										
150	ZK	H1	plr	grbr										/5
160		V1	z	br										/3 riet
170		V3	z	br										riet
180		V3	z	br										riet
190		V3	z	br										riet
200		V3	z	br										# riet
210		V3	z	br										# riet, zw laagje 5 cm versp?
220		V3	z	br										riet, zw laagje 5 cm (versp?)
230		V3	z	br										riet
240		V3	z	br										riet, 1 cm kleiband
250		V1	z	br										riet, 1 cm zwart bandje
260	LK		r	gr										
270														GM
280														# GM, Einde Boring!

Einde boring: 201801038

Appendix E

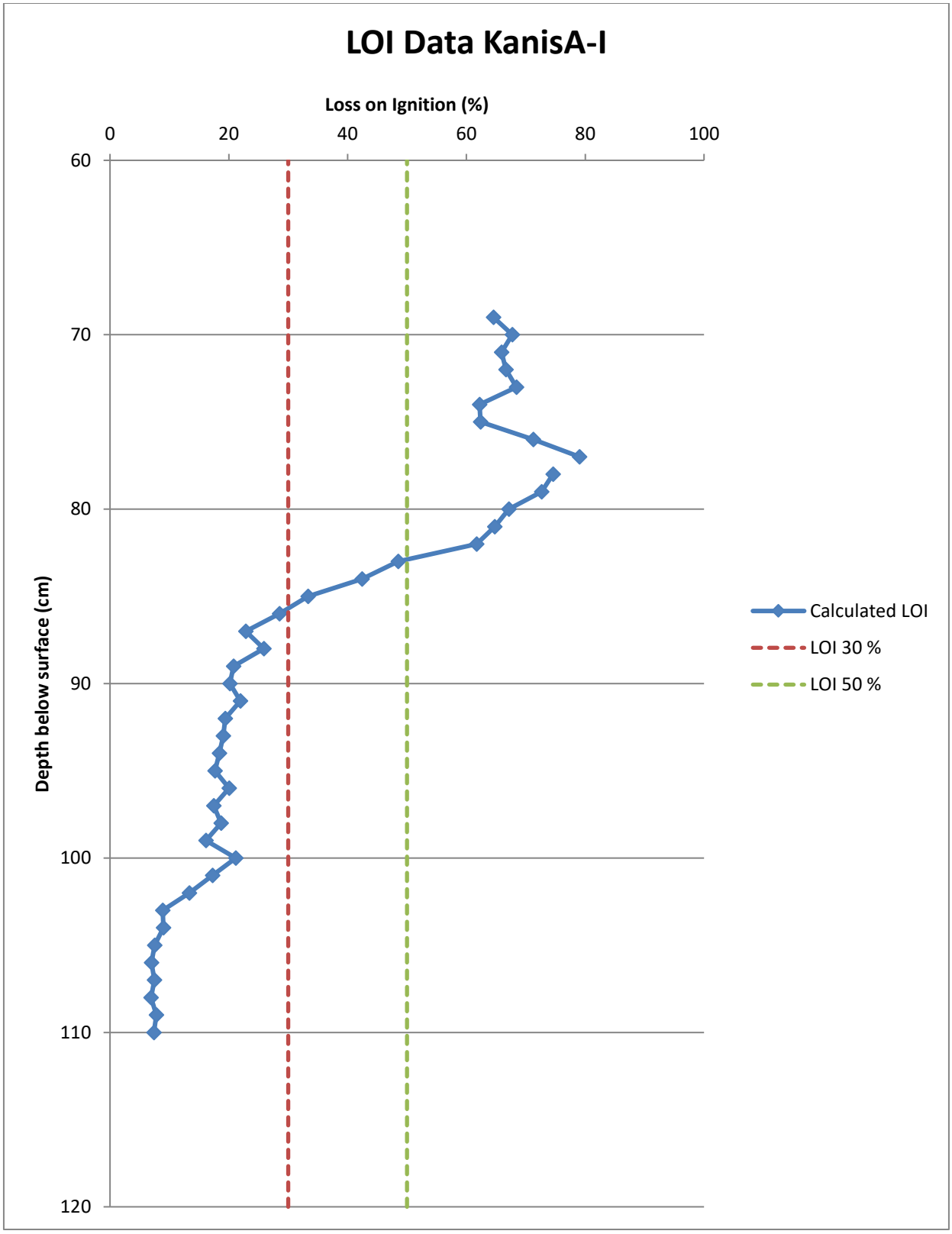
LOI Data KanisA-I
Loss on Ignition (%)
0
20
40
60
80
100
60
70
80
90
100
110
120
Depth below surface (cm)
Calculated LOI
LOI 30 %
LOI 50 %

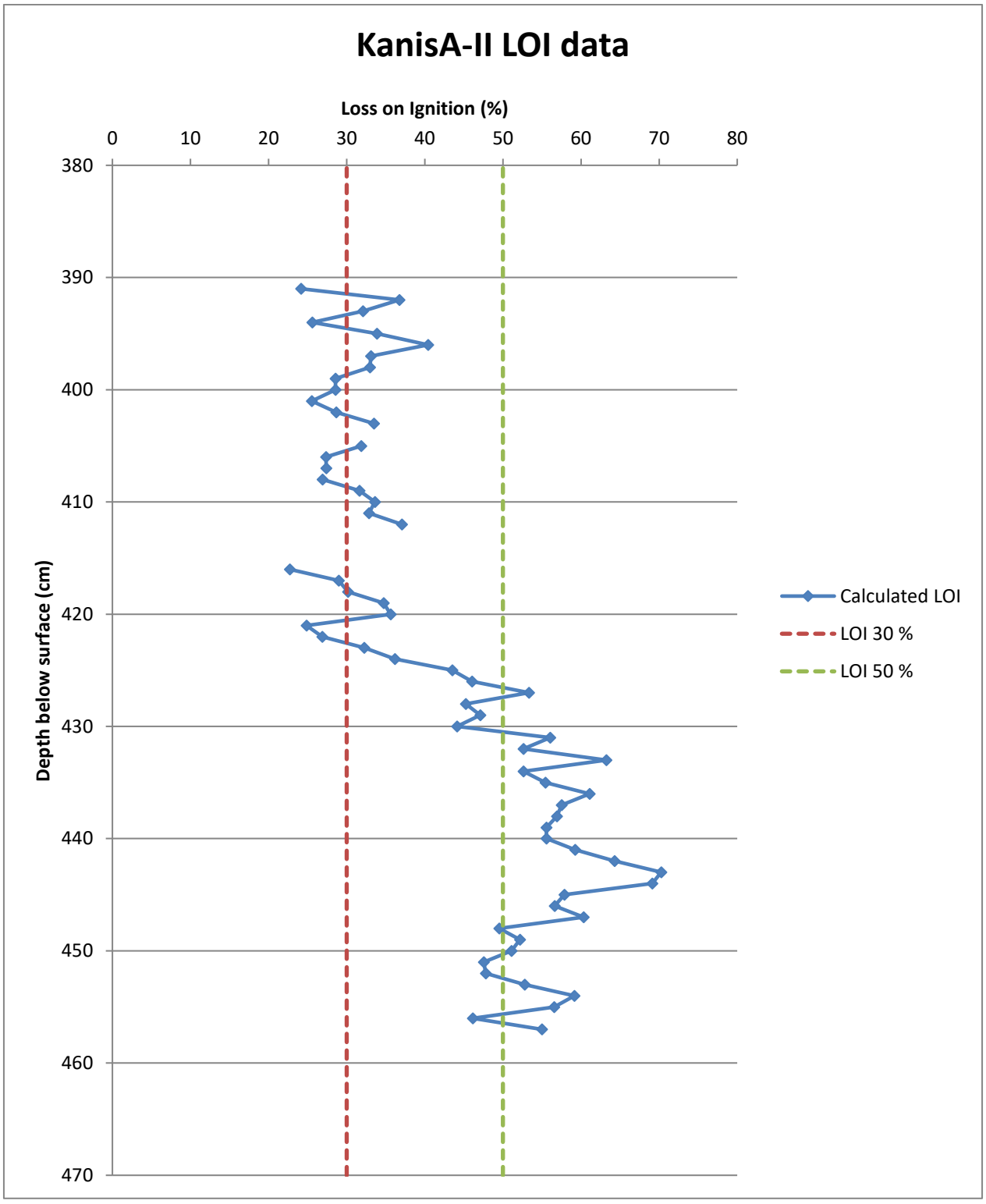
KanisA-II LOI data
Loss on Ignition (%)
0
10
20
30
40
50
60
70
80
380
390
400
410
420
430
440
450
460
470
Depth below surface (cm)
Calculated LOI
LOI 30 %
LOI 50 %

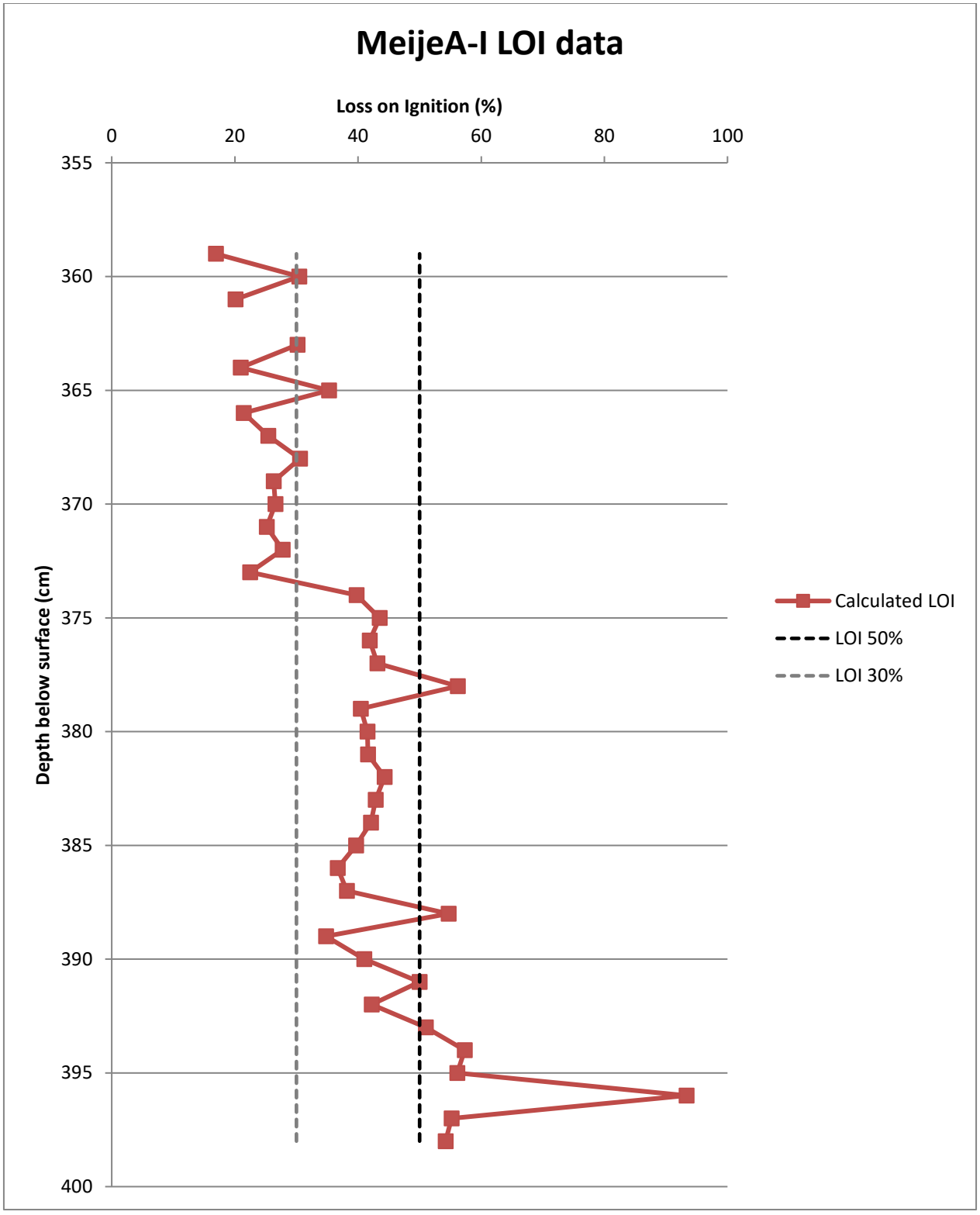
MeijeA-I LOI data
Loss on Ignition (%)
0
20
40
60
80
100
355
360
365
370
375
380
385
390
395
400
Depth below surface (cm)
Calculated LOI
LOI 50%
LOI 30%

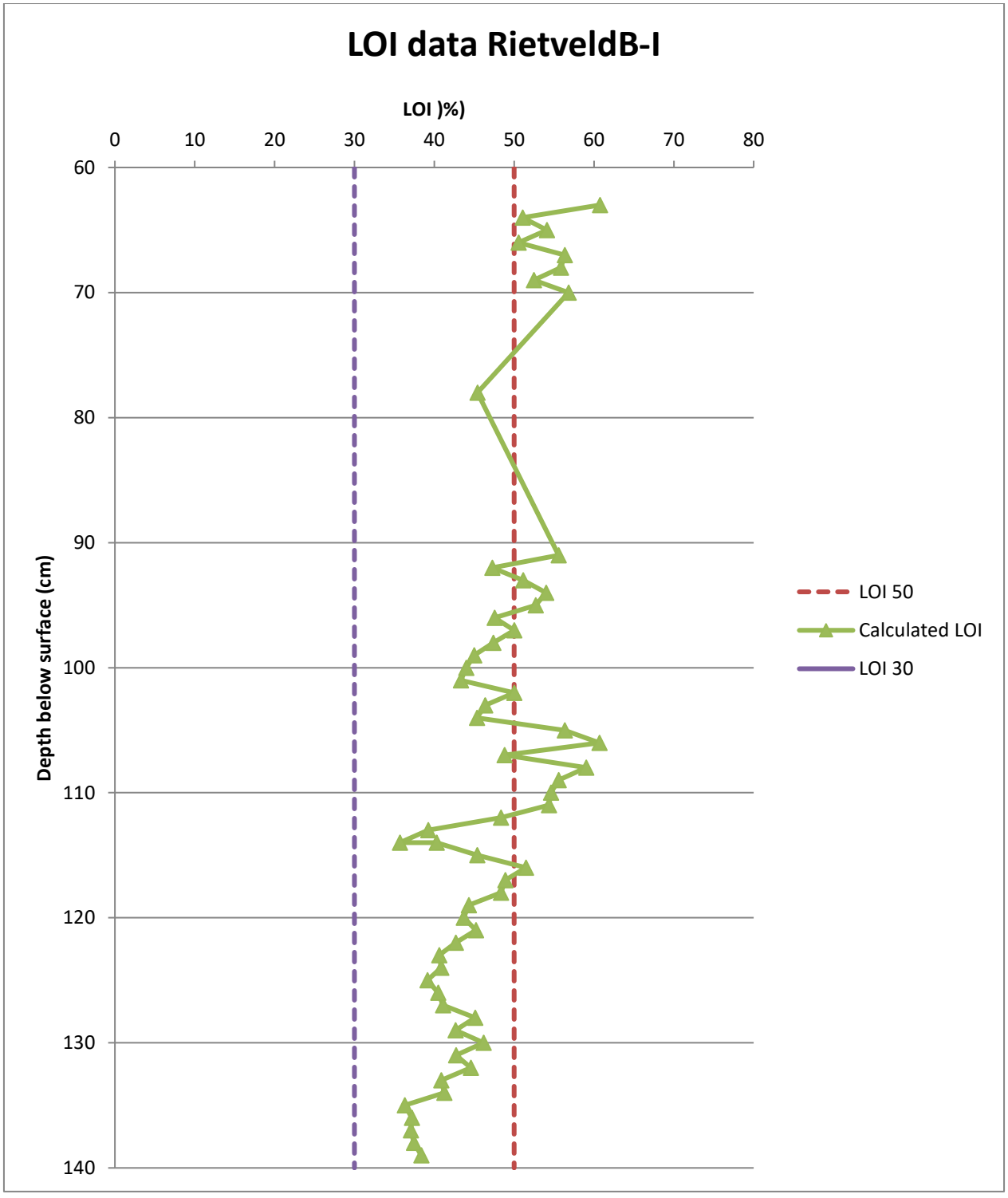
LOI data RietveldB-I
LOI)%)
0
10
20
30
40
50
60
70
80
Depth below surface (cm)
60
70
80
90
100
110
120
130
140
LOI 50
Calculated LOI
LOI 30

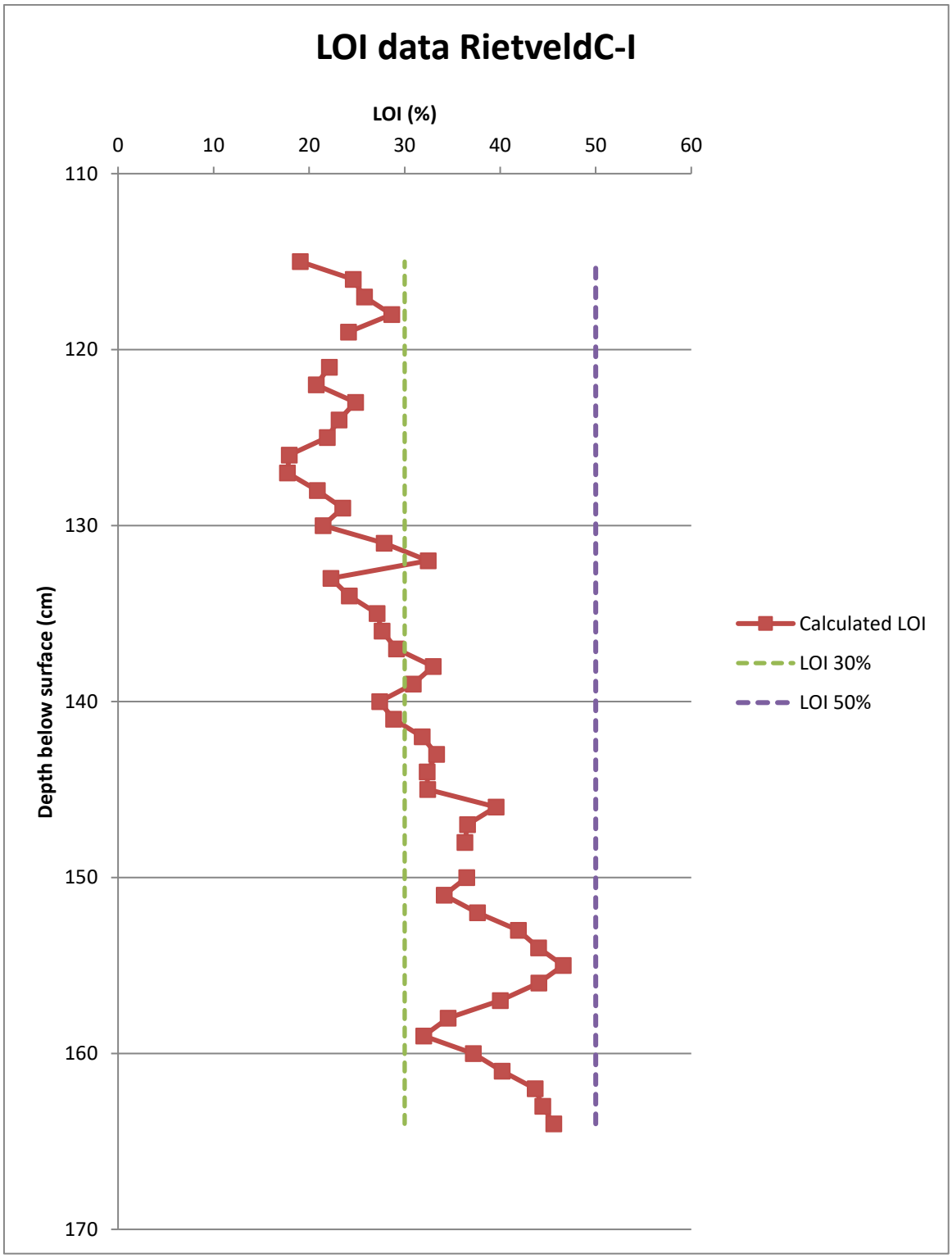
LOI data RietveldC-I
LOI (%)
0
10
20
30
40
50
60
110
120
130
140
150
160
170
Depth below surface (cm)
Calculated LOI
LOI 30%
LOI 50%

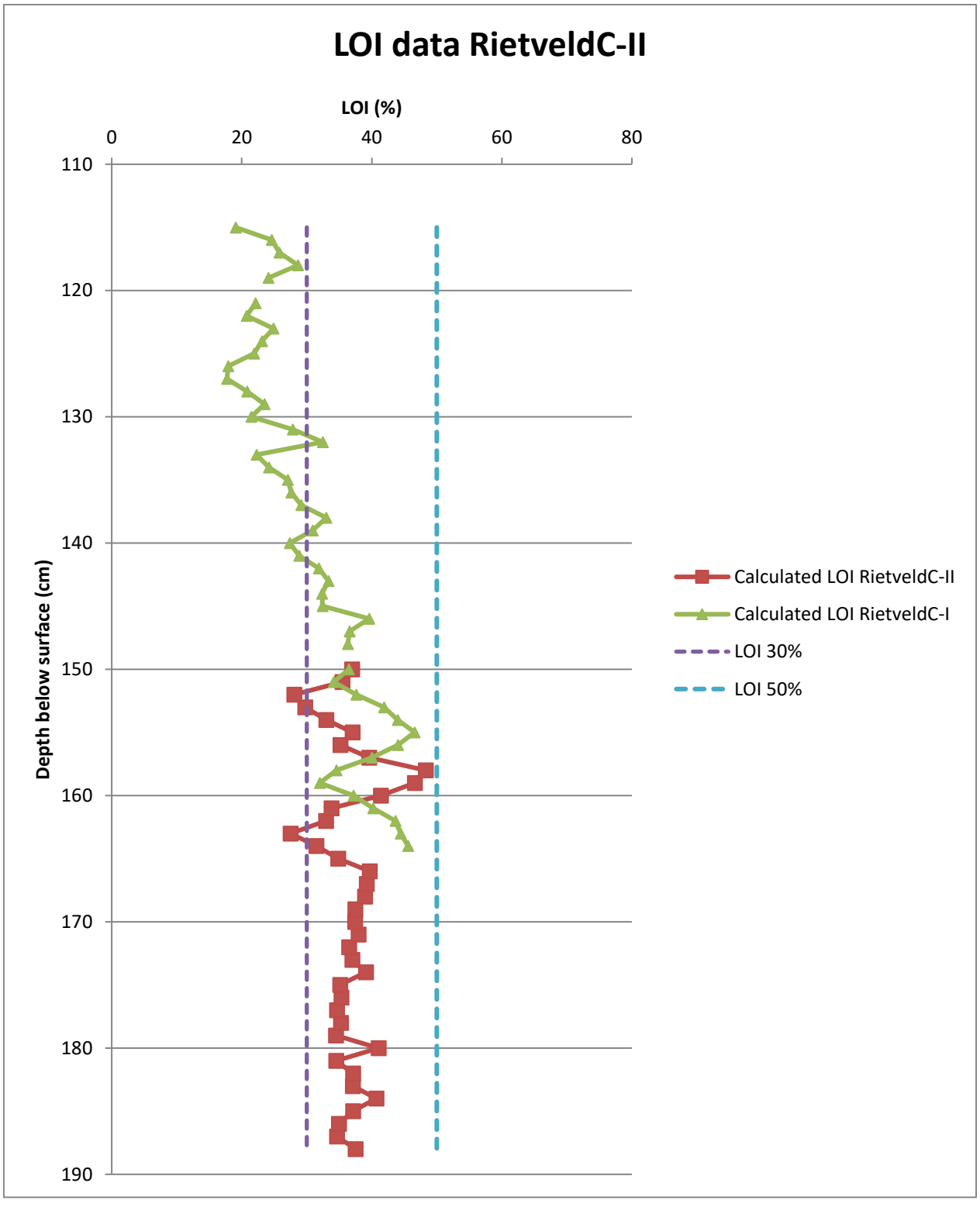
LOI data RietveldC-II
LOI (%)
0
20
40
60
80
110
120
130
140
150
160
170
180
190
Depth below surface (cm)
Calculated LOI RietveldC-II
Calculated LOI RietveldC-I
LOI 30%
LOI 50%

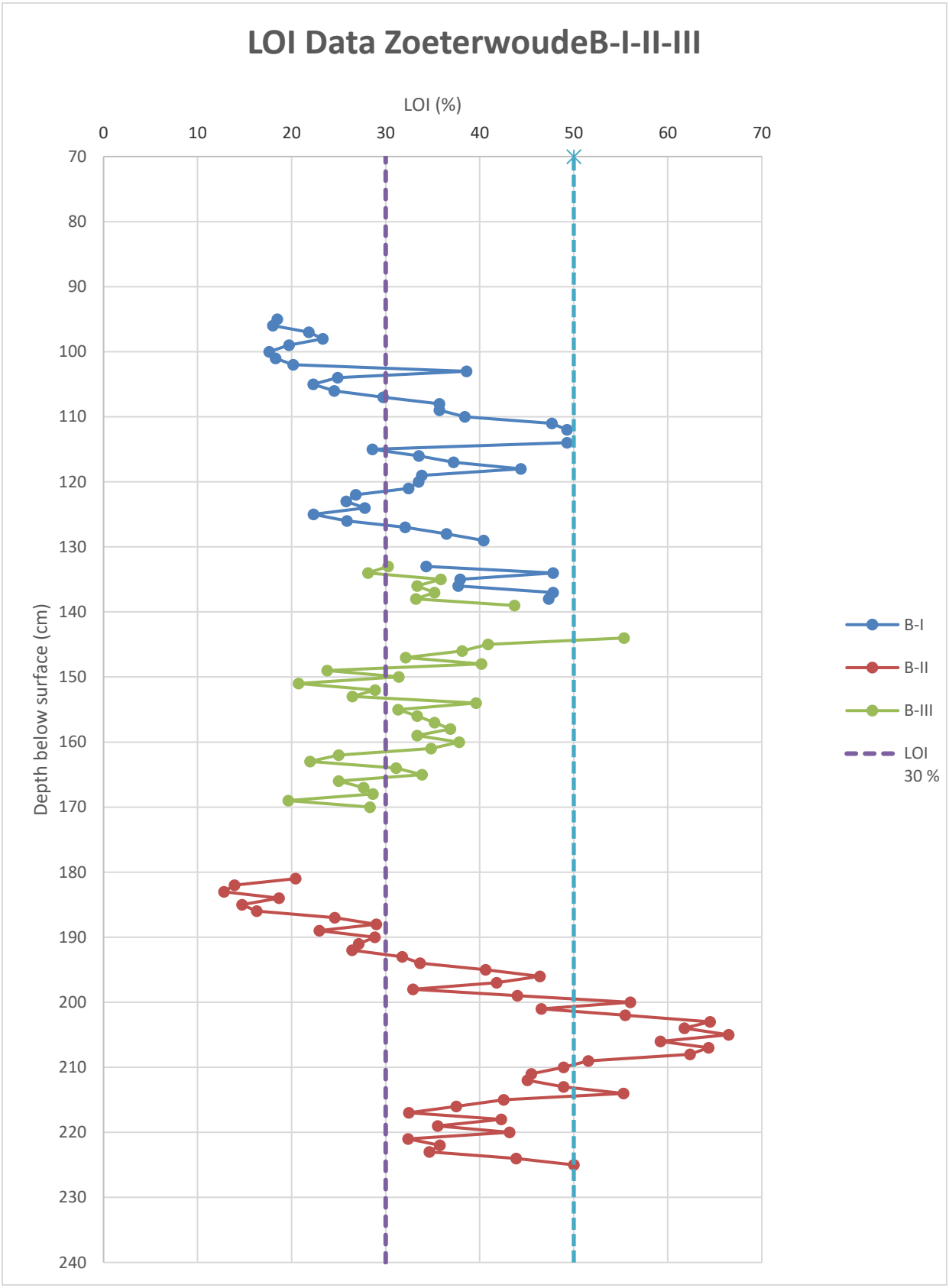
LOI Data ZoeterwoudeB-I-II-III
LOI (%)
0
10
20
30
40
50
60
70
Depth below surface (cm)
70
80
90
100
110
120
130
140
150
160
170
180
190
200
210
220
230
240
B-I
B-II
B-III
LOI
30 %

Appendix F

Samples

Required data				Extra Isotopes analysis				Weight	More	Customer pretreat		Sample locati	Town / Lake /					Additional info		Sample Position [m]			ref. surface						Expected Age	
Sample	Material	Sample	Other co	C-13	O-18	H-2	N-15	mg or ml	available	Done?	Pretreatme	Country /	Province	Mountair	Latitude	Longitud	GPS coo	Local co	Collectio	Sample	From…	To…	with resp	elevation	Layer	Type of i	Field of s	Prehist. /	Stratigr.	Age	Time scale
Hazerswc	(charred)	Eleocharis palustris/uniglumis 19, Carex sp. 6, Alnus glutino						?	x		AAA, ultra	The Neth	Zuid-Holla	Hazerswoude				97496-46	#####	Sediment	1.89	1.91	below sur	-1.15	upper	Boring	Geology		Holland P	4000-250	BP
Hazerswc	(charred)	Alnus glutinosa 33 v, katschub 12						?	x		AAA, ultra	The Neth	Zuid-Holla	Hazerswoude				97496-46	#####	Sediment	1.72	1.74	below sur	-1.15	upper	Boring	Geology		Holland P	3500-250	BP
Kerkvaar	(charred)	Eleocharis palustris/uniglumis 16, Lythrum salicaria 9, Mentl						?	x		AAA, ultra	The Neth	Zuid-Holla	Alpen aan den Rijn				107648-4	#####	Sediment	2.95	2.97	below sur	-1.15	upper	Boring	Geology		Holland P	4000-250	BP
Kerkvaar	(charred)	Carex sp 8, Urtica dioca, 1, Alnus glutionasa 8						?	x		AAA, ultra	The Neth	Zuid-Holla	Alpen aan den Rijn				107733-4	#####	Sediment	1.11	1.13	below sur	-1.52	upper	Boring	Geology		Holland P	3000-200	BP
Kerkvaar	(charred)	Alnus glutinosa 10v, 1 katje						?	x		AAA, ultra	The Neth	Zuid-Holla	Alpen aan den Rijn				107733-4	#####	Sediment	1.22	1.3	below sur	-1.52	lower	Boring	Geology		Holland P	3500-250	BP
KanisA-I-	(charred)	Apiaceae 5; Mentha aquatica 1; Alisma plantago-aquatica 4						?	x		AAA, ultra	The Neth	Utrecht	Kanis, gemeente Woerden				120864-4	#####	Sediment	0.76	0.82	below sur	-1.58	lower	Boring	Geology		Holland P	3000-150	BP
KanisA-II	(charred)	Alnus glutinosa 1 v; Rubus sp. 1 frgm; Carex sp. 1; Menth						?	x		AAA, ultra	The Neth	Utrecht	Kanis, gemeente Woerden				120864-4	#####	Sediment	4.25	4.37	below sur	-1.58	upper	Boring	Geology		Holland P	5000-200	BP
MeijjeA-I-	(charred)	Alnus glutinosa 22 v, katje 1 frgm, katschub 3; Carex sp.						?	x		AAA, ultra	The Neth	Zuid-Holla	Meije,gem. Bodegraven				112137-4	#####	Sediment	3.73	3.75	below sur	-1.67	upper	Boring	Geology		Holland P	5000-200	BP
RietveldA	(charred)	Leaf remains						?	x		AAA, ultra	The Neth	Zuid-Holla	Rietveld, gem. Alphen ad Rijn				103888-4	#####	Sediment	3	3.1	below sur	-1.6	middle	Boring	Geology		Holland P	3000-150	BP
RietveldC	(charred)	Alnus glutinosa 22 v, katje 1 frgm, katschub 3; Carex sp.						?	x		AAA, ultra	The Neth	Zuid-Holla	Rietveld, gem. Alphen ad Rijn				103860-4	#####	Sediment	1.65	1.67	below sur	-1.82	upper	Boring	Geology		Holland P	5000-200	BP
Zoeterwo	(charred)	Leaf remains						?	x		AAA, ultra	The Neth	Zuid-Holla	gemeente Zoeterwoude				95881-45	#####	Sediment	2.65	2.7	below sur	-1.95	middle	Boring	Geology		Holland P	3000-150	BP
Zoeterwo	(charred)	Alnus glutinosa 1 katje						?	x		AAA, ultra	The Neth	Zuid-Holla	gemeente Zoeterwoude				95881-45	#####	Sediment	1.28	1.31	below sur	-1.95	middle	Boring	Geology		Holland P	3000-150	BP
Zoeterwo	(charred)	Alnus glutinosa 15 v + 13 v frgm, katschub 12; Carex sp.						?	x		AAA, ultra	The Neth	Zuid-Holla	gemeente Zoeterwoude				95817-45	#####	Sediment	1.08	1.14	below sur	-2.05	upper	Boring	Geology		Holland P	5000-200	BP
Zoeterwo	(charred)	Alnus glutinosa 8 v, 1 katje, 4 katschub						?	x		AAA, ultra	The Neth	Zuid-Holla	gemeente Zoeterwoude				95817-45	#####	Sediment	2.01	2.03	below sur	-2.05	upper	Boring	Geology		Holland P	5000-200	BP
Zoeterwo	(charred)	Alnus glutinosa 3 v, 2 katje, katschub 5						?	x		AAA, ultra	The Neth	Zuid-Holla	gemeente Zoeterwoude				95817-45	#####	Sediment	1.58	1.6	below sur	-2.05	lower	Boring	Geology		Holland P	5000-200	BP
Zoeterwo	(charred)	Alnus glutinosa 12 v, 1 katje, 10 katschub						?	x		AAA, ultra	The Neth	Zuid-Holla	gemeente Zoeterwoude				95817-45	#####	Sediment	1.46	1.48	below sur	-2.05	lower	Boring	Geology		Holland P	5000-200	BP

Appendix G

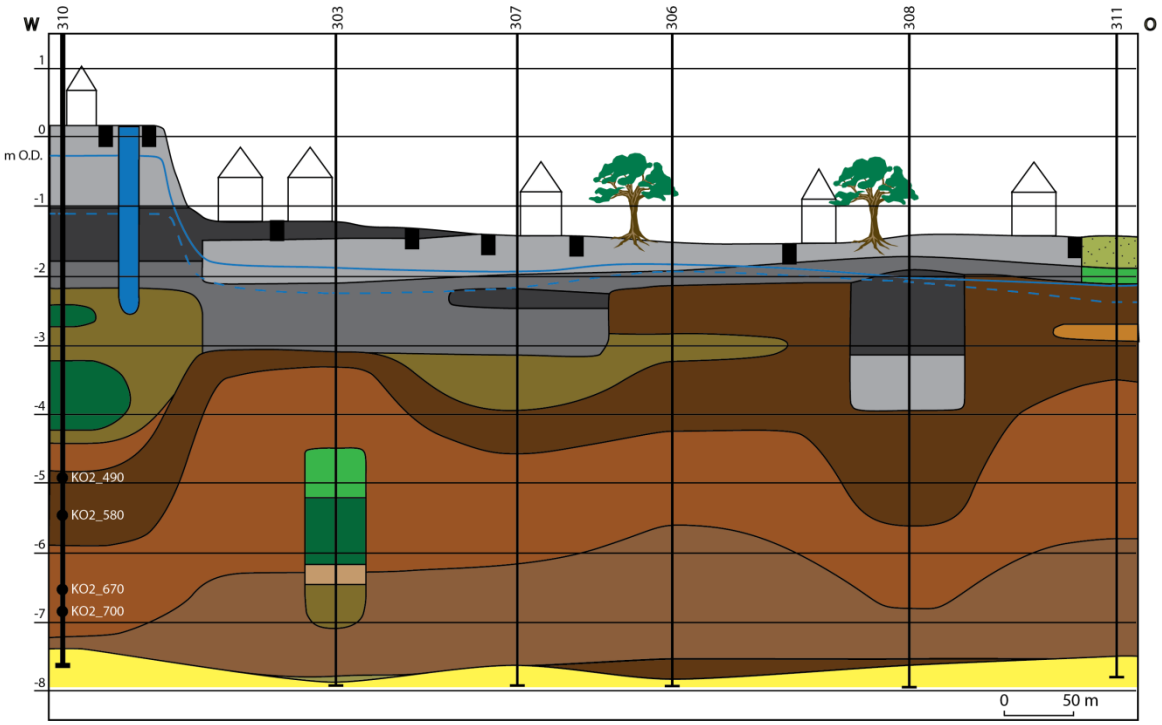

Figure E.4. *Cross section of the Holocene sequence beneath Kockengen south. For location of the cross section see Figure 2. This cross section dissects the old part of the village. The anthropogenic layer varies in thickness between 0.6 and 2.4 m. The Holocene sequence composition is similar to the northern cross section in Kockengen, including an up-to-2-m thick layer of clayey floodbasin deposits (clayey peat, peaty clay) of the Spengen channel, embedded in the top wood-peat layer (borehole numbers 306, 307 and 310). At borehole number 303 (crevasse) channel deposits have been found at a deeper level, dissecting the sedge-reed peat layer. This is probably connected to the Old Rhine channel system (active between ca 6500 and 725 cal yr BP; [Cohen et al., 2012]).*

Figure E.4 and caption adopted from the supplementary data to Van Asselen *et al*. (2018)

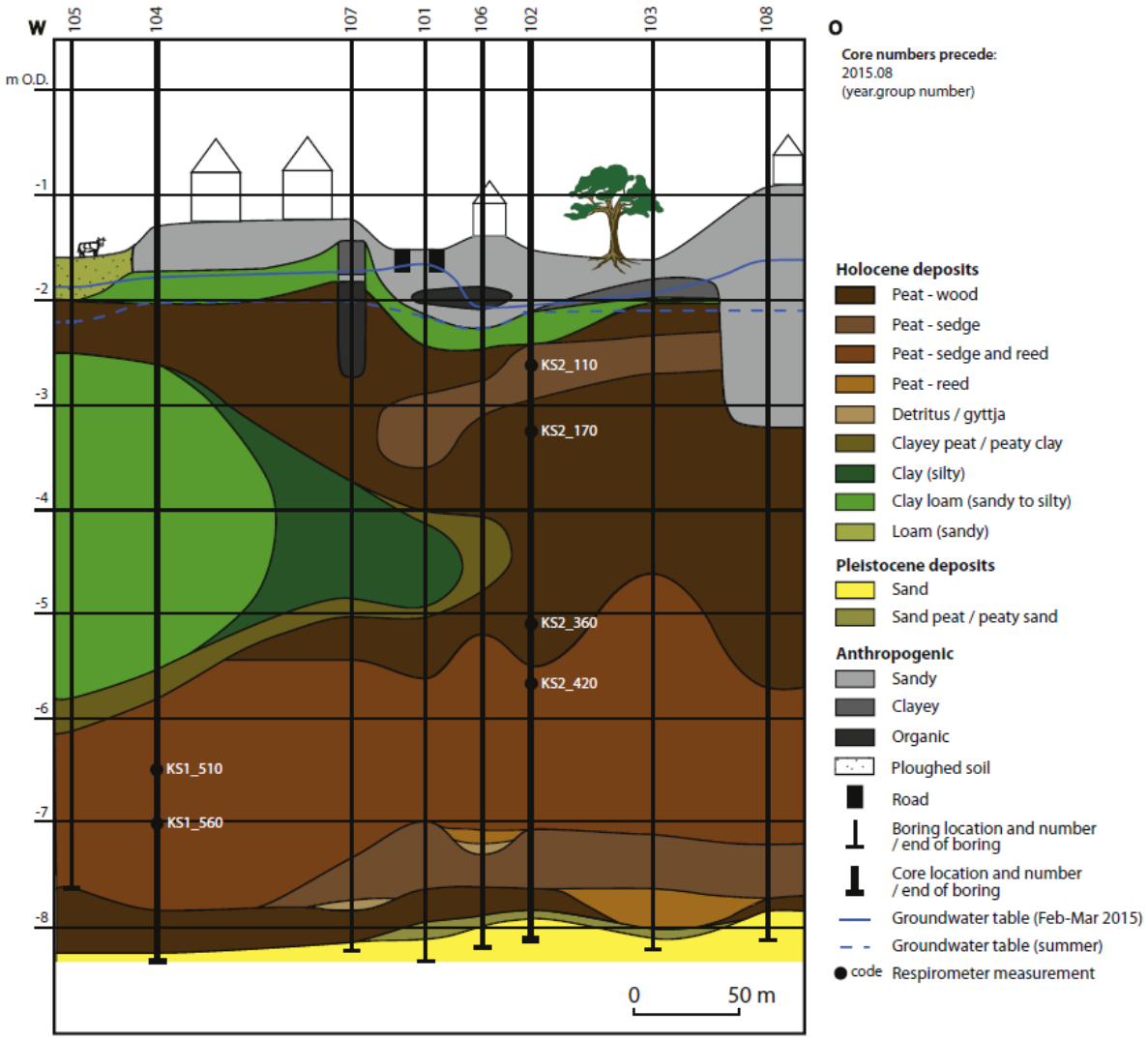

Fig. 4. Cross section of the Holocene sequence beneath Kanis. For the location of the cross section see Fig. 2. The clayey deposits embedded in the peat layer probably belong to the earlier phase of the Grecht channel system, which was active from ca 2900–1850 cal yr BP (Cohen et al., 2012; radiocarbon dates are calibrated using Oxcal 4.1 (Bronk Ramsey, 2001) with the *IntCal13* calibration curve (Reimer et al., 2013)). Other cross sections constructed for this study are presented in Figs. E.1–E.4.

Figure 4 adopted from Van Asselen *et al*. (2018)